Mathematical methods for the Boltzmann equation in the context of chemically reactive gases

Filipe Manuel Sampaio de Carvalho

UMinho | 2012

Universidade do Minho
Escola de Ciências

Filipe Manuel Sampaio de Carvalho

Mathematical methods for the Boltzmann equation in the context of chemically reactive gases

Setembro de 2012

Universidade do Minho
Escola de Ciências

Filipe Manuel Sampaio de Carvalho

Mathematical methods for the Boltzmann equation in the context of chemically reactive gases

Tese de Doutoramento em Ciências
Especialidade em Matemática

Trabalho realizado sob a orientação da
Professora Doutora Ana Jacinta Pereira da Costa Soares
e do
Professor Doutor Filipe Serra de Oliveira

Setembro de 2012

Universidade do Minho, ___/___/______

Assinatura: ____

Acknowledgments

To my supervisor professor Ana Jacinta Soares, for giving true meaning to the role she accepted to take in this work and moreover for the patience, encouragement and enthusiasm she used to guide our meetings. In her I found an excellent teacher, a colleague and above all a friend.

To my master's degree and PhD supervisor professor Filipe Oliveira, for encouraging me to pursuit scientific research and conveying confidence in my skills to do so.

To professor Jacek Polewczak for his collaboration, especially in what concerns this work's last chapter.

To my sons for forgiving the countless stories that remained untold and to their mother for the consecutive shifts she had to take to replace mines.

To Instituto Politécnico de Viana do Castelo for the support given during the process of producing this dissertation.

To University of Minho, Mathematics Department of School of Sciences for the conditions offered to this project and the warm host.

This thesis was supported by:

Fundação para a Ciência e Tecnologia through the PhD-grant SFRH/BD/28795/2006.

Centro de Matemtica da Universidade do Minho through the FCT Pluriannual Funding Program, FEDER Funds, *Programa Operacional Factores de Competitividade* COMPETE and Project Est-C/MAT/UI0013/2011.

Project FCT-PTDC/MAT/68615/2006.

Abstract

In this work we develop some mathematical methods for the Boltzmann equation in the context of chemically reactive gases. The problems here addressed have practical applications on several areas, namely combustion and other engineering applications as well as chemical physics.

First, we study the reaction heat influence on the steady detonation wave. Then, we analyze the influence of both the reaction heat and the activation energy, on the stability spectrum of the steady detonation wave. Finally, we thoroughly construct the simple reacting spheres theory for a quaternary reactive mixture, derive the mathematical properties related to the consistency of the SRS theory and deduce the explicit expressions of the collisional operators' kernels of the linearized SRS system.

We tried to present this work as clear and complete as possible in order to allow to those less familiarized with the kinetic theory of gases to the understand the developments presented.

Although it was not our purpose to describe exhaustively the existing works on the matters here addressed, those we considered important on the contextualization and grounding of the work developed in this thesis are presented.

Resumo

Nesta tese desenvolveram-se alguns métodos matemáticos para tratar a equação de Boltzmann no contexto dos gases quimicamente reativos. Os problemas aqui abordados têm diversas aplicações práticas, refira-se por exemplo a combusto e outras aplicações da engenharia bem como da física e química.
Primeiro estuda-se a influência do calor de reação na onda de detonação estacionária. Em seguida, analisa-se a influência do calor de reação, bem como da energia de activação, no espetro de estabilidade da onda de detonação estacionária. Finalmente, contrói-se, de forma detalhada, a teoria das "siple reacting spheres" para uma mistura quaternária reativa, deduzem-se as propriedades matemáticas relacionadas coma consistência da teoria SRS e deduzem-se as expressções explícitas dos núcleos dos operadores colisionais para o sistema SRS linearizado.
Procurou-se estruturar a tese de uma forma clara e to completa quanto o possvel, de modo a possibilitar que aqueles menos familiarizados com a teoria cinética de gases fossem capazes de acompanhar os desenvolvimentos apresentados.
Apesar de não ser nosso objectivo descrever de forma exaustiva os diversos trabalhos que abordam os temas aqui tratados, não deixamos de apresentar os que consideramos serem importantes na contextualização e fundamentação do trabalho desenvolvido.

List of symbols

$\mathcal{A}$	affinity
A_i	gas mixture constituent
$\boldsymbol{c}_i$	velocity of a particle of the constituent A_i
D	detonation wave velocity
E_i	formation energy of the constituent A_i
f_i	distribution function of the constituent A_i
$\hat{f}_i$	weighted distribution function of the constituent A_i
f_i^M	Maxwellian distribution function of mechanical equilibrium
$\mathbf{g_{si}}$	relative velocity $\boldsymbol{c}_i - \boldsymbol{c}_s$
$\mathcal{H}$	residual function in linear stability calculations
H	Boltzmann H-function
k	Boltzmann constant
$\mathcal{L}_i^E$	linearized elastic operator of the constituent A_i
$\mathcal{L}_i^R$	linearized reactive operator of the constituent A_i
$\hat{\mathcal{L}}_i$	linearized weighted operator of the constituent A_i
m_i	molecular mass of the constituent A_i
M_i	Maxwellian distribution function of thermodynamical equilibrium
M	molecular mass of the reactants $(m_1 + m_2)$ and products $(m_3 + m_4)$
n_i	number density of the constituent A_i
p_i	pressure of the constituent A_i
Q_R	reaction heat
$\mathcal{Q}_i^E$	elastic collisional operator of the constituent A_i
$\mathcal{Q}_i^R$	reactive collisional operator of the constituent A_i
Q_i	weighted linearized elastic operator
p_{lr}^i	pressure tensor component of the constituent A_i

q_l^i	heat flux component of constituent A_i
R_i	weighted linearized reactive operator
T	temperature of the gas mixture
T_i	weighted linearized "hybrid" operator
t_c	characteristic time
x_F	spacial position of the final state in the steady detonation structure
x_s	normalized steady variable in the detonation structure
x_0	spatial position of the shock front in the steady detonation structure
x^+	spatial position of the state ahead of the shock front in the steady detonation structure
u_i	diffusion velocity of the constituent A_i
v_i	velocity of the constituent A_i
z^*	steady detonation solution in the stability analysis
$\bar{z}$	space disturbance in the stability analysis
α	perturbation growth rate of the normal mode approach in the stability analysis
β	perturbation frequency of the normal mode approach in the stability analysis
β_{ij}	steric factor for the collision between constituents A_i and A_j
δ_{rl}	Kronecker's delta
ϵ	unit vector along the the line passing through the centers of the spheres at the moment of impact
Γ_{ij}	threshold velocity of the reactive collisions in the SRS theory
γ	ratio of specific heats
γ_i	relative translational energy
σ_{is}^2	elastic cross section of constituents A_i and A_s
σ	microscopic entropy
${\sigma_{ij}^{\star}}^2$	reactive cross section of constituents A_i and A_j
μ_i	chemical potential of the constituent A_i
μ_{ij}	reduced mass of constituents A_i and A_j

ν_i	stoichiometric coefficient of the constituent A_i
ρ_i	mass density of the constituent A_i
τ_i	reaction rate of the constituent A_i
Θ	Heaviside step function
ε_i	activation energy of the constituent A_i
ξ_1, ξ_2, ξ	relative velocity $\boldsymbol{c}_1 - \boldsymbol{c}_2$
ξ_3, ξ_4, ξ'	relative velocity $\boldsymbol{c}_3 - \boldsymbol{c}_4$
ζ_i	peculiar velocity of the constituent A_i

Contents

Introduction

The dynamics of rarefied gases is a complex subject with several real life applications. In aerospace engineering its application is obvious because the atmospheric density decreases with altitude. In addition, there are several other fields in which this subject has been applied, namely environmental engineering, vacuum industry, ionized gases, electrons behavior, swarms and crawls dynamics and nano-science, among others [19, 31].
As it deals with chemically reactive systems, the dynamics of rarefied mixtures can be applied to engineering problems, such as combustion crystal growth, atmospheric reentry or chemical reactor on the modulation of pollutant formation, chemical vapor deposition reactors, laminar flame extinction limits or gas dissociation behind shocks around space vehicles [36].
The classical fluid dynamics, using the Navier-Stokes partial differential equations, describes very accurately the spatio-temporal evolution of a gas. These equations model the behavior of some macroscopic variables such as density, velocity or temperature. They are derived using the conservation principles and additional hypothesis that relate qualitatively the transportation of mass, linear momentum and energy with macroscopic variables. These hypothesis introduce unknown transport coefficients of diffusion, viscosity and thermic conductivity on the fluid dynamics equations, for which experimental data is available only in some particular cases.
One of the main goals of the kinetic theory is to explain the macroscopic evolution of a rarefied gas through the analysis of the microscopic dynamics

of the constituent gas particles [31, 51, 69].
When one presents a description of the gas dynamics, starting from the kinetic theory, the transport coefficients, as well as all the macroscopic variables, are explicitly obtained through the molecular interaction laws. In fact, the kinetic theory allows the establishment of connections between the different coefficients and provides qualitative results which agree with the ones obtained trough the classical gas dynamics. Moreover, its constructive process allows the correction of the qualitative hypothesis adopted by the classical gas dynamics [31].
The exact dynamics of all particles that constitute the gas, in terms of the Newton equation, could be used to describe the behavior of the gas. However, in practice, this conceptual tool cannot be used, since it requires too much information. On the other hand, a strictly stochastic description would not permit the connection between the Newton equations, which describe the individual movement of each particle, and the spacio-temporal evolution of the macroscopic properties of a gas. The Boltzmann equation lies between those two extremes playing a central role in the kinetic theory [69].
The Boltzmann equation, created in 1872 by Ludwing Boltzman, is an integro-differential equation which describes the evolution of the state of a rarefied gas. Its properties description, its multiple applications as well as its limitations will be addressed throughout this work.
Solving the Boltzmann equation is a rather complex task. To cope with this problem, a series of methods were created and simplifications were made.

Analytical methods of approximate solutions, as those proposed by Grad and by Chapman and Enskog, as well as some simplified collisional models, like the Bhatnagar-Gross-Krook, BGK, discrite velocity models and linear models, enable the maintenance of the major properties of the original equation simplifying the problem. On the other hand, the range of applications of the Boltzmann equation have grown way beyond the original one, i.e., dealing with the behavior of a rarefied gas with only one constituent. In

fact, several generalizations of the Boltzmann equation have been developed by several authors to include relativistic or quantic effects, energy dissipation phenomena and chemical reactions. For a descriptive overview about methods of approximate solutions, simplified collisional models and some relevant extensions of the Boltzmann equation to more evolved systems, see for example, the handbook by Villani [85] and the references therein cited.
It should be noticed that a series of numerical techniques have been developed in order to overcome the underlaying analytic difficulties. Furthermore, the numerical simulations have permitted to ease the constraints that arise from the lack of information concerning the experimental studies [19].
In this work, we deal with chemically reactive mixture. In this context we study the detonation wave problem and the linear stability of the steady detonation wave. In both these problems we investigate the contribution of the reaction heat. We also construct a specific kinetic model, starting from some properties of the classical mechanics and some basic physical laws.

Thesis' structure

The work developed in this thesis is organized in four chapters. Chapter 1 contains a general presentation of the relevant concepts and main properties of the reactive Boltzmann equation. After a brief discussion on the original Boltzmann equation, we explain how the microscopic variables can be used to obtain the macroscopic variables. Some important concepts, such as the elastic and chemical equilibrium and the Maxwell distribution function, are presented. We also present the H-theorem and discuss its relation with the concept of entropy. All these contents have already been presented in literature and are here briefly reviewed in order to exhibit the consistency of this reactive extension of the Boltzmann equation.
In Chapter 2 we address the steady detonation waves. We start by positioning the problem and the adopted model, mentioning some of its main characteristics and limitations and doing some comparisons with other existing

theories. Then we describe the microscopic dynamics, the adopted distribution function and the motivation for that choice. Afterwards we briefly describe the generic features of a steady detonation wave and present the mathematical description for the steady detonation wave that results from the adopted model and distribution function. Finally we present and discuss some numerical results, giving special emphasis on the influence that the reaction heat has on the behavior of the steady detonation wave.

In Chapter 3 we deal with the problem of linear stability of the steady detonation wave. After a brief presentation of the motivations for the study of this problem we address some of the most important works that dealt with the same problem. We give special attention to the ones that were the start point for the approach here used. Then we deduce the problem formulation in which a closure condition is required. The physical meaning and the reason for our choice is also discussed. Before presenting the numerical results and respective discussions we describe, in detail, a numerical technique developed in this work. This technique conjugates different ideas from Erpenbeck and Lee and Stewart and its main goal is to make the search for instabilities more efficient.

In Chapter 4 we construct the kinetic modeling for a chemically reactive gas mixture with hard-sphere potential. After mentioning some previous works on chemically reactive gas mixtures in Section 4.1, we introduce the kinetic adopted model in Section 4.2. In Section 4.3 we explore some of the properties of the collisional operator presented in the previous section and in Section 4.4 we prove the existence of a Lyapunov function and present the characterization of equilibrium states. In Section 4.6 we deduce the linearized Boltzmann equation and explore some of its properties. In this section we also present the explicit expressions for the kernels and the frequency operator of the linearized collisional operator.

In the conclusions we discuss the work presented in this thesis and mention some interesting issues to be investigated in future works.

Main contributions

The original contributions of this thesis appear in Chapters 2, 3 and 4. More in detail, in Chapter 2 we include, for the first time, the contribution of the reaction heat effect on the detonation wave's profile. This study was already presented in the international conference "Waves and Stability in Continuous Media" and published in its proceedings [13]. The study performed in Chapter 3 is based on paper [15] and constitutes the first study on the linear stability problem, on the scope of the kinetic theory, that includes the contribution of the reaction heat and the activation theory on the stability spectrum. Finally, in Chapter 4 we present a new work, still in progress, about the existence and asymptotic stability of the solutions of the Linear Boltzmann equation. The main results of this chapter constitute the content of paper [65], whose final form will be submitted in a near future.

Chapter 1

Kinetic modeling (general description)

For the convenience of presentation and discussion, we introduce, in this chapter, some important concepts and properties of kinetic theory that will be necessary throughout this work, and explain their physical meaning. We also present the physical assumptions and the corresponding mathematical conditions that are usually considered to derive the Boltzmann equation.
The "classical" Boltzmann equation for one component gas is introduced in Section 1.1. In Section 1.2 we present and explore the reactive Boltzmann equation that describes the evolution of a specific chemically reactive gas mixture. Neither the classical nor the reactive Boltzmann equations are here derived in detail, we only present an informal derivation. Moreover, some definitions and fundamental properties related to both equations are presented without their detailed derivation. They can be found, for example, in [17, 51]. Our objective is to discuss the consistency of the kinetic modeling and explain the physical meaning of the properties. The proofs are omitted here.
At last, in Section 1.3 we express the macroscopic variables as suitable averages of microscopic quantities. The passage from the microscopic description

to the hydrodynamic limit is carried out in the construction of the macroscopic equations that describe mean quantities in the gas dynamics. We present some of the connections between the classical theory and the kinetic theory of gas dynamics, and explore some of their differences.

1.1 Boltzmann equation

The kinetic theory is a branch of the nonequilibrium statistical physics. One of its main objectives is to describe the macroscopic properties of a system (a gas, a plasma or another one with a large number of particles) through the microscopic variables associated to the particles that constitute the system. It is important to notice that we do not consider relativistic and quantum effects and we also do not take into account any degrees of freedom. Therefore the microscopic variables are only the velocity components (c_1, c_2, c_3). These components, together with the macroscopic variables of the physical position $\boldsymbol{x}$, define the particle phase space. The state of the gas is modeled, in the phase space, by a distribution function $f \equiv f(\boldsymbol{x}, \boldsymbol{c}, t)$ for any fixed time t, in such a way that $fd\boldsymbol{x}d\boldsymbol{c}$ represents the particle density in the volume element $d\boldsymbol{x}d\boldsymbol{c}$ around position $\boldsymbol{x}$ and velocity $\boldsymbol{c}$ at time t. The function $f(\boldsymbol{x}, \boldsymbol{c}, t)$ is used under the assumption that a bounded domain in the physical space contains only a finite number of particles. In this work, we consider that the evolution domain of the gas is $\mathbb{R}^3$ and thus, the previous assumption about the physical space leads to the mathematical condition $\int_{\mathbb{R}^3} \int_K f(\boldsymbol{x}, \boldsymbol{c}, t) d\boldsymbol{x}d\boldsymbol{c} < +\infty$ for any compact in the spatial domain, $K \subset \mathbb{R}^3$, and for any fixed time t.

The number of particles which constitute the gas, their diameter, the time between two consecutive collisions of one particle and the distance that the particle travels between those collisions are some of the parameters that we have to consider in order to derive the Boltzmann equation. In fact, this equation is only valid for some values of these parameters. We do not intend

to develop here the range of validity of the Boltzmann equation, we only want to stress the importance of its discussion. There are many works, such as [17, 18, 38, 85], that deal with the problem.
If we consider that there are no interactions (collisions) between the particles that constitute the gas then, according to Newton's principle, each particle travels at a constant velocity, in a straight line, and the gas density is constant along the characteristic lines defined by $d\boldsymbol{x}/dt = r$ for any $r \in \mathbb{R}$. Then, if we know the initial density, it is easy to compute the value of the density at time t, using the condition $f(\boldsymbol{x}, \boldsymbol{c}, t) = f(\boldsymbol{x} - t\boldsymbol{c}, \boldsymbol{c}, 0)$. However, this is not the case in situations where collisions between particles are considered. When we consider that particles collide, the state evolution of the gas depends on how these collisions occur. In order to introduce the interaction between particles we have to consider the following assumptions:

Assumption 1: The gas is rarefied enough in order to neglect the collisions of more than two particles. Each collision results in a change of pre-collisional velocities into post-collisional velocities, say $(\boldsymbol{c}, \boldsymbol{c}_*) \to (\boldsymbol{c}', \boldsymbol{c}'_*)$, and implies the rearangement of linear momentum and energy.

Assumption 2: The collisions are micro-reversible, which means that the probability that velocities $(\boldsymbol{c}, \boldsymbol{c}_*)$ are transformed into $(\boldsymbol{c}', \boldsymbol{c}'_*)$ is equal to the probability that velocities $(\boldsymbol{c}', \boldsymbol{c}'_*)$ are transformed into $(\boldsymbol{c}, \boldsymbol{c}_*)$.

Assumption 3: The velocities of two particles that are about to collide are uncorrelated. This assumption is called the Boltzmann chaos assumption.

After a collision, the velocities of the two particles are no longer uncorrelated. In fact they are determined by the pre-collisional velocities. In a one constituent gas, the conservation of momentum and energy in a collision read

$$\boldsymbol{c} + \boldsymbol{c}_* = \boldsymbol{c}' + \boldsymbol{c}'_*, \tag{1.1}$$

$$\boldsymbol{c}^2 + \boldsymbol{c}_*^2 = \boldsymbol{c}'^2 + \boldsymbol{c}'^2_*. \tag{1.2}$$

Using conditions (1.1) and (1.2), the post-collisional velocities are completely determined by the pre-collisional velocities.

In the absence of external forces, and on the basis of the considered Assumptions 1, 2 and 3, the time-space evolution of f is given by the integro-differential Boltzmann equation, see[17],

$$\frac{\partial}{\partial t} f + \sum_{i=1}^{3} c_i \frac{\partial}{\partial x_i} f = \int_{\mathbb{R}^3} \int_{\mathbb{S}^2} (f' f'_* - f f_*) B(\boldsymbol{c} - \boldsymbol{c}_*, \epsilon) d\epsilon d\boldsymbol{c}_* \tag{1.3}$$

where $f' \equiv f(\boldsymbol{x}, \boldsymbol{c}', t)$, $f'_* \equiv f(\boldsymbol{x}, \boldsymbol{c}'_*, t)$, $f \equiv f(\boldsymbol{x}, \boldsymbol{c}, t)$, $f_* \equiv f(\boldsymbol{x}, \boldsymbol{c}_*, t)$, ϵ is a unit vector along the line passing through the centers of the particles, at the moment of impact, and $B(\boldsymbol{c} - \boldsymbol{c}_*, \epsilon)$ is the Boltzmann collisional kernel. This kernel is a nonnegative function which depends only on $\|\boldsymbol{g}\|$, where $\boldsymbol{g} = \boldsymbol{c}_* - \boldsymbol{c}$, and on the scalar product $\langle \frac{\boldsymbol{g}}{\|\boldsymbol{g}\|}, \epsilon \rangle$. Its relation with the cross section, σ^2, is given by the identity $B(\boldsymbol{g}, \epsilon) = \|\boldsymbol{g}\| \sigma^2(\boldsymbol{g}, \epsilon)$. The Boltzmann kernel takes different expressions depending on the adopted potential. A particular case of great importance is the hard-sphere model, for which

$$B(\boldsymbol{g}, \epsilon) = d^2 \langle \boldsymbol{g}, \epsilon \rangle, \tag{1.4}$$

where d is the diameter of the particles. The right-hand side of the Boltzmann equation (1.3) is the collisional operator, which discribes the effect of the collisions on the distribution function f. It is usually represented by $\mathcal{Q}(f, f)$ and can be written as $\mathcal{Q}(f, f) = \mathcal{Q}^+(f, f) - \mathcal{Q}^-(f, f)$, where $\mathcal{Q}^+(f, f)$ and $\mathcal{Q}^-(f, f)$ are the gain and the loss terms, respectively. The gain term, $\mathcal{Q}^+(f, f) = \int_{\mathbb{R}^3} \int_{\mathbb{S}^2} f' f'_* B(\boldsymbol{c} - \boldsymbol{c}_*, \epsilon) d\epsilon d\boldsymbol{c}_*$, counts the number of particles with velocity $\boldsymbol{c}$ that result from collisions between particles with velocity $\boldsymbol{c}'$ and $\boldsymbol{c}'_*$, whereas the loss term, $\mathcal{Q}^-(f,f) = \int_{\mathbb{R}^3}\int_{\mathbb{S}^2} f f_* B(\boldsymbol{c}-\boldsymbol{c}_*,\epsilon) d\epsilon d\boldsymbol{c}_*$, counts the number of particles with velocity $\boldsymbol{c}$ that are lost in collisions between particles with velocity $\boldsymbol{c}$ and $\boldsymbol{c}_*$.

Note 1.1.1. *Assumption 2 results in the relation* $B(\boldsymbol{g},\epsilon) = B(\boldsymbol{g}',\epsilon)$, *with* $\boldsymbol{g}' = \boldsymbol{c}' - \boldsymbol{c}'_*$, *which is crucial in some symmetry properties of the collisional operator.*

The Boltzmann equation (1.3) constitutes a fundamental model in the kinetic theory of gases, that describes the dynamics of the gas particles. At the same time, in the hydrodynamic limit, it leads to a description in terms of suitable and physically meaningful macroscopic quantities and related balance equations. The mathematical properties of the collisional operator, in particular its consistency in terms of conservation equations, entropy inequality and trend to equilibrium, are fundamental for its validity and for the construction of several variants of the Boltzmann equation, when quantum or relativistic effects are taken into account or when chemical reactions are considered.

In particular, the extension of the Boltzmann equation to chemically reactive mixtures will be treated in the next subsection and constitutes the central model of the present work. The fundamental properties of the Boltzmann equation and other relevant mathematical aspects of the theory are the subject of the forthcoming sections in the context of the reactive mixtures.

1.2 Reactive Boltzmann equation

In this section we present the reactive Boltzmann equation that describes the evolution of this gas mixture and some of its properties. We give special attention to mechanical and thermodynamical equilibrium conditions and to the H-theorem that regards the trend to equilibrium. In the presentation of this theorem we make a brief excursion to one component gases. This is justified for the historical significance of the theme. It was Boltzmann, with the H-theorem, who first tried to explain the irreversibility of natural processes in gases, showing how the molecular collisions tend to increase the entropy.

1.2.1 Modeling

We consider a gas mixture with four components, say A_1, A_2, A_3 and A_4, with molecular masses m_1, m_2, m_3 and m_4, and formation energies E_1, E_2, E_3 and E_4, respectively, whose particles undergo binary elastic collisions as well as reactive collisions according to the following reversible reaction

$$A_1 + A_2 \rightleftharpoons A_3 + A_4. \tag{1.5}$$

The reaction heat, Q_R, is given by the difference between the formation energies of the products and those of the reactants. For the considered reaction we have $Q_R = E_3 + E_4 - E_1 - E_2$. Thus, $Q_R > 0$ if the direct reaction is endothermic and $Q_R < 0$ if it is exothermic. The influence of this parameter on the profile of the detonation wave and in the linear stability of the detonation wave receives special attention in this work, specifically in Chapters 2 and 3.

Since we now have more than one component, we have to adjust the notation used in the previous subsection. To identify each constituent we adopt a subscript (or superscript) i in the variables, with $i = 1, 2, 3, 4$. For instance, the distribution function of each constituent A_i is denoted by $f_i(\boldsymbol{x}, \boldsymbol{c}_i, t)$, $f_i(\boldsymbol{c}_i)$ or simply f_i, but the $l-th$ spatial component of the velocity $\boldsymbol{c}_i$ is represented by c_l^i, with $l = 1, 2, 3$.

At the collisional level, the physical conservation laws of mass, linear momentum and total energy of the particles, during the reactive encounters, are specified by the following mathematical conditions

$$m_1 + m_2 = m_3 + m_4, \tag{1.6}$$

$$m_1\boldsymbol{c}_1 + m_2\boldsymbol{c}_2 = m_3\boldsymbol{c}_3 + m_4\boldsymbol{c}_4, \tag{1.7}$$

$$E_1 + \tfrac{1}{2}m_1\boldsymbol{c}_1^2 + E_2 + \tfrac{1}{2}m_2\boldsymbol{c}_2^2 = E_3 + \tfrac{1}{2}m_3\boldsymbol{c}_3^2 + E_4 + \tfrac{1}{2}m_4\boldsymbol{c}_4^2. \tag{1.8}$$

These conditions play an important role in the derivation of the reactive Boltzmann equation.

If we do not take into account external forces, the reactive Boltzmann equation for the distribution function f_i can be written in the following form, see [51]:

$$\frac{\partial}{\partial t} f_i + \sum_{l=1}^{3} c_l^i \frac{\partial}{\partial x_l} f_i = \mathcal{Q}_i^E + \mathcal{Q}_i^R, \tag{1.9}$$

with

$$\mathcal{Q}_i^E = \sum_{s=1}^{4} \int_{\mathbb{R}^3} \int_{\mathbb{S}^2} (f_i' f_s' - f_i f_s) \|\boldsymbol{g}_{si}\| \sigma_{is}^2 d\epsilon d\boldsymbol{c}_s, \tag{1.10}$$

$$\mathcal{Q}_{1(2)}^R = \int_{\mathbb{R}^3} \int_{\mathbb{S}^2} \left[f_3 f_4 \left(\frac{m_1 m_2}{m_3 m_4} \right)^3 - f_1 f_2 \right] \|\boldsymbol{g}_{21}\| {\sigma_{12}^{\star}}^2 d\epsilon d\boldsymbol{c}_{2(1)}, \tag{1.11}$$

$$\mathcal{Q}_{3(4)}^R = \int_{\mathbb{R}^3} \int_{\mathbb{S}^2} \left[f_1 f_2 \left(\frac{m_3 m_4}{m_1 m_2} \right)^3 - f_3 f_4 \right] \|\boldsymbol{g}_{43}\| {\sigma_{34}^{\star}}^2 d\epsilon d\boldsymbol{c}_{4(3)}. \tag{1.12}$$

In the above equations, $\boldsymbol{g}_{si} = \boldsymbol{c}_i - \boldsymbol{c}_s$ is the pre-collisional relative velocity, ${\sigma_{is}}^2$ is the elastic cross section of constituents A_i and A_s, and ${\sigma_{12}^{\star}}^2$ and ${\sigma_{34}^{\star}}^2$ are the differential reactive cross sections for forward and backward reactions, respectively.

We now have four coupled Boltzmann equations for the four distribution functions $f_i, i = 1, ..., 4$. The first term on the right-hand side of Eq. (1.9) refers to the elastic interactions among the particles and represents the elastic operator. The second term refers to the chemical reaction and represents the reactive operator.

The meaning of the elastic collisional operator $\mathcal{Q}_i^E$ in Eq. (1.9) is similar to that of the integral operator on the right-hand side of Eq. (1.3), since both refer to elastic encounters. However, in the present case, the elastic operator $\mathcal{Q}_i^E$ contains the mixture effects represented by the summation over the index $s = 1, ..., 4$.

The reactive collisional operator can also be splitted into a gain and a loss term. In particular, for the reactive collisional operator of constituent A_1 the gain term counts the number of particles with velocity $\boldsymbol{c}_1$ that are created from reactive collisions between particles of constituents A_3 and A_4 with velocities $\boldsymbol{c}_3$ and $\boldsymbol{c}_4$, respectively. The corresponding loss term counts the number of particles with velocity $\boldsymbol{c}_1$ that are consumed in collisions between particles of constituents A_1 and A_2 with velocities $\boldsymbol{c}_1$ and $\boldsymbol{c}_2$, respectively. An analogous interpretation can be made for the reactive collisional operator of the other constituents.

In the definition of the collisional operators given in Eqs. (1.10), (1.11) and (1.12), the so called micro-reversibility principle, which generates a generalized Assumption 2 of Section 1.1, was taken into account. The relation

$$d\boldsymbol{c}_3 d\boldsymbol{c}_4 = \frac{m_1 m_2 \|\boldsymbol{g}_{43}\|}{m_3 m_4 \|\boldsymbol{g}_{21}\|} d\boldsymbol{c}_1 d\boldsymbol{c}_2, \tag{1.13}$$

together with

$$\sigma_{34}^{\star\;2} = \left(\frac{m_1 m_2}{m_3 m_4}\right)^2 \left(\frac{\|\boldsymbol{g}_{21}\|}{\|\boldsymbol{g}_{43}\|}\right)^2 \sigma_{12}^{\star\;2}, \tag{1.14}$$

is used to obtain the micro-reversibility condition in the form

$$f_3 f_4 \|\boldsymbol{g}_{43}\| \sigma_{34}^{\star\;2} d\epsilon d\boldsymbol{c}_3 d\boldsymbol{c}_4 = f_3 f_4 \left(\frac{m_1 m_2}{m_3 m_4}\right)^3 \|\boldsymbol{g}_{21}\| \sigma_{12}^{\star\;2} d\epsilon d\boldsymbol{c}_1 d\boldsymbol{c}_2, \tag{1.15}$$

which, in turn, is used to express the gain term in the form presented in Eq. (1.11). The gain term in Eq. (1.12) is obtained in a similar way. A more detailed description can be found, for example, in [51]. Although the micro-reversibility principle is pointed out as a basic assumption, apart from some exception, it has not been established whether it is satisfied for realistic particle potentials in general, see [43]. In Chapter 4 we adopt a potential that, under simple assumptions, satisfies this principle.

1.2.2 Properties of the collisional terms

Now we present some of the basic properties of the collisional terms given by Eqs. (1.10), (1.11) and (1.12). We aim to introduce the properties that must be verified to assure the consistency of a kinetic model and explain their physical meaning. The detailed derivations are omitted here, since they are presented in Chapter 4 with reference to a particular kinetic modeling.

Proposition 1.2.1. *The elastic collisional terms are such that*

$$\int_{\mathbb{R}^3} \mathcal{Q}_i^E d\boldsymbol{c}_i = 0 \qquad i = 1, ..., 4. \tag{1.16}$$

This proposition states that the number of particles of each constituent does not change during elastic interactions.

Proposition 1.2.2. *The reactive terms satisfy the following property:*

$$\int_{\mathbb{R}^3} \mathcal{Q}_1^R d\boldsymbol{c}_1 = \int_{\mathbb{R}^3} \mathcal{Q}_2^R d\boldsymbol{c}_2 = -\int_{\mathbb{R}^3} \mathcal{Q}_3^R d\boldsymbol{c}_3 = -\int_{\mathbb{R}^3} \mathcal{Q}_4^R d\boldsymbol{c}_4. \tag{1.17}$$

Equalities (1.17) come from the fact that, with the chemical bimolecular reaction (1.5) the variation of the number of particles of constituents A_1 and A_2 is equal and symmetric to the variation of the number of particles of constituents A_3 and A_4. Thus, the reaction rates defined by $\tau_i = \int_{\mathbb{R}^3} \mathcal{Q}_i^R d\boldsymbol{c}_i$ are such that $\tau_1 = \tau_2 = -\tau_3 = -\tau_4$.

Another fundamental property of the collisional operator states the existence of suitable collisional invariants, this is, certain functions which do not change during the collisional process. This property is related to the conservation laws presented in Eqs. (1.6), (1.7) and (1.8).

Definition 1.2.1. *A function* $\psi = (\psi_1, \psi_2, \psi_3, \psi_4)$ *is a* **collisional invariant** *in the velocity space if*

$$\sum_{i=1}^{4} \int_{\mathbb{R}^3} \psi_i \left(\mathcal{Q}_i^E + \mathcal{Q}_i^R \right) d\boldsymbol{c}_i = 0. \tag{1.18}$$

Proposition 1.2.3. *The functions* $\psi = (1,0,1,0)$, $\psi = (1,0,0,1)$, $\psi = (0,1,1,0)$, *and the functions* $\psi = (\psi_1, \psi_2, \psi_3, \psi_4)$ *defined by* $\psi_i = m_i c_1^i$, $\psi_i = m_i c_2^i$, $\psi_i = m_i c_3^i$, *and* $\psi_i = E_i + \frac{1}{2}\mathbf{c}_i^2 m_i$ *are collisional invariants.*

The first three invariants assure the conservation of the number of particles of constituents A_1 and A_3, A_1 and A_4 and A_2 and A_3, respectively. This is a consequence of the bimolecular chemical law. The conservation of the total number of particles of the reactive mixture results from these partial conservations. The next three invariants assure the conservation of the linear momentum components of the gas mixture and the last invariant assures the conservation of the total energy of the gas mixture.
All functions, which are a linear combination of the above six invariants are also collisional invariants. They can be defined by

$$\psi_i(\boldsymbol{c}_i) = G_i + \mathbf{H} \cdot m_i \boldsymbol{c}_i + J(E_i + \frac{1}{2}\mathbf{c}_i^2), \tag{1.19}$$

where G_i and J are scalar functions, with G_i being such that $G_1 + G_2 = G_3 + G_4$, and $\mathbf{H}$ a vectorial function, all of them being independent of $\boldsymbol{c}_i$.

1.2.3 Mechanical and chemical equilibrium

When the gas reaches the equilibrium the elastic and reactive collisions do not stop, they become balanced. This means that the collisional process does not modify the number of particles which enter and leave a volume element in the phase space per unit time.

Definition 1.2.2. *A gas is in mechanical equilibrium when*

$$\mathcal{Q}_i^E = 0, \qquad i = 1, ..., 4. \tag{1.20}$$

It is in chemical equilibrium when

$$\mathcal{Q}_{1(2)}^R = \mathcal{Q}_{3(4)}^R = 0 \tag{1.21}$$

and in thermodynamical equilibrium when

$$\mathcal{Q}_i^E + \mathcal{Q}_i^R = 0, \qquad i = 1, ..., 4. \tag{1.22}$$

The relation between elastic, chemical and thermodynamical equilibrium is established in the next proposition.

Proposition 1.2.4. *For each $i = 1, ..., 4$, the following conditions are equivalent:*

a) $\mathcal{Q}_i^E + \mathcal{Q}_i^R = 0$;

b) $\mathcal{Q}_i^E = \mathcal{Q}_i^R = 0$.

Proposition 1.2.4 shows that the entire collisional operator vanishes only when both the elastic and the reactive collisional operators vanish separately. In other words, it is not possible to reach thermodynamical equilibrium without reaching both mechanical and chemical equilibrium.

Proposition 1.2.5. *If all constituents are at the same temperature, the only distribution function that assures the mechanical equilibrium is the Maxwellian distribution given by*

$$f_i^M(\boldsymbol{c}_i) = n_i \left(\frac{m_i}{2\pi kT}\right)^{\frac{3}{2}} \exp\left[-\frac{m_i(\boldsymbol{c}_i - u)^2}{2kT}\right]. \tag{1.23}$$

Above, k is the Boltzmann constant and n_i, T and u represent the number density of constituent A_i and the temperature and velocity of the mixture, respectively, which are macroscopic quantities that will be defined in terms of microscopic variables in Section 1.3. This result is well known and a formal proof can be found in many books, see for example [17] for a one single specie and [51] for a reactive mixture.

Note 1.2.1. *In a non-reactive gas mixture the Maxwellian function characterizes the equilibrium state. However this is not the case for a mixture with a chemical reaction since to obtain thermodynamical equilibrium it is necessary to reach not only mechanical equilibrium but also chemical equilibrium.*

To obtain the chemical equilibrium conditions we may introduce the chemical potential of the constituent A_i, say μ_i, given by

$$\mu_i = E_i - kT\left[\frac{3}{2}\ln T - \ln n_i + \frac{3}{2}\ln\left(\frac{2\pi m_i k}{h^2}\right)\right], \tag{1.24}$$

where h is the Plank constant. The deviation from chemical equilibrium can be characterized by the affinity

$$\mathcal{A} = -\sum_{i=1}^{4} \nu_i \mu_i, \tag{1.25}$$

where ν_i is the stoichiometric coefficient of the constituent A_i. For the considered chemical reaction, these coefficients are such that $\nu_1 = \nu_2 = -\nu_3 = -\nu_4 = -1$ and the chemical equilibrium condition is $\sum_{i=1}^{4} \nu_i \mu_i^{\mathrm{eq}} = 0$, where the superscript "eq" indicates equilibrium values. This condition may take the form of the mass action law, as described in the following proposition.

Proposition 1.2.6. *The chemical equilibrium is characterized by Maxwellians (1.23) constrained by*

$$(m_3 m_4)^3 f_1^M(\boldsymbol{c}_1) f_2^M(\boldsymbol{c}_2) = (m_1 m_2)^3 f_3^M(\boldsymbol{c}_3) f_4^M(\boldsymbol{c}_4),$$

which is equivalent to the mass action law expressed by

$$\frac{Q_R}{kT} = \frac{3}{2} \ln \left(\frac{m_3 m_4}{m_1 m_2} \right) + \ln \left(\frac{n_1^{\text{eq}} n_2^{\text{eq}}}{n_3^{\text{eq}} n_4^{\text{eq}}} \right). \tag{1.26}$$

1.2.4 Boltzmann H-theorem

The objective of this subsection is to study the tendency to equilibrium of a chemically reactive gas mixture and this is done using the Boltzmann H-theorem. This theorem shows the important feature of the irreversibility of the Boltzmann equation and states the trend to equilibrium. These features were the source of many discussions and gave rise to some known paradoxes. Some people could not accept that an equation which is based on classical reversible mechanics had an irreversible feature. Some arguments for and against this property can be found, for instance, in [17, 51, 85]. This theorem is also related to the concept of entropy. In thermodynamics, the entropy S is defined in equilibrium states by the equation

$$dS = \frac{\delta Q}{T},$$

where δQ represents the amount of heat received by the gas. If a gas is in equilibrium, a change in its state is only possible with external disturbances. It is important to state that the symbol δQ is used instead of dQ because Q is not a state variable.

It is known that in any thermodynamical process between an initial equilibrium state I and the final equilibrium state F the following inequality holds true:

$$S_F \geq S_I + \int_I^F \frac{\delta Q}{T}.$$

In the specific case of isolated gases we obviously have that $\delta Q = 0$ and thus $S_F \geq S_I$ which is the same as

$$\Delta_S = S_F - S_I \geq 0.$$

This is the second principle of thermodynamics, see for example [19, 31, 51]. It is also known that if a gas system is isolated there is a maximal value for the entropy and that this value corresponds to the equilibrium state. These are known macroscopic features of gas dynamics.

To be able to prove the H-theorem in gas mixtures, it is necessary to consider some additional conditions to the Boltzmann equation. There are some works that proved the existence of an H-function for reactive mixtures on the space-homogeneous case, see [42, 50, 71], for example. For non-homogeneous cases it is necessary to consider a certain type of domain or to impose suitable boundary conditions. In particular, a space domain with periodic boundary conditions or a bounded space domain with specular reflection, see [19, 27]. For the space-homogeneous case we have the following proposition.

Proposition 1.2.7. *If we consider the distribution function f_i uniform in space for every $i = 1, ..., 4$, the functional H defined by*

$$\mathsf{H}(t) = \sum_{i=1}^{4} \int_{\mathbb{R}^3} f_i \log\left(\frac{f_i}{m_i^3}\right) d\boldsymbol{c}_i \tag{1.27}$$

respects the following conditions:

a) $\frac{d}{dt}\mathsf{H}(t) \leq 0$

b) $\frac{d}{dt}\mathsf{H}(t) = 0$ *if and only if the gas mixture is in thermodynamical equilibrium.*

The result stated in Proposition 1.2.7 proves the asymptotic stability of the Boltzmann equation solution, since $\mathsf{H}(t)$ reaches its minimum value only at the unique equilibrium distribution function, namely the Maxwellian distribution function defined in expression (1.23).

To end this section we present a note on how Boltzmann tried to explain the temporal evolution of a gas with one constituent through microscopic interactions. This brief derivation from the context of reactive gas mixtures is needed due to the historical importance of this development in the kinetic theory.

Historical note:
To make the connection between the classical reversible mechanics of the molecular collisions and the irreversible evolution of gases, Boltzmann proposed a definition of the entropy of a gas in terms of the microscopic states. An H-function was proposed for a rarefied gas constituted by N particles and occupying a spatial region $R \in \mathbb{R}^3$, as follows

$$\mathsf{H}(t) = \int_R H(\boldsymbol{x}, t) d\boldsymbol{x}, \tag{1.28}$$

where $H(\boldsymbol{x}, t)$ is given by

$$H(\boldsymbol{x}, t) = \int f(\boldsymbol{x}, \boldsymbol{c}, t) \log f(\boldsymbol{x}, \boldsymbol{c}, t) d\boldsymbol{c}. \tag{1.29}$$

With this function Boltzmann proposed the following definition of the microscopic entropy σ,

$$\sigma(t) = -kN\mathsf{H}(t), \tag{1.30}$$

where k is the Boltzmann constant.
Generally speaking, the H-theorem states that if f is a solution of the Boltzmann equation (1.3) of an isolated gas, then $\mathsf{H}(t)$ decreases in time and reaches its minimum value in the equilibrium state. With this result it is possible to sustain that the Boltzmann equation creates a connection between statistical mechanics and gas mechanics. The H-theorem proof regarding to monotonic gases is well known, see for example [17].

1.3 Macroscopic equations

The connection between the microscopic variables and the macroscopic quantities is based on the idea that all measurable macroscopic variables can be expressed in terms of microscopic averages of the distribution functions. We introduce below the more relevant macroscopic quantities associated to each constituent, denoted with the subscript i, as well as those referring to the whole mixture, denoted with plain symbols.

Number density

$$n_i = \int_{\mathbb{R}^3} f_i d\mathbf{c}_i \quad \text{and} \quad n = \sum_{i=1}^{4} n_i \tag{1.31}$$

Mass density

$$\varrho_i = \int_{\mathbb{R}^3} m_i f_i d\mathbf{c}_i \quad \text{and} \quad \varrho = \sum_{i=1}^{4} \varrho_i \tag{1.32}$$

Momentum density

$$\varrho_i v_l^i = \int_{\mathbb{R}^3} m_i c_l^i f_i d\mathbf{c}_i \quad \text{and} \quad \varrho v_l = \sum_{i=1}^{4} \varrho_i v_l^i \tag{1.33}$$

where v denotes the velocity of the mixture.

Diffusion velocity

$$u_l^i = \frac{1}{\varrho_i} \int_{\mathbb{R}^3} m_i \zeta_l^i f_i d\mathbf{c}_i \tag{1.34}$$

where $\zeta_l^i = c_l^i - v_l$ is a peculiar velocity.

Pressure

$$p_i = \frac{1}{3} \int_{\mathbb{R}^3} m_i \zeta_i^2 f_i d\mathbf{c}_i \quad \text{and} \quad p = \sum_{i=1}^{4} p_i \tag{1.35}$$

Pressure tensor components

$$p_{lr}^{i} = \int_{\mathbb{R}^3} m_i \zeta_l^i \zeta_r^i f_i d\mathbf{c}_i \quad \text{and} \quad p_{lr} = \sum_{i=1}^{4} p_{lr}^{i} \tag{1.36}$$

Temperature

$$T_i = \frac{p_i}{n_i k} \quad \text{and} \quad T = \sum_{i=1}^{4} \frac{n_i}{n} T_i = \frac{p}{nk} \tag{1.37}$$

Heat flux components

$$q_l^i = \int_{\mathbb{R}^3} \frac{1}{2} m_i \zeta_i^2 \zeta_l^i f_i d\boldsymbol{c}_i \quad \text{and} \quad q_l = \sum_{i=1}^{4} \left(q_l^i + n_i E_i u_l^i \right) \tag{1.38}$$

where the term $n_i E_i u_l^i$ refers to the formation energy transfer of the constituent A_i due to diffusion.

With the macroscopic variables defined as microscopic averages of the distribution function, we can use the Boltzmann equation to deduce appropriate balance equations for the evolution of the macroscopic variables of the reactive gas mixture. The evolution of the general average macroscopic variable $\int_{\mathbb{R}^3} \psi_i d\boldsymbol{c}_i$ is given by the transfer equation for the constituent A_i. This equation is obtained from the Boltzmann equations (1.9) by taking the product with the function $\psi_i \equiv \psi(\boldsymbol{x}, \boldsymbol{c}_i, t)$ and integrating over the velocity $\boldsymbol{c}_i$, getting

$$\frac{\partial}{\partial t} \int_{\mathbb{R}^3} \psi_i f_i d\boldsymbol{c}_i + \sum_{l=1}^{3} \frac{\partial}{\partial x_l} \int_{\mathbb{R}^3} \psi_i c_l^i f_i d\boldsymbol{c}_i - \int_{\mathbb{R}^3} \left(\frac{\partial}{\partial t} \psi_i + \sum_{l=1}^{3} c_l^i \frac{\partial}{\partial x_l} \psi_i \right) f_i d\boldsymbol{c}_i$$
$$= \int_{\mathbb{R}^3} \psi_i \left(\mathcal{Q}_i^E + \mathcal{Q}_i^R \right) d\boldsymbol{c}_i. \tag{1.39}$$

From this equation, we can obtain the balance equation for the relevant macroscopic variables, when the function ψ_i is suitably defined. The balance equation for the number density of the constituent A_i follows from the transfer equation (1.39) by choosing $\psi_i = 1$, resulting

$$\frac{\partial}{\partial t} n_i + \sum_{l=1}^{3} \frac{\partial}{\partial x_l} \left(n_i u_l^i + n_i v_l \right) = \int_{\mathbb{R}^3} \left(\mathcal{Q}_i^E + \mathcal{Q}_i^R \right) d\mathbf{c}_i. \tag{1.40}$$

The balance equation for the momentum density component of the constituent A_i follows from the transfer equation (1.39) by choosing $\psi_i = m_i c_l^i$, resulting

$$\frac{\partial}{\partial t}(\varrho_i v_l^i) + \sum_{r=1}^{3} \frac{\partial}{\partial x_r} \left(p_{lr}^i + \varrho_i u_l^i v_r + \varrho_i u_r^i v_l + \varrho_i v_l v_r \right)$$
$$= \int_{\mathbb{R}^3} m_i c_l^i \left(\mathcal{Q}_i^E + \mathcal{Q}_i^R \right) d\mathbf{c}_i. \tag{1.41}$$

The balance equation of the total energy of the constituent A_i follows from the transfer equation (1.39) by choosing $\psi_i = E_i + \frac{1}{2} m_i \mathbf{c}_i^2$, resulting

$$\frac{\partial}{\partial t} \left[\frac{3}{2} p_i + n_i E_i + \varrho_i u_l^i v_l + \frac{1}{2} \varrho_i v^2 \right] + \sum_{l=1}^{3} \frac{\partial}{\partial x_l} \left[q_l^i + p_{lr}^i v_r \right.$$
$$\left. + n_i E_i u_l^i + \frac{1}{2} \varrho_i u_l^i v^2 + \left(\frac{3}{2} p_i + n_i E_i + \varrho_i u_l^i v_l + \frac{1}{2} \varrho_i v^2 \right) v_i \right]$$
$$= \int_{\mathbb{R}^3} \left(\frac{1}{2} m_i c_i^2 + E_i \right) \left(\mathcal{Q}_i^E + \mathcal{Q}_i^R \right) d\mathbf{c}_i. \tag{1.42}$$

The balance equations for the number density, linear momentum and total energy of the gas mixture are obtained by summing the corresponding Eqs. (1.40), (1.41) and (1.42) over all constituents. From Proposition 1.2.3 and Definition 1.2.1, we easily conclude that the resulting balance equations for the gas mixture are of conservative type, because the right-hand side of the equations vanish. They are given by

$$\frac{\partial}{\partial t} n + \sum_{l=1}^{3} \frac{\partial}{\partial x_l}(n v_i) = 0, \tag{1.43}$$

$$\frac{\partial}{\partial t}(\varrho v_l) + \sum_{r=1}^{3} \frac{\partial}{\partial x_r}(p_{lr} + \varrho v_l v_r) = 0, \tag{1.44}$$

$$\frac{\partial}{\partial t}\left[\frac{3}{2} nkT + \sum_{i=1}^{4} n_i E_i + \frac{1}{2}\varrho v^2\right] + \sum_{l=1}^{3} \frac{\partial}{\partial x_l}\left[q_l + p_{lr} v_r + \left(\frac{3}{2} nkT + \sum_{i=1}^{4} n_i E_i + \frac{1}{2}\varrho v^2\right) v_l\right] = 0. \tag{1.45}$$

The so called system of evolution equations is formed by the balance equations (1.40) for the number densities of the constituents, the conservation equations (1.44) and (1.45) for the linear momentum and total energy (1.45) of the whole mixture constitutes. Such system is not closed. In classical gas dynamics it is closed assuming that p_{lr} and q_l respect Newton's law,

$$p_{lr} = p\delta_{lr}, \qquad q_l = 0, \tag{1.46}$$

giving rise to the Euler equations, or assuming that they respect the Stokes' law and the Fourier's law,

$$p_{lr} = p\delta_{lr} - \nu\left(\frac{\partial v_l}{\partial x_r} + \frac{\partial v_r}{\partial x_l} - \frac{2}{3}\frac{\partial v_s}{\partial x_s}\delta_{lr}\right) - \nu_B \frac{\partial v_s}{\partial x_s}\delta_{lr}, \qquad q_l = -\lambda \frac{\partial T}{\partial x_l}, \tag{1.47}$$

giving rise to the Navier-Stokes equations. Above, δ_{lr} is the Kronecker's delta, ν is the viscosity, ν_B is the bulk viscosity and λ is the thermal conductivity of the gas mixture.

In kinetic theory, the system of evolution equations is closed by determining the distributions function as an appropriate solution of the Boltzmann equation consistent with the considered mechanical and chemical regime. Kinetic approaches to chemically reactive gas mixtures can be used as a consistent and justified tool to derive adequate hydrodynamic equations for reactive mixtures. One particular case is the Maxwellian distribution function. This particular choice for the distribution function gives the same result as considering Newton's law in classical gas dynamics, both giving rise to the Euler equations. These are the evolution equations of a gas mixture in mechanical equilibrium.

The kinetic approach can help to understand, or even explain and predict, the chemical reaction that plays a crucial role in the evolution process.

Chapter 2

Dynamics of the steady detonation wave

In this chapter we study the propagation of steady detonation waves, starting from the kinetic modeling of the explosive reactive mixture in terms of the description made in Section 1.2. First, we present a brief description of the main theories about detonation in gas mixtures. We do so in order to recall the relevant physical aspects of the phenomenon and introduce the mathematical models used to describe the propagation of detonation waves. Then we present our results on the steady representation of the detonation wave solution, based on the so-called Zeldovich-von Neuman and Doering (ZND) detonation theory. More in detail, we consider the kinetic modeling of a binary reactive mixture undergoing a symmetric bimolecular chemical reaction and then we pass to the hydrodynamic limit at the Euler level. The resulting macroscopic equations are used to determine the steady detonation wave solution. Finally, some numerical simulations are performed to obtain representative profiles of the solution.

2.1 Preliminaries

In this subsection we introduce some fundamental concepts related to the detonation fenomena, with the aim of presenting the necessary background to follow the central problem of this chapter.

Deflagration and detonation

In some situations, when we have a reactive mixture, a propagation wave may appear. If this wave is subsonic, it is considered a deflagration wave and its front is called flame. In this type of waves, downstream perturbations may change the state of the mixture before the arrival of the wave itself. Thus, the deflagration wave velocity depends, not only on the properties of the initial mixture, but also on the way that the mixture is changed by the perturbations that pass through the wave from the downstream mixture. On the other hand, when the wave is supersonic, it is considered a detonation wave and its front is called shock front. In this type of wave, the thermodynamical variables vary abruptly. Since the wave velocity is supersonic, the initial mixture does not change until the arrival of the wave, and thus its velocity only depends on the properties of the initial mixture.

On specific situations, a deflagration wave may transit into a detonation wave. This transition involves several interesting aspects which are the subject of many works, namely [54, 90]. The problem of deflagration to detonation transition (DDT), as well as the problem of deflagration waves, are not addressed this work. Note that the transition is not the only way of starting a detonation; for instance, it may start directly from an ignition source without passing through a deflagration. The way of starting a detonation is also not part of this work.

Chapman-Jouguet theory

One of the fundamental features of the detonation is its propagating velocity. Chapman and Jouguet studied this problem using an idealized model in which the flux is considered one dimensional in space; the shock front is plan and the chemical reaction is instantaneous. Therefore, the chemical equilibrium is reached immediately after the shock front. Unlike non reactive shock waves that admit any velocity greater then the sound velocity, the detonation waves do not admit any velocity below a certain minimum value. Chapman and Jouguet postulated that a self-sustained detonation wave must have this minimum velocity, that is called the CJ velocity, see [33, 81, 82]. The Chapman Jouguet theory does not make any reference to the detonation wave structure, that is, to the transition process from the two different equilibrium states: before and after the detonation wave. After determining the wave velocity the final state is determined by the conservation laws of mass, linear momentum and total energy. Since it is considered that the mixture reaches equilibrium immediately after the shock front, it is possible to determine the chemical composition through the thermodynamical variables and the amount of released energy.

Zeldovich, von Neumann and Doering theory.

The ZND model, proposed independently by Zeldovich, von Neumann and Doering, uses the Euler equations to describe the detonation. This is also an idealized model in which the flux is one dimensional and the shock front is plan. The main difference between the CJ model and the ZND model is that the latter considers that the chemical reaction does not occur instantaneously in the shock front but rather it starts at the shock front and proceeds with a finite reaction rate until reaching the equilibrium. The conservation laws are valid anywhere, in particular in the final equilibrium state. Thus, the CJ hypothesis is still valid for any reaction rate, even if it is finite. This hypothesis is usually used to determine the velocity of self-sustained detonation waves.

Less idealized theories
In order to cope with the differences between theoretical and experimental results, some new models have been proposed. The theory advanced by Wood and Kirkwood also uses the Euler equations but allows the existence of many different chemical reactions. Other theories use the Navier-Stokes equations to describe the state of the mixture and thus, do consider the influence of the thermal conductivity, diffusion and viscosity. These less idealized theories bring many mathematical difficulties and are not treated in this work.

The ZND as well as the CJ theory may seem inadequate to direct application on real detonations. In fact, although the shock front of a real detonation is approximately plane and its velocity is approximately constant, experimental observations show the existence of three dimensional structures which are dependent on time. Nevertheless, the one dimensional solutions are important for theoretical developments and to create a solid base for more complete and complex approaches.
All the presented models and theories are based on macroscopic aspects of the gas mixture behavior. For a better understanding on the way that microscopic aspects of the chemical reaction influence the detonation wave solutions we approach this problem using the kinetic theory of gases.
For velocities greater then the CJ velocity, there are two different solutions for the detonation wave, the strong and the week solutions. The strong solution or overdriven solution is supported by a piston, its pressure is greater than the pressure of the CJ-detonation and the flux velocity of the final state, with respect to the reference frame moving with the shock front, is subsonic. On the other hand, the week solution or pathological solution has less pressure than the one of the CJ-detonation. Furthermore the flux velocity of the final state, with respect to the reference frame moving with the shock front, is supersonic [33]. In this work, we always use the detonation wave velocity as a parameter and it takes values greater than the CJ velocity. Furthermore,

we deal with both, overdriven and pathological solutions.

2.2 Kinetic background

In this section we present the kinetic background used to approach the steady detonation wave problem as well as the linear stability problem which is the object of the following Chapter. We study the detonation wave problem starting from the Boltzmann equation for the reactive gaseous mixture and also the influence of the reaction heat on the behavior of the wave. This study is carried out for both the steady detonation of overdriven solution with exothermic chemical reaction and for the second branch of the pathological solution with endothermic chemical reaction.
We start by describing a model for the distribution function which is obtained from a small deviation from the Maxwellian distribution [49]. This model was adopted in order to emphasize the influence of the reaction heat on the detonation wave solution. Then we use the model to investigate the detonation wave problem and obtain some numerical results concerning the profile of the detonation wave solution.
The results presented in this chapter have been published in papers [13, 14].

2.2.1 Adopted kinetic modeling

The detonation system is a binary reacting gaseous mixture described by a simple kinetic model, corresponding to a particular case of the one presented in Section 1.2. Accordingly, we consider two constituents, say A and B, with the same molecular mass m, whose particles undergo binary elastic collisions as well as inelastic collisions with reversible chemical reaction of type $A + A \rightleftharpoons B + B$.
The kinetic equations, describing the behavior of the mixture, can be obtained from the general equations (1.9), (1.10), (1.11) and (1.12) referring to

the particular adopted modeling, namely to a binary mixture with symmetric reaction, hard-sphere cross sections for elastic collisions and step cross sections with activation energy for reactive collisions.

$$\sigma_i^{\star 2} = \begin{cases} 0 & \text{for } \gamma_i < \varepsilon_i^\star \\ d_r^2 & \text{for } \gamma_i > \varepsilon_i^\star \end{cases} \qquad i = A, B, \tag{2.1}$$

where $\gamma_i = \frac{m g_i^2}{4kT}$ is the relative translational energy.
The details and properties of this kinetic model have been treated in paper [49] and are not object of investigation in this thesis.

On paper [49], using the Chapman-Enskog method and the Sonine polynomial approximation to the coefficients of the distribution function, the authors obtained an approximate solution of the kinetic equations, containing the non-equilibrium effects of the reaction heat and activation energy. In the Euler hydrodynamic limit, in a slow reaction regime, this solution leads to a closed macroscopic system of hydrodynamic equations with excellent mechanical and chemical kinetic properties to study the propagation of detonation waves and its hydrodynamic stability. The closure aspects and the application of the resulting macroscopic equations to the detonation problem can be considered the innovative and key idea developed in this work.
Coming to the mathematical details of the closure procedure and macroscopic equations, the approximate solution of the kinetic equations obtained in paper [49] is

$$f_i^{(0)} = f_i^M \left[1 + \omega \left(\frac{15}{8} - \frac{5m(c_i - v)^2}{4kT} + \frac{m^2 (c_i - v)^4}{8k^2 T^2} \right) \right], \tag{2.2}$$

where f_i^M is the Maxwellian distribution, and ω is given by

$$\omega = -x_A^2 \left(\frac{d}{d_r} \right)^2 \frac{Q_R^\star}{8} \left(1 - Q_R^\star - Q_R^\star \varepsilon_A^\star + \varepsilon^\star - 2\varepsilon_A^{\star 2} \right) e^{-\varepsilon_A^\star}. \tag{2.3}$$

Above, $x_A = n_A/n$ is the concentration of the A-constituent, d and d_r the elastic and reactive diameters, $\varepsilon_A^\star$ the activation energy of the forward reaction in units of kT and $Q_R^\star = Q_R/kT$ the reaction heat in units of kT. Moreover, $Q_R = 2\,(E_B - E_A)$, indexreaction! heatso that $Q_R > 0$ when the forward reaction is endothermic whereas $Q_R < 0$ when it is exothermic. The solution given by Eqs. (2.2) and (2.3) exhibits an appreciable influence of the reaction heat and activation energy.
The closed system of hydrodynamic Euler equations, obtained with the non-equilibrium distribution $f_i^{(0)}$ given by expressions (2.2) and (2.3), have the form:

$$\frac{\partial}{\partial t} n_A + \sum_{l=1}^{3} \frac{\partial}{\partial x_l}(n_A v_i) = \tau_A, \tag{2.4}$$

$$\frac{\partial}{\partial t}(n_A + n_B) + \sum_{l=1}^{3} \frac{\partial}{\partial x_l}((n_A + n_B) v_l) = 0, \tag{2.5}$$

$$\frac{\partial}{\partial t}(\varrho v_l) + \sum_{r=1}^{3} \frac{\partial}{\partial x_r}(p\delta_{lr} + \varrho v_l v_r) = 0, \quad l = 1, 2, 3, \tag{2.6}$$

$$\frac{\partial}{\partial t}\left[\frac{3}{2} nkT + \sum_{i=A}^{B} n_i E_i + \frac{1}{2}\varrho v^2\right] + \sum_{l=1}^{3} \frac{\partial}{\partial x_l}\left[\sum_{r=1}^{3} p\delta_{lr} v_r + \left(\frac{3}{2} nkT + \sum_{i=A}^{B} n_i E_i + \frac{1}{2}\varrho v^2\right) v_l\right] = 0, \tag{2.7}$$

where the macroscopic quantities are defined in terms of the distribution functions f_i as explained in Chapter 1, for the considered binary mixture. Moreover, the reaction rate τ_A has the following form

$$\tau_A = -4 n_A^2 d_r^2 \sqrt{\frac{\pi kT}{m}}\, e^{-\varepsilon_A^\star}\left[1 + \varepsilon_A^\star + \frac{x_A^2}{128}\left(\frac{d}{d_r}\right)^2 Q_R^\star \times \left(1 + Q_R^\star + Q_R^\star \varepsilon_A^\star + \varepsilon_A^\star - 2\varepsilon_A^{\star 2}\right)\left(4\varepsilon_A^{\star 3} - 8\varepsilon_A^{\star 2} - \varepsilon_A^\star - 1\right) e^{-\varepsilon_A^\star}\right], \tag{2.8}$$

where the non-equilibrium effects of the reaction heat $Q_R^\star$ and activation energy $\varepsilon_A^\star$ are visible.

2.3 Detonation wave solution

In this section we present some details of the ZND theory, in order to clarify the adopted nomenclature. Then, we derive the governing equations for the description of the detonation wave solutions. Using these equations, we deduce the Rankine-Hugoniot conditions that connect the pre-reaction state ahead of the wave and any state within the reaction zone behind the wave, or even the final state.

2.3.1 Mathematical formulation

The closed hydrodynamic reactive system of governing Eqs. (2.4), (2.5), (2.6) and (2.7) define the mathematical analog of the detonation problem and is used to determine the steady detonation solution. It is well known

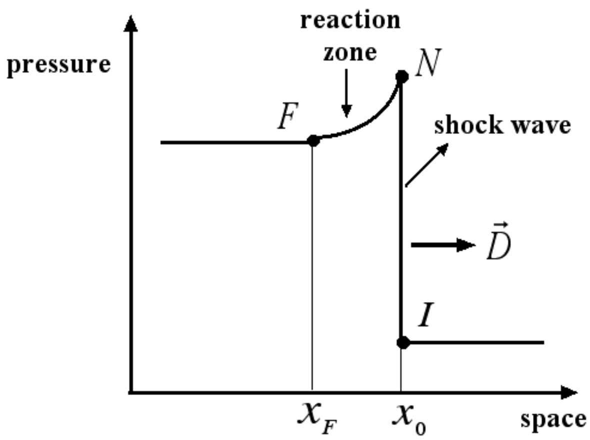

Figure 2.1: ZND configuration of a steady detonation wave profile for the mixture pressure.

that such hyperbolic equations, in their one-space-dimensional formulation,

admit steady traveling detonation wave solutions. These solutions describe a combustion regime in which a strong planar shock front ignites the mixture and the burning keeps the shock advancing and proceeds to equilibrium behind the shock.
The ZND idealized model, represented in Fig. 2.1, gives a good and accepted description of such detonation wave solutions, whose configuration consists of a leading, planar, non-reactive shock wave propagating with constant velocity, followed by a finite reaction zone where the chemical reaction takes place. With reference to the ZND model, the shock wave is assumed to propagate in the x-direction, from left to right, with velocity D. The shock front is located at $x = x_0$, and the reaction zone remains from x_0 to x_F. The state just behind the shock, located at $x = x_0$, is the von Neumann state N, where the chemical reaction is triggered, and the one located at $x = x_F$, at the end of the reaction zone, is the final state S, where the chemical reaction reaches equilibrium. Ahead of the shock front, that is for $x > x_0$, the quiescent mixture is at rest in its initial state I, where the rate of the chemical reaction is negligible. Inside the reaction zone, for $x_F < x < x_0$, the mixture evolves through their intermediate states R of partial reaction until reaching the final state.

2.3.2 One-dimensional steady states

Since the entire ZND configuration is steady in the shock attached frame, a new reference frame moving with the shock is considered and the normalized steady variable x_s is introduced, namely

$$x_s = \frac{x - Dt}{Dt_c}, \qquad t_c = \frac{1}{4n^+d^2}\sqrt{\frac{m}{\pi k T^+}}, \tag{2.9}$$

where the superscript $+$ refers to the initial state I and t_c is a characteristic time. For sake of simplicity, the normalized steady variable x_s is still denoted with the plane symbol x.

The mechanical and thermodynamical evolution of the detonating mixture is described by the hydrodynamic governing equations in its closed form, Eqs. (2.4), (2.5), (2.6) and (2.7) written in one-space-dimension,

$$\frac{\partial}{\partial t} n_A + \frac{\partial}{\partial x}(n_A v) = \tau_A, \tag{2.10}$$

$$\frac{\partial}{\partial t}(n_A + n_B) + \frac{\partial}{\partial x}((n_A + n_B)v) = 0, \tag{2.11}$$

$$\frac{\partial}{\partial t} v + \frac{1}{\varrho}\frac{\partial}{\partial x} p + v\frac{\partial}{\partial x} v = 0, \tag{2.12}$$

$$kT\frac{\partial}{\partial t} n + vkT\frac{\partial}{\partial x} n + \frac{5}{3} nkT\frac{\partial}{\partial x} v + \frac{2}{3}\sum_{i=A}^{B} E_i \tau_i = 0. \tag{2.13}$$

We should notice that this closed system of equations contitutes the set of the reactive Euler equations, where τ_A is given by expression (2.8). Then, to characterize steady detonation wave solutions, this system is transformed to the steady frame attached to the shock, namely

$$\frac{d}{dx}\Big[(v - D)\, n_A\Big] = Dt_c \tau_A, \tag{2.14}$$

$$\frac{d}{dx}\Big[(v - D)\,(n_A + n_B)\Big] = 0, \tag{2.15}$$

$$\frac{d}{dx}\Big[(v - D)\,\varrho v + nkT\Big] = 0, \tag{2.16}$$

$$\frac{d}{dx}\left[(v - D)\left(\frac{3}{2} nkT + \frac{\varrho v^2}{2} + E_A n_A + E_B n_B\right) + nkTv\right] = 0. \tag{2.17}$$

The spatial structure of the ZND detonation wave is determined by means of the Rankine-Hugoniot conditions, connecting the fluxes of the macroscopic quantities preserved across the shock front, together with the rate law, describing the advancement of the chemical process in the reaction zone. Accordingly, the conservative ODEs (2.15), (2.16) and (2.17) are integrated across the shock front, between the quiescent initial state $(n_A^+, n_B^+, 0, T^+)$ and an arbitrary state $\big(n_A(x), n_B(x), v(x), T(x)\big)$, $x \in [x_F, x_0]$, within the reaction zone, leading to the Rankine-Hugoniot conditions,

$$(n_A + n_B)(v - D) = -\left(n_A^+ + n_B^+\right) D, \tag{2.18}$$

$$\varrho v (v - D) + nkT = n^+ kT^+, \tag{2.19}$$

$$\left(\frac{3}{2}nkT + \frac{\varrho v^2}{2} + E_A n_A + E_B n_B\right)(v - D) + nkTv = -\left(\frac{3}{2}n^+ kT^+ + E_A n_A^+ + E_B n_B^+\right) D. \tag{2.20}$$

After some rearrangements, Eqs. (2.18), (2.19) and (2.20) take the form

$$n_B(n_A) = \frac{\left(n_B^+ + n_A^+\right) D}{D - v} - n_A, \tag{2.21}$$

$$T(n_A) = \frac{(D - v)\left(\varrho^+ Dv + n^+ kT^+\right)}{n^+ kD}, \tag{2.22}$$

$$v(n_A) = \frac{2Q_R^* n_A + 3\varrho^+ D^2 - 5n^+ kT^+ + \sqrt{P(n_A)}}{8\varrho^+ D}, \tag{2.23}$$

where

$$P(n_A) = \left(2Q_R^* n_A + 3\varrho^+ D^2 - 5n^+ kT^+\right)^2 - 32\varrho^+ Q_R^* D^2 \left(n_A - n_A^+\right). \tag{2.24}$$

The rate law comes from Eq. (2.14) in the form

$$\frac{d}{dx} n_A = \frac{D t_c \tau_A}{v - D + n_A \frac{dv}{dn_A}}, \tag{2.25}$$

and gives the x-evolution of the constituent number density n_A in the reaction zone, specifying the chemical composition of the reactive mixture. The algebraic equations (2.21), (2.22) and (2.23) together with the differential equation (2.25), with D and Q_R^* as parameters, characterize any arbitrary state within the reaction zone, in dependence of the initial state.

2.4 Numerical results and detonation profiles

In this section, we describe the numerical procedure implemented to determine the detonation solution, and present some representative results for the steady detonation problem. In the discussion, we give special attention to the influence of reaction heat on the results, in agreement with our announced objectives.

2.4.1 Numerical technique

The methodology for solving Eqs.(2.21), (2.22) and (2.23) and (2.25) comprises two steps. First, the von Neumann state N, just ahead the shock, is characterized by Eqs. (2.21), (2.22) and (2.23) together with a further jump condition of Rankine-Hugoniot type, which is consistent with the still unreacted character of the von Neumann state. This RH-condition is obtained by integrating across the shock the further conservative ODE resulting from the rate equation (2.25) with τ_A settled equal to zero. Then, in the second step, all the intermediate states inside the reaction zone ($x_0 < x < x_F$), as well as the final state at the end of the reaction zone ($x = x_F$), are obtained by integrating the rate equation (2.25) with initial condition at the von Neumann state, using a fourth order Runge-Kutta routine, and then solving the algebraic Eqs. (2.21), (2.22) and (2.23) for the considered state. In particular, the equilibrium final state is obtained when the above referred integration gives a vanishing reaction rate τ_A. This final state x_F is defined in the numerical computations by the value x for which $\frac{dn_A}{dx} = 10^{-6}$.

The detonation problem is numerically solved for both types of exothermic and endothermic chemical reaction and some simulations are performed for one elementary reaction of the chain branching of a theoretical detonating mixture. We have presented a preliminary analysis in paper [13]. The detonation velocity D and the kinetic and thermodynamical reference input parameters are assumed as follows

$$
\begin{aligned}
&D\!=\!1700\,ms^{-1}, \quad n_A^+ = 0.35\,mol/l, \quad n_B^+ = 0\,mol/l, \quad \varepsilon_A^\star = 7.5, \\
&m = 0.01\,Kg/mol, \quad T^+ = 298.15\,K, \quad E_A = 2400. \qquad (2.26)
\end{aligned}
$$

Figures 2.2, 2.3, 2.4 and 2.5 show some representative steady detonation profiles for the number density n, temperature T, mean velocity v and mixture pressure p, respectively, in dependence of the algebraic distance behind the shock wave. The left frames of these figures refer to two exothermic chemical reactions with reaction heat $Q_R^* = -2$ and $Q_R^* = -1$. Conversely, the right frames refer to two endothermic chemical reactions with reaction heat $Q_R^* = 1$ and $Q_R^* = 2$. One can extract from these figures that the extent of the reaction zone is larger when the reaction heat Q_R^* has greater magnitude (dashed lines). This is an expected feature, in agreement with other numerical and experimental works, see [78], for example. Moreover, the n, v and p profiles of Figs. 2.2, 2.4 and 2.5 show that the steady detonation solution is a reactive rarefaction wave for an exothermic reaction (left frames) and a reactive compression wave for an endothermic reaction (right frames). Concerning the temperature, Fig. 2.3 shows that the steady detonation solution is a reactive compression wave for an exothermic reaction (left frame) and a reactive rarefaction wave for an endothermic reaction (right frame). The left frames reproduce the typical configuration of an overdriven steady detonation wave arising in a real explosive gas mixture with one exothermic chemical reaction [33, 34]. On the other hand, the right frames replicate the essential features of the dynamics of the endothermic stage of a typical chain-branching reactive gas mixture with pathological detonation, more specifically, the branch between the so called pathological point and the strong final state of a overdriven detonation [33, 34, 73, 75].

The value of the macroscopic variables in the final state x_F were also analyzed for the reaction heat in the range $-2 < Q_R^\star < 2$. In Figs. 2.6

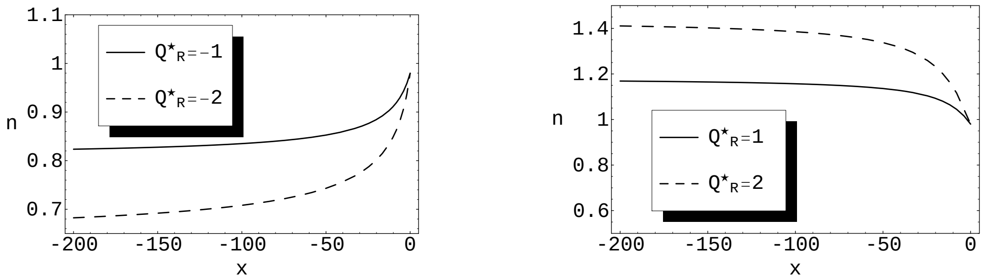

Figure 2.2: Steady detonation profile for the mixture number density n. *Left:* exothermic chemical reaction with $Q_R^\star = -1$ (solid line) and $Q_R^\star = -2$ (dashed line). *Right:* endothermic chemical reaction with $Q_R^\star = 1$ (solid line) and $Q_R^\star = 2$ (dashed line).

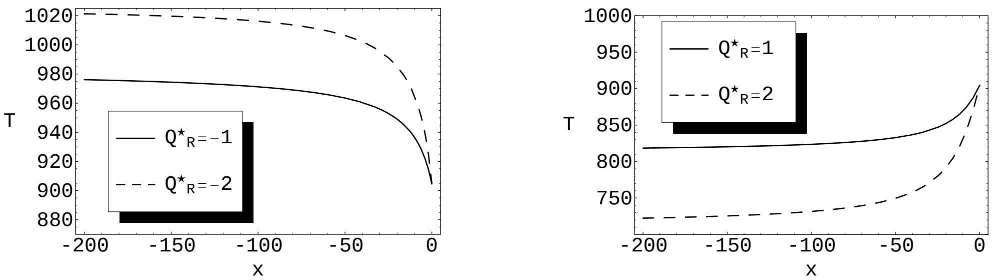

Figure 2.3: Steady detonation profile for the mixture temperature T. *Left:* exothermic chemical reaction with $Q_R^\star = -1$ (solid line) and $Q_R^\star = -2$ (dashed line). *Right:* endothermic chemical reaction with $Q_R^\star = 1$ (solid line) and $Q_R^\star = 2$ (dashed line).

and 2.7 we can see that the number density, pressure and velocity are larger for greater values of $Q_R^\star$. The temperature shows an opposite behavior, with lower values for greater values of $Q_R^\star$. These results are in agreement with the trend shown in the corresponding detonation profiles of the previous Figs. 2.2, 2.3, 2.4 and 2.5 for the particular values of the reaction heat $Q_R^\star = -2, -1, 1, 2$. Furthermore, the dependence of these macroscopic variables on the reaction heat is not linear. In fact, the number density and temperature at the final state show a more pronounced behavior for greater values of the reaction heat, whereas the mean velocity and pressure show a more pronounced behavior for lower values of the reaction heat.

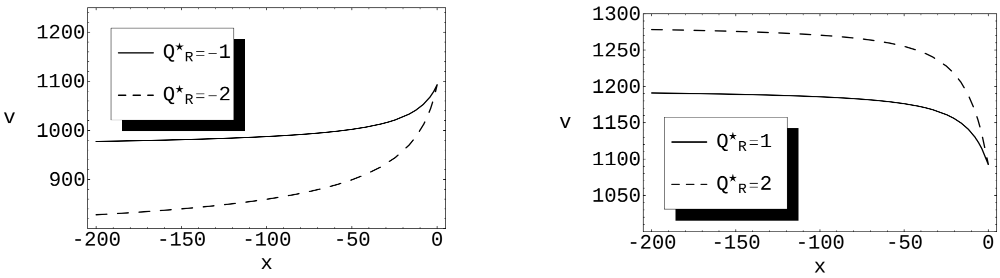

Figure 2.4: Steady detonation profile for the mixture mean velocity v. *Left:* exothermic chemical reaction with $Q_R^\star = -1$ (solid line) and $Q_R^\star = -2$ (dashed line). *Right:* endothermic chemical reaction with $Q_R^\star = 1$ (solid line) and $Q_R^\star = 2$ (dashed line).

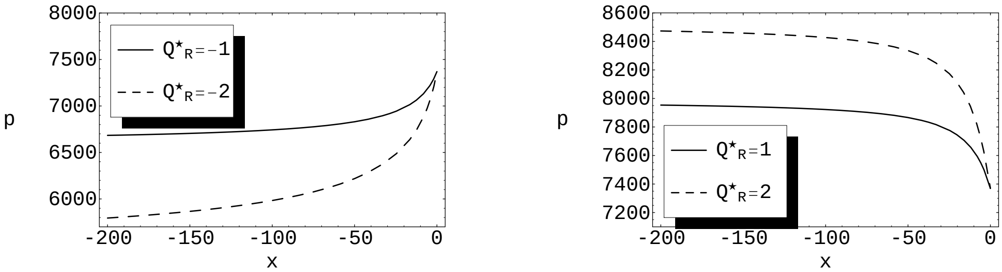

Figure 2.5: Steady detonation profile for the mixture pressure p. *Left:* exothermic chemical reaction with $Q_R^\star = -1$ (solid line) and $Q_R^\star = -2$ (dashed line). *Right:* endothermic chemical reaction with $Q_R^\star = 1$ (solid line) and $Q_R^\star = 2$ (dashed line).

2.5 Final remarks

The propagation of steady detonation waves within kinetic theory of chemically reacting gases has been investigated in some previous works [22, 23], starting from the system of reactive Euler equations in a specific chemical regime, together with the related Rankine-Hugoniot conditions. However, the effects of the reaction heat on the behavior of the detonation wave solutions has been disregarded, since the considered kinetic model does not include the deviations on the Maxwellian distributions induced by the heat of the chemical process. In the present work, with reference to the kinetic model

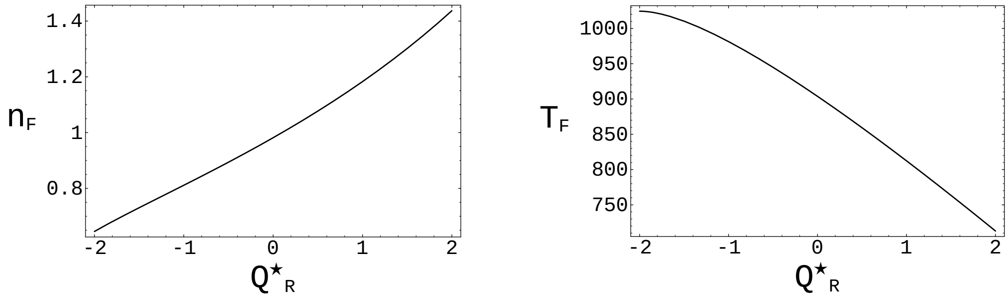

Figure 2.6: *Left:* Number density at the final stage as a function of $Q_R^\star$, $n_F(Q_R^\star)$ *Right:* Temperature at the final stage as a function of $Q_R^\star$, $T_F(Q_R^\star)$

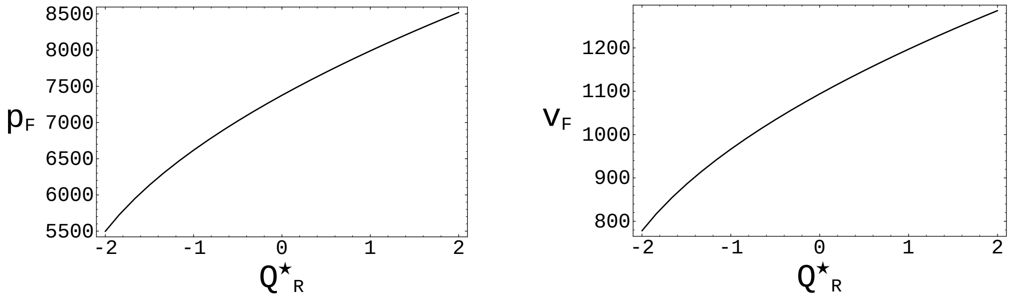

Figure 2.7: *Left:* Pressure at the final stage as a function of $Q_R^\star$, $p_F(Q_R^\star)$ *Right:* Gas mixture velocity at the final stage as a function of $Q_R^\star$, $v_F(Q_R^\star)$

of paper [49], and using a similar procedure to the one employed in papers [22, 23], we study the propagation of steady detonation waves. Our main objective is to investigate the influence of the reaction heat on such type of solutions and, in particular, to analyze how the structure of the wave solution varies with the reaction heat.

As discussed in previous papers about the non-equilibrium effects induced by the chemical reaction [77], the reaction heat changes the Maxwellian distribution function and therefore it has a significant influence in the description of the reactive mixture. Thus, it seems important to include the contribution of the reaction heat on the structure of the detonation wave solution. This feature is reflected in the present study and constitutes a major result for our study about detonation wave solutions.

Chapter 3

Linear Stability of the steady detonation wave

This chapter is dedicated to the linear hydrodynamic stability of the steady detonation wave studied in Chapter 2. There, the influence of the reaction heat on the steady wave profile was analyzed. Following a similar line of study, in this chapter we investigate the influence of the reaction heat on the linear stability of the steady detonation solution. Moreover, we dedicate special attention to the effects of the activation energy on the stability spectrum.

We begin with a brief description of the stability problem and some of its main developments, in order to introduce the relevant aspects of the subject. Then, in Section 3.2, the governing equations in the perturbed shock frame are explicitly derived and the stability problem for the eigenfunctions and growth rate perturbation is formulated. The radiation condition used to close the perturbed equations is also presented. In Section 3.3 the numerical technique used in the simulations is described and some representative computational results for the stability behavior in the parameter space are given and discussed.

The study developed in this chapter, as well as the results here presented, have been published in papers [14, 15].

3.1 Background and motivation

In this section we introduce the stability problem and present some of the most important ideas and developments of the subject. With this introduction we intend to explain the importance of the problem itself and the motivation for the kinetic approach here adopted.
Experimental and computational studies show that the detonation tends to be structurally unstable and that the instabilities propagate in a quasi-periodic oscillating manner [33, 54]. The reaction zone behind the shock is extremely sensitive to small rear boundary perturbations and, as a result, the detonation wave presents, in general, an unstable configuration.
The dynamics of such propagating instabilities can provide useful information about the unsteady structure and elucidate about the detonation mechanism. The usual first step is a hydrodynamic stability analysis of the steady detonation solution. Assuming that the perturbations are small, a linearized theory is used to describe their evolution and determine the instability modes. The results of this linear analysis are relevant for detonation waves in channels or square tubes and give important information about the growth rate of the instabilities and the influence of the detonation parameters in the instability behavior [1, 76].
An extensive and valuable study of the linear stability problem was developed by Erpenbeck using a Laplace transform approach and a numerical technique based on the Nyquist-winding theorem to determine the number of unstable solutions [28, 30]. The works by Abouseif and Toong [1, 2], Buckmaster, Ludford and Neves [10, 11], and Majda and Rosales [56] gave important analytical and numerical contributions for the physical interpretations of the instability behavior.
A further relevant contribution to the linear detonation stability was given by

Lee and Stewart in paper [53], using a normal mode approach and a numerical shooting technique to find the unstable modes. An extensive literature based on similar approaches and using rather sophisticated numerical techniques, include, among others, the papers [8, 37, 44, 45, 47, 55, 58, 61, 72, 78, 79, 82] for ZND detonation, and [73, 74, 75, 79] for pathologic-type detonations. Modern computer facilities allowed to produce several experimental and computational studies, as for example those of papers [3, 21, 26, 62].
Although a linear stability analysis can describe some relevant physical effects of the perturbations [1], it requires that the steady character of the detonation wave can only be slightly perturbed and therefore its validity is restricted to the initial stage of very small amplitude oscillations. A nonlinear stability analysis is needed for detonation waves whose structure is very far from that of the steady wave. A typical case is the curved detonation wave propagating through an unconfined material, for which more real effects of multi-dimensional instabilities are observed, such as bifurcations to multi-mode and irregular oscillations, and "diamond" or "fish scale" patterns are produced [54, 76].
The hydrodynamic linear stability of steady detonation waves, concerning the detonation stability analysis in the context of the kinetic theory for chemically reactive gas mixtures, has been investigated for the first time in paper [6]. The emphasis of this paper is on the mathematical formulation and solutions to the stability problem in the kinetic frame, for a quaternary gas mixture with a reversible bimolecular chemical reaction. Some numerical results and visualizations are shown regarding the time evolution of the eigenfunctions for both instability and stability pictures as well as at conditions of neutral stability. However, the considered kinetic modeling does not include the effects of the reaction heat neither those of the activation energy, therefore the stability picture remains incomplete.
In this chapter, starting from the kinetic formulation proposed in [6], we investigate linear stability of the steady detonation solution characterized

in Chapter 2. The main objective is to develop a detailed hydrodynamic stability analysis, and investigate the influence of the reaction heat and activation energy on the stability behavior. A first contribution in this direction was presented in paper [14], where some numerical simulations have been shown about the structure of the detonation wave and its linear stability. This preliminary stability analysis was then expanded and detailed in paper [15] exploiting the non-equilibrium effects due to the heat of the chemical reaction.

Both the mathematical formulation of the stability problem and the numerical method of solution are explained in detail in this chapter. Some numerical simulations are performed and the results are presented and discussed.

3.2 Formulation of the linear stability problem

In this section we formulate the one dimensional linear stability problem. This is considered the standard preliminary step of any formal treatment of stability analysis [82]. We want to investigate the effect of a small rear boundary perturbation in the steady configuration of the detonation wave solution. The rear perturbation induces a deviation in the shock wave position which, in turn, affects the steady character of the detonation wave solution. In particular, the state variables in the reaction zone are perturbed. The evolution of these perturbations determines the stability of the steady detonation solution. More in detail, when any perturbation grows in time, the steady solution is said to be hydrodynamically unstable, and if all perturbations decay in time, the steady solution is stable. A normal mode approach is assumed for the perturbations and the growth or decay of the disturbances are determined by the complex eigenvalues of the stability equations. We are not interested in the eigenvalues with negative real part

because they represent perturbations that decay in time and therefore do not add any important information about the instabilities. Conversely, the existence of eigenvalues with positive real part means that the perturbations grow in time. Consequently, a steady solution is unstable if it admits at least one eigenvalue with positive real part, which is called an instability mode.
From the mathematical point of view, the hydrodynamic stability problem requires the transformation to the perturbed shock attached frame, and then the linearization of the governing equations and Rankine-Hugoniot shock conditions around the steady detonation solution. This will be done in the next subsection, adopting the normal mode approach first proposed by Lee and Stewart in paper [53] and then followed by several authors, see for example paper [82] and the references therein cited.

3.2.1 Governing equations in the perturbed shock frame

The mathematical analog is defined by the stability equations derived from the one-space dimensional version of the hydrodynamic equations, see Eqs. (2.10), (2.11), (2.12) and (2.13), through a linearization around the steady solution assuming an exponential time-dependence for the perturbations. First, we introduce dimensionless time and space variables into the hydrodynamic equations (2.10), (2.11), (2.12) and (2.13) defined by $t_a = t/t_c,\ \ y = x/Dt_c$. For sake of simplicity, we relabel the new time coordinate t_a with the previous symbol t.
The following step consists in transforming the resulting equations to the perturbed shock attached frame. In order to do so we introduce the shock front displacement from the unperturbed position, $\widetilde{\psi}(t)$, so that the perturbed shock is located at $\psi(t) = Dt + \widetilde{\psi}(t)$ and its velocity is $D(t) = D + \widetilde{\psi}\,'(t)$. Note that the considered wave coordinate, $x = y - \psi(t)$, measures the distance from the perturbed shock and the instantaneous position of the perturbed shock wave is $x = 0$ in the new shock-attached coordinate system. The

corresponding transformed equations are

$$D\frac{\partial}{\partial t}n_A + \left(v - D - D\frac{d}{dt}\widetilde{\psi}(t)\right)\frac{\partial}{\partial x}n_A + n_A\frac{\partial}{\partial x}v = Dt_c\tau_A, \quad (3.1)$$

$$D\frac{\partial}{\partial t}n + \left(v - D - D\frac{d}{dt}\widetilde{\psi}(t)\right)\frac{\partial}{\partial x}n + n\frac{\partial}{\partial x}v = 0, \quad (3.2)$$

$$\varrho D\frac{\partial}{\partial t}v + \frac{\partial}{\partial x}p + \varrho\left(v - D - D\frac{d}{dt}\widetilde{\psi}(t)\right)\frac{\partial}{\partial x}v = 0, \quad (3.3)$$

$$D\frac{\partial}{\partial t}p + \frac{5p}{3}\frac{\partial}{\partial x}v + \left(v - D - D\frac{d}{dt}\widetilde{\psi}(t)\right)\frac{\partial}{\partial x}p = \frac{Q_R D t_c \tau_A}{3}. \quad (3.4)$$

The next step consists in the linearization of the transformed hydrodynamic equations around the steady state, assuming a normal mode expansion, for the state variables n_A, n_B, v and p, with exponential time dependent perturbations. Introducing the state vector z defined by $z = [n_A \;\; n \;\; v \;\; p]^T$, the expansions are assumed in the form

$$z(x,t) = z^*(x) + e^{at}\,\overline{z}(x), \qquad \psi(t) = \overline{\psi}e^{at}, \qquad a, \overline{\psi} \in \mathbb{C}, \quad (3.5)$$

where $z^*(x)$ represents the steady solution and $\overline{z}(x)$ the unknown space disturbances, with $\overline{z} \in \mathbb{C}$. Moreover, $\overline{\psi}$ is a perturbation parameter and $a = \alpha + i\beta$, with α being the perturbation growth rate and β the perturbation frequency. Since the assigned perturbations are small, the transformed governing equations in the perturbed shock frame are linearized about the steady solution $z^*(x)$, by means of the expansions (3.5). Performing a further normalization of the state variables with respect to the complex amplitude parameter $\overline{\psi}$, namely $\overline{w} = \overline{z}/\overline{\psi}$, one obtains the evolution equations in the wave coordinate x, for the complex disturbances. Rewriting $\overline{z}$ instead of $\overline{w}$, the resulting equations, for $x \in]x_F, 0[$, are

$$Da\overline{n}_A + (v^* - D)\,\frac{d}{dx}\overline{n}_A + (\overline{v} - Da)\,\frac{d}{dx}n_A^* + \overline{n}_A\frac{d}{dx}v^* + n_A^*\frac{d}{dx}\overline{v} = \overline{\tau}_A, \tag{3.6}$$

$$Da\overline{n} + (v^* - D)\,\frac{d}{dx}\overline{n} + (\overline{v} - Da)\,\frac{d}{dx}n^* + \overline{n}\frac{d}{dx}v^* + n^*\frac{d}{dx}\overline{v} = 0, \tag{3.7}$$

$$\varrho^* Da\overline{v} + \frac{d}{dx}\overline{p} + \varrho^*(\overline{v} - Da)\,\frac{d}{dx}v^* + \overline{\varrho}\,(v^* - D)\,\frac{d}{dx}v^* + \varrho^*(v^* - D)\,\frac{d}{dx}\overline{v} = 0, \tag{3.8}$$

$$Da\overline{p} + \frac{5}{3}\left(p^*\frac{d}{dx}\overline{v} + \overline{p}\frac{d}{dx}v^*\right) + (v^* - D)\frac{d}{dx}\overline{p} + (\overline{v} - Da)\frac{d}{dx}p^* = \frac{Q_R^* Dt_c\overline{\tau}_A}{3}. \tag{3.9}$$

In the above equations, $\overline{\tau}_A$ denotes the linearized reaction rate perturbation of constituent A, given by

$$\overline{\tau}_A = -4d_r^2\sqrt{\frac{\pi k}{m}}e^{-\epsilon^\star}\left[\left(2n_A^*\overline{n}_A\sqrt{T^*} + \frac{\overline{p} + \frac{\overline{n}}{n^*}p^*}{2n^*k\sqrt{T^*}}{n_A^*}^2\right)\left(1 + \epsilon^\star + \Gamma {x_A^*}^2\right) + 2\sqrt{T^*}\frac{{n_A^*}^3}{n^*}\left(-n_A^*\overline{n}_B + n_B^*\overline{n}_A\right)\right], \tag{3.10}$$

where

$$\Gamma = \frac{1}{128}\left(\frac{d}{d_r}\right)^2 Q_R^\star\left(1 + Q_R^\star + Q_R^\star\varepsilon_A^\star + \varepsilon_A^\star - 2\varepsilon_A^{\star 2}\right)\left(4\varepsilon_A^{\star 3} - 8\varepsilon_A^{\star 2} - \varepsilon_A^\star - 1\right)e^{-\varepsilon_A^\star}.$$

Equations (3.6), (3.7), (3.8) and (3.9) constitute the stability equations for the present modeling, giving the spatial evolution of the complex perturbations $\overline{z}(x)$ in the reaction zone, from the perturbed shock position $x=0$ to the equilibrium final state $x=x_F$. They constitute a system of eight first-order homogeneous linear ordinary differential equations with spatially varying coefficients, for the real and imaginary parts of the complex perturbations.

3.2.2 Initial conditions

The initial conditions to be joined to the stability equations (3.6), (3.7), (3.8) and (3.9) are the linearized perturbed Rankine-Hugoniot relations which connect the value of the disturbances at the von Neuman state to their zero value ahead the perturbed shock. They are provided by the Rankine-Hugoniot relations (2.18), (2.19) and (2.20) together with the further jump condition for the von Neuman state obtained as explained in Subsection 2.3.2. After transforming to the wave coordinate, linearizing around the steady state and normalizing with respect to $\overline{\psi}$, the resulting jump conditions at the von Neuman state are obtained in the form

$$\overline{n}_i(0) = \frac{\left(n_i^* - n_i^+\right) a - n_i^* \overline{v}(0)}{v^* - D}, \qquad i = A, B, \tag{3.11}$$

$$\overline{v}(0) = \frac{3\varrho^+ v^{*2} + \frac{3}{2}\left(p^* - p^+\right) - \frac{3}{2} D \varrho^+ v^* + 2E_A n^+ + Q_R^* n_B^+}{-\varrho^* \left(v^* - D\right)^2 + \frac{5}{2} p^*}\, a, \tag{3.12}$$

$$\overline{p}(0) = -\varrho^+ a v^* - \left(v^* - D\right) \varrho^* \overline{v}(0). \tag{3.13}$$

Equations (3.11), (3.12) and (3.13) give the initial conditions for the stability equations (3.6), (3.7), (3.8) and (3.9). The stability system involves the complex parameter a and thus, the system is not closed.

3.2.3 Closure condition

The required closure condition, which gives the dispersion relation for the normal modes (3.5), is the acoustics radiation condition adopted in many previous works on detonation stability as, for example, in papers [6, 10, 37, 45, 53, 78, 82]. Such condition states that the inherent instability of the detonation wave solution results exclusively from the interplay between the leading shock and the reaction zone and cannot be affected by further disturbances traveling towards the shock from a great distance from the reaction zone. Thus the closure condition is a boundary condition assigned at the equilibrium final state as

$$\overline{v}(x_F) + a = \frac{-1}{\gamma \varrho_{eq}^* c_{eq}^*}\, \overline{p}(x_F), \tag{3.14}$$

where γ is the ratio of specific heats, c^*_{eq} and ϱ^*_{eq} the isentropic sound speed and gas mixture density at the equilibrium final state, for $x = x_F$. Equation (3.14) is usually regarded as the necessary condition to define the dynamics of the complex growth rate a. It was originally derived in paper [10] through an acoustic analysis performed at the end of the reaction zone. Important discussions about the closure condition and detailed derivations can be found in papers [45, 53, 82], for example. These papers show that the closure condition can be alternatively derived following two distinct approaches, one being physically based on an accurate acoustic analysis and another one being justified by a boundedness condition which requires that the asymptotic structure of the perturbed solution is independent from elementary unbounded solutions. Different closure conditions can be imposed to assure the determinacy of the stability problem, as for example a piston-type condition which requires the vanishing of the velocity perturbation at a piston located far downstream of the shock wave. However, as discussed in paper [45], the further interaction of the piston with the shock wave would alter the instability spectrum leading to different stability results in comparison to those coming from the intrinsic mechanism between the shock wave and the reaction zone.

Concluding this section, the one-dimensional linear stability problem of the steady detonation is formulated in terms of the complex disturbances $\overline{z}(x)$ and complex growth rate a, by means of the ordinary differential equations (3.6), (3.7), (3.8) and (3.9) for $x \in]x_F, 0[$, with initial conditions (3.11), (3.12) and (3.13) at $x = 0$ and closure condition (3.14) at $x = x_F$. This problem will be treated numerically as described in the next section.

3.3 Numerical treatment of the stability problem

The stability problem is treated numerically with the aim of obtaining an extensive investigation of the stability spectrum for the eigenfunction perturbations $\overline{z}$ and eigenvalue perturbation parameter a, in terms of the parameters characterizing the steady solution. For a given set of thermodynamical and chemical parameters describing the steady detonation solution, the disturbances $\overline{z}(x)$ and perturbation parameter a are determined applying an iterative shooting technique based on the numerical method proposed by Lee and Stewart in paper [53].

3.3.1 Discussion on the numerical scheme

A trial value of a in a fixed bounded domain $\mathcal{R}$ of the complex plane is considered and then equations (3.6), (3.7) and (3.8) are integrated in the reaction zone $]x_F, 0[$ with initial conditions (3.11), (3.12) and (3.13) at $x = 0$, using a fourth order Runge-Kutta routine. The solution $\overline{z}(x)$, $x \in [x_F, 0]$, obtained for the considered trial value of a is then specialized for $x = x_F$ to inquire if the boundary condition (3.14) is verified. However, for a given steady detonation solution, an arbitrary value of a does not satisfy the closure condition (3.14) and thus it does not produce a solution of the stability problem. To overcome this difficulty, the residual function $\mathcal{H}(a)$, defined from the closure condition (3.14) by the expression

$$\mathcal{H}(a) = \overline{v}(x_F) + a + \frac{1}{\gamma \varrho_{eq}^* c_{eq}^*} \, \overline{p}(x_F), \quad a \in \mathcal{R}, \tag{3.15}$$

is estimated at each trial value of a. Only those solutions $\overline{z}(x)$ obtained for values of a for which the residual function $\mathcal{H}(a)$ vanishes within a given tolerance are accepted. The search for trial values of the complex parameter a constitutes the key problem in the stability analysis. There exist some numerical techniques to search for these values, as for example those used by Erpenbeck in papers [28, 30] and by Lee and Stewart in paper [53]. However, in the present study, a different numerical scheme is proposed, recovering the Erpenbeck's idea of counting the number of zeros of $\mathcal{H}$ in a fixed domain of the complex plane, combined with the shooting method proposed by Lee and Stewart.

In some situations we only need to know if there exist any instability mode since, as we mentioned before, the existence of one instability mode is enough to conclude that the steady detonation wave is hydrodynamically unstable. In these situations, it is sufficient to implement the search procedure just once to know if the steady detonation wave is hydrodynamically unstable.

To be able to identify the instability modes, and determine the growth rate and frequency, we use a three-dimensional plot of $|\mathcal{H}|$. In order to construct a suitable plot of $|\mathcal{H}|$ it is necessary to define a thin grid in the region $\mathcal{R}$ and then estimate the value of $|\mathcal{H}|$ in each point of the grid. The number of trial points where we need to evaluate $|\mathcal{H}|$ vary with the size of the region $\mathcal{R}$. In order to reduce the number of trial points, and thus reduce both the computational effort and the time spent in the identification of the instability modes, the three-dimensional plot of $|\mathcal{H}|$ is constructed in a considered refinement of $\mathcal{R}$ in which there are at least one instability mode. This refinement is obtained through an iterative manner by using successively the numerical procedure in different subregions of $\mathcal{R}$.

3.3.2 Numerical technique

Instability modes correspond to a positive growth rate $\mathrm{Re}\, a$, so that the zeros of the residual function $\mathcal{H}$ are searched in a domain $\mathcal{R}$ on the right half of the complex plane. On the other hand, since these modes occur in conjugate pairs, it is enough to choose a domain $\mathcal{R}$ in the upper-right quarter of the complex plane.

The numerical method proposed in this work provides a rapid and efficient procedure to investigate if the domain $\mathcal{R}$ contains any zero of $\mathcal{H}$, meaning that the corresponding detonation solution is unstable. Moreover, the effective determination of the approximate locations of the zeros of $\mathcal{H}$ in the domain $\mathcal{R}$, and the identification of the corresponding growth rate $\operatorname{Re} a$ and frequency $\operatorname{Im} a$, requires a further refinement of the domain $\mathcal{R}$ as well as a three-dimensional plot of $|\mathcal{H}|$ in the refinement.

Preliminaries. The argument principle used by Erpenbeck in paper [30], combined with the shooting method proposed by Lee and Stewart in paper [53], is adopted here to count the number of zeros of the residual function $\mathcal{H}$ and approximate their location. This principle states that the difference between the number Z of zeros and P of poles of the function $\mathcal{H}$ within the region $\mathcal{R}$, provided that there are no zeros in its contour, is given by

$$Z - P = \frac{1}{2\pi i} \int_{\zeta} \frac{\mathcal{H}'(u)}{\mathcal{H}(u)}\, du, \tag{3.16}$$

or equivalently by

$$Z - P = \frac{1}{2\pi i} \int_{k}^{\ell} \frac{\mathcal{H}'(\zeta(t))}{\mathcal{H}(\zeta(t))} \parallel \zeta'(t) \parallel dt, \tag{3.17}$$

where $\zeta : [k, \ell] \to \mathbb{C}$ is a path smooth by parts, describing the contour of $\mathcal{R}$ in the positive sense. Since $\mathcal{H}$ has no poles in the complex plane, one has $P = 0$ and the expression (3.17) gives the number of zeros of $\mathcal{H}$ inside the region $\mathcal{R}$, that is

$$Z = \frac{1}{2\pi i} \int_{k}^{\ell} \frac{\mathcal{H}'(\zeta(t))}{\mathcal{H}(\zeta(t))} \parallel \zeta'(t) \parallel dt. \tag{3.18}$$

It is important to note that the requirement that the residual function $\mathcal{H}$ has no zeros in the contour of $\mathcal{R}$ does not constitute an actual limitation for the application of expressions (3.18) in the present numerical computation. In fact, the method starts with the residual values $\mathcal{H}(a_j)$ for a very huge number of points a_j in the contour of $\mathcal{R}$. If there is any zero of $\mathcal{H}$ in the contour of $\mathcal{R}$ then, at least one of the considered points a_j should be close enough to this zero and the location of such point allows to identify the zero without using any further strategy.

General description of the numerical technique. The starting point for the implementation of the numerical technique is the random selection of a great number of trial values for the perturbation parameter a in the contour of a fixed domain $\mathcal{R}$, say a_j, $j = 1, 2, \ldots, n$, such that $a_j = \zeta(t_j)$, for $j = 1, 2, \ldots, n$. Then the integral in expression (3.18) is estimated using a rather cumbersome procedure. More in detail, the mean value theorem gives

$$\int_k^\ell \frac{\mathcal{H}'(\zeta(t))}{\mathcal{H}(\zeta(t))} \parallel \zeta'(t) \parallel dt = \mu(\ell - k), \tag{3.19}$$

where μ represents the mean value in the interval $[k, \ell]$ of the function $h : [k, \ell] \to \mathbb{R}$ defined by

$$h(t) = \frac{\mathcal{H}'(\zeta(t))}{\mathcal{H}(\zeta(t))} \parallel \zeta'(t) \parallel, \quad t \in [k, \ell]. \tag{3.20}$$

The mean value μ of h, in turn, is approximated with the mean value μ_S of the set

$$S = \left\{ \frac{\mathcal{H}'(\zeta(t_j))}{\mathcal{H}(\zeta(t_j))} \parallel \zeta'(t_j) \parallel : \ j = 1, 2, \ldots, n \right\}. \tag{3.21}$$

The derivative $\mathcal{H}'(\zeta(t_j)) = \mathcal{H}'(a_j)$ is estimated by choosing a suitable point close enough to a_j, say b_j, with Re $b_j =$ Re $a_j + 10^{-6}$ and Im $a_j =$ Im b_j, as follows

$$\mathcal{H}'(a_j) \approx \frac{\mathcal{H}(b_j) - \mathcal{H}(a_j)}{b_j - a_j}, \quad j = 1, 2, \ldots, n. \tag{3.22}$$

Moreover, it is well known that if n is large enough, then the mean value of the sample S, μ_S, can be treated as a statistical variable following a normal distribution with mean value μ and standard deviation $\sigma_S/\sqrt{n}$, with σ_S being the standard deviation of S. Therefore, the mean value μ of the function h

can be inferred in a confidence interval by the mean value μ_S of the sample S. The amplitude of the confidence interval can be reduced enlarging, as much as necessary, the number n of points in the set S. Here, all the calculations have been performed with a confidence level of 99%. Consequently, the number of zeros of the residual function $\mathcal{H}$ inside the domain $\mathcal{R}$ is estimated as follows

$$\frac{\ell - k}{2\pi i}\left(\mu_S - 2.58\,\frac{\sigma_S}{\sqrt{n}}\right) < Z < \frac{\ell - k}{2\pi i}\left(\mu_S + 2.58\,\frac{\sigma_S}{\sqrt{n}}\right). \tag{3.23}$$

3.3.3 Numerical solution

Having the above preliminary ideas in mind, the numerical solution of the stability problem is determined through the following steps.

Step 1 (choice of the domain $\mathcal{R}$). A bounded domain $\mathcal{R}$ in the upper-right complex plane is considered, and a path $\zeta : [k, \ell] \to \mathbb{C}$, which is smooth by parts and describes the contour of $\mathcal{R}$ in the positive sense, is fixed.

Step 2 (selection of the trial values for a). A great number of points, say a_j with $j = 1, \dots, n$, are selected at random in the contour of $\mathcal{R}$. For each point a_j, one determines the unique point $t_j \in [k, \ell]$ such that $a_j = \zeta(t_j)$. Moreover, for each point a_j one chooses another point close enough, say b_j, such that $\text{Re}\ b_j = \text{Re}\ a_j + 10^{-6}$ and $\text{Im}\ a_j = \text{Im}\ b_j$, for $j = 1, \dots, n$.

Step 3 (integration of the ODE's). Assuming each point a_j and b_j, for $j = 1, \dots, n$, as a trial value for the perturbation parameter a, the differential equations (3.6), (3.7), (3.8) and (3.9) are integrated with initial conditions (3.11), (3.12) and (3.13), using a fourth order Runge-Kutta routine.

Step 4 (evaluation of the residual function). The solutions $\overline{z}(x)$, $x \in [x_F, 0]$, obtained in the previous step for the considered trial values a_j and b_j are used to evaluate the residual function $\mathcal{H}$ defined by expression (3.15) at each point a_j and b_j, for $j = 1, \dots, n$.

Step 5 (estimation of the derivative of the residual function). The derivative $\mathcal{H}'(a_j)$ is estimated with the quotient between the differences $\mathcal{H}(b_j) - \mathcal{H}(a_j)$ and $b_j - a_j$, as indicated in Eq. (3.22).

Step 6 (mean value of the sample S). The mean value μ_S of the sample S introduced in expression (3.21) is evaluated as the mean value of a statistical variable following a normal distribution with standard deviation given by $\sigma_S/\sqrt{n}$, where σ_S is the standard deviation of S.

Step 7 (mean value of the function h). The mean value μ of the function h defined by expression (3.20) is inferred from the mean value μ_S of the sample S, using a 99% confidence interval.

Step 8 (estimation of the number of zeros of $\mathcal{H}$). The integral in Eq. (3.18) is approximated by the quantity $(k - \ell)\mu$. The number of zeros of the residual function $\mathcal{H}$ within the region $\mathcal{R}$ is approximated using the estimation (3.23). The amplitude of the interval can be controlled by the number n of points in the set S in such a way that there is only one integer in the interval.

3.3.4 Remarks on the numerical approach

A direct approach such as the representation of the three-dimensional plot of $|\mathcal{H}|$ in all region $\mathcal{R}$ would give the necessary information for the stability study, since it would allow to identify all the zeros of $\mathcal{H}$ in $\mathcal{R}$. However, as we said before, in order to obtain a suitable plot of $|\mathcal{H}|$, it would be necessary a really great number of trial points in the region $\mathcal{R}$. This number is much larger then the number of trial points that are needed to count the number of zeros in the same region (*Step 2*). The procedure that we propose here is not direct but allows the obtainment of valuable results in much less time.
In some situations it is only required to know if there is any eigenvalue in the region $\mathcal{R}$. In these situations the procedure gives all the needed information. Conversely, in those situations in which it is necessary to determine the zeros of $\mathcal{H}$, we combine this search procedure with a three-dimensional plot of

$|\mathcal{H}|$. We start in region $\mathcal{R}$ and count the number of zeros of $|\mathcal{H}|$. If there are no zeros we conclude that the detonation wave is stable in the region parameter $\mathcal{R}$. On the other hand, if there is at least one zero, then the detonation is unstable and we may identify this zero. Next we split the region $\mathcal{R}$ into two different subregions, $\mathcal{R}_1$ and $\mathcal{R}_2$, and use the search procedure in subregion $\mathcal{R}_1$. This allows to count the zeros in this subregion. At the same time, it allows to count the remaining zeros in $\mathcal{R}_2$. This method is used iteratively, excluding subregions of $\mathcal{R}$ that have no zeros of $\mathcal{H}$ and obtaining smaller subregions of $\mathcal{R}$ with at least one zero of $\mathcal{H}$. After some iterations we obtain subregions of $\mathcal{R}$ that are much smaller then $\mathcal{R}$ and we plot a three-dimensional representation of $|\mathcal{H}|$ in these small subregions, identifying all the zeros of $\mathcal{H}$ in region $\mathcal{R}$.
It is important to stress that, even in situations that require the determination of the zeros of $\mathcal{H}$, the proposed combined procedure uses much less time. In fact, if we decide to plot directly the representation of $|\mathcal{H}|$ in all region $\mathcal{R}$, without a pre-selection criteria, the computational time and effort increase significantly. It is also important to underline that, in spite of the several approximations used in this procedure, its results remain valid. The large number of plots of $|\mathcal{H}|$, that we did during the preparation of this work, confirmed this validity.

For a given set of thermodynamical and chemical parameters, and considering certain bounds for the perturbation parameter a, the numerical method described above has been applied to investigate the linear stability of the steady detonation solution. The main objective is to describe the structure of unstable detonation waves and provide more detailed information about the instability parameter regimes. Some numerical simulations have been performed and several visualizations will be provided in the next section.

3.4 Numerical results

The response of the steady detonation solution to the rear boundary perturbations, as well as the influence of the reaction heat on the stability spectra, is investigated numerically. The stability problem formulated in terms of perturbation parameter a and spatially disturbances $\overline{z}$ by the ODE's (3.6), (3.7), (3.8) and (3.9) with initial conditions (3.11), (3.12) and (3.13) and closure boundary condition (3.14) is treated with the numerical shooting technique described in Subsection 3.3.2. A rectangular domain $\mathcal{R}$ in the upper-right complex plane is considered in order to locate the unstable modes, namely $0.001 < Re(a) < 0.02$ and $0.001 < Im(a) < 0.1$. This particular choice of the domain allows to avoid numerical difficulties coming from the possible existence of a neutral mode, $a = 0$, as well as other instability modes on the coordinate axes. The missing area in the domain $\mathcal{R}$, namely the region $[0, 0.001] \times [0, 0.1] \cup [0.001, 0.02] \times [0, 0.001]$, is rather small when compared with the domain $\mathcal{R}$ and can be studied separately.
All the results presented here about the linear stability problem are in dimensionless form. The numerical simulations have been performed assuming the following data in what concerns the kinetic and thermodynamical input parameters as well as the initial state of the fresh mixture,

$$\begin{aligned} &D{=}1700\ ms^{-1}, \quad E_A = 2400\ K, \quad m = 0.01\ Kg/mol, \\ &n_A^+ = 0.35\ mol/l, \quad n_B^+ = 0\ mol/l, \quad T^+ = 298.15\ K. \end{aligned} \tag{3.24}$$

The considered detonation velocity corresponds to an overdriven detonation. The reaction heat is varying in the range $-2 \leq Q_R^* \leq 2$, allowing to investigate the stability for both types of exothermic and endothermic chemical reactions. Furthermore, the equilibrium final state at the end of the reaction zone is assumed to be that point where the derivative of the number density of the constituent A reaches the value 10^{-6}. Fig. 3.1 shows the stability boundary in the parameter plane defined by the reaction heat Q_R^* and

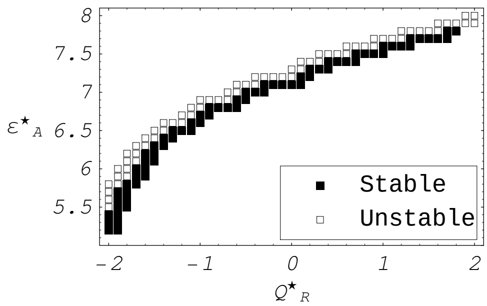

Figure 3.1: Stability boundary in the Q_R^*–$\varepsilon_A^\star$ plane, for the considered region $\mathcal{R}$.

forward activation energy $\varepsilon_A^\star$, for the considered domain $\mathcal{R}$ in the complex plane, and for the selected detonation velocity. One can interpret this representation as follows: a pair $(Q_R^*, \varepsilon_A^\star)$ in the stability zone indicates that for the corresponding values of the reaction heat and activation energy, no instability modes have been found in the domain $\mathcal{R}$; analogously, a pair $(Q_R^*, \varepsilon_A^\star)$ in the instability zone indicates that for the corresponding values of the reaction heat and activation energy, one instability mode, at least, has been found in the domain $\mathcal{R}$. Moreover, Fig. 3.1 reveals that for a fixed value of the activation energy, the detonation becomes stable for larger values of the reaction heat, whereas for a fixed value of the reaction heat, the detonation becomes stable for smaller values of the activation energy. These results are consistent with previous experimental works and numerical simulations, which show that increasing the reaction heat, or decreasing the activation energy, tends to stabilize the detonation. See, for example, the book [54] by J. H. S. Lee and the references therein cited.
A further and detailed analysis can provide a more deep description of the instability spectrum. In particular, if one sets the forward activation energy equal to a fixed value, namely $\varepsilon_A^\star = 7$, and left the reaction heat Q_R^* varying in a certain range as the parameter of interest, the numerical method allows to count the instability modes. Table 3.1 reveals the number of instability modes that have been found in the domain $\mathcal{R}$, for different values of the

reaction heat in the range $-2 \leq Q_R^* \leq 2$. One can see that the number of instability modes in the region $\mathcal{R}$ is zero when $Q_R^* \geq -0.6$ and increases for lower values of Q_R^*. These results are in agreement with the behavior recognizable in Fig. 3.1 as well as with the general trend described above.

Q_R^*	number of modes		Q_R^*	number of modes
2	0		-0.62	1
1.5	0		-0.65	2 to 3
1	0		-0.7	4 to 7
0	0		-1	18 to 24
-0.5	0		-1.5	57 to 70
-0.6	0		-2	215 to 252

Table 3.1: Number of the instability modes in the domain $\mathcal{R}$, for fixed forward activation energy, $\varepsilon_A^\star = 7$, and different values of the reaction heat in the range $-2 \leq Q_R^* \leq 2$.

Table 3.1 suggests the idea that for the considered value of the forward activation energy, $\varepsilon_A^\star = 7$, the number of instability modes increases indefinitely when the reaction heat decreases. Similar results have been obtained in some previous works, see [53] for example.

Figure 3.2 shows a three-dimensional plot of $|\mathcal{H}(a)|$, for an exothermic chemical reaction with $Q_R = -0.1$ and forward activation energy $\varepsilon_A^\star = 7.5$. This plot was obtained with increased resolution in a refinement of the region $\mathcal{R}$, namely in the sub-region $[0.00102, 0.00117] \times [0.089, 0.091]$. A very thin uniform grid is used, with step 10^{-4} for the imaginary part and 10^{-5} for the real part. The points a_j of this grid are assumed as trial values to evaluate the magnitude of the residual function and the instability modes are obtained as the zeros of $|\mathcal{H}(a)|$. Figure 3.2 shows the existence of four instability modes. A thinner grid should produce accurate approximations for these modes, however the computational effort should become rather intensive. Applying this procedure with grids occupying different regions, one obtains the instability spectra represented bellow, in Fig. 3.4, for different values of the reaction heat Q_R^*. In particular, the spectrum of Fig. 3.4, for $Q_R^* = -0.1$,

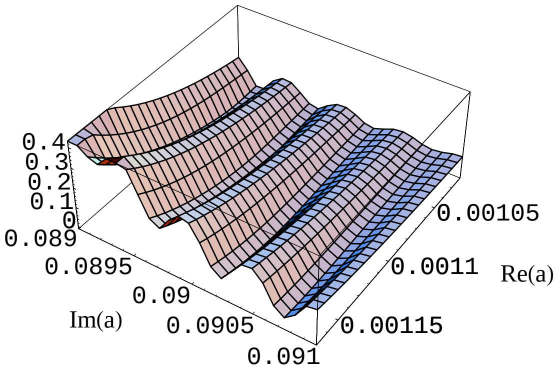

Figure 3.2: Three-dimensional plot of the magnitude of the residual function, $|\mathcal{H}(a)|$, in the sub-domain of $\mathcal{R}$ defined by $Re\,(a) \in [0.00102, 0.00117]$, $Im\,(a) \in [0.089, 0.091]$, for reaction heat and forward activation energy given by $Q_R = -0.1$ and $\varepsilon_A^\star = 7.5$.

includes the four instability modes of Fig. 3.2.

Another study concerning the effect of the reaction heat on the stability behavior is represented in Figs. 3.3 and 3.4. Figure 3.3 shows the migration of the fundamental instability mode, corresponding to the lowest perturbation frequency (small imaginary part), for the activation energy $\varepsilon_A^\star = 7.5$, as the reaction heat Q_R^* is varied from -0.5 to 0.5. This choice for the range of the reaction heat allows to follow the migration of the fundamental mode when it passes, in particular, through the inert gas mixture characterized by the vanishing of the reaction heat, $Q_R^* = 0$. Note that the plot range of Fig. 3.3 is not contained in the domain $\mathcal{R}$, already defined, but they intercept each other. In Fig. 3.3, the inert gas mixture is represented by the square labeled point, which is located on the right-hand-side of the frame. All the points labeled with the cross correspond to $Q_R^* < 0$, or ZND detonation with exothermic chemical reaction, whereas the points labeled with the black triangle correspond to $Q_R^* > 0$, or pathological stage of the detonation with endothermic chemical reaction. The mode departs from the crossed point

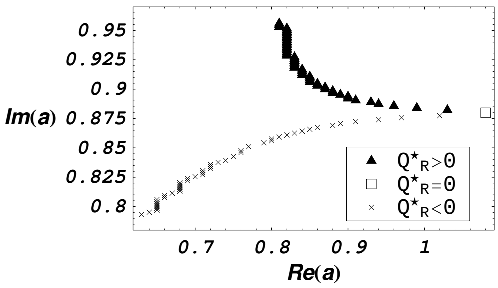

Figure 3.3: Migration of the fundamental instability mode (lowest perturbation frequency) for the activation energy $\varepsilon_A^\star = 7.5$, as the reaction heat Q_R^* is varied, with a step of 10^{-2}, from -0.5 to 0.5. $\mathrm{Re}\, a$ is scaled by the factor 10^3 and $\mathrm{Im}\, a$ by the factor 10.

located on the left-hand-side of the frame, corresponding to $Q_R^* = -0.5$, and starts moving above and to the right, until Q_R^* reaches its zero value at the square labeled point. This trend means that the perturbation frequency and the growth rate increases, so that a destabilizing effect of the detonation is verified. Then, when Q_R^* increases from its zero value to positive values, the mode moves above and to the left. This behavior signifies that the perturbation frequency increases but the growth rate decreases, so that a stabilizing effect of the detonation is observed. Therefore one can conclude that the endothermic reaction ($Q_R^* > 0$) has a stabilizing effect on the detonation wave. The results shown in Fig. 3.3 are in agreement with those provided in other previous works on detonation stability, see for example [37, 53, 72, 79].

The unstable spectra in the domain $\mathcal{R}$ are represented in Fig. 3.4, when the forward activation energy is $\varepsilon_A^\star = 7.5$, and the reaction heat takes the values $Q_R^* = -0.1$, $Q_R^* = 0$, $Q_R^* = 0.1$. All the instability modes in the domain $\mathcal{R}$ are located in the upper-left sub-domain $[0.1, 0.22] \times [0.79, 1]$ considered in Fig. 3.4. These modes were obtained using various three-dimensional plots of $|\mathcal{H}(a)|$ similar to the one drawn in Fig. 3.2. Each curve of Fig. 3.4 consists of all instability modes that have been found in the considered searching window, for the corresponding value of the reaction heat. In particular,

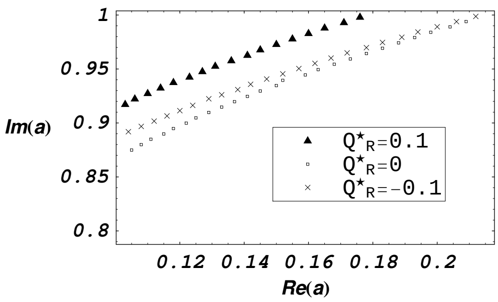

Figure 3.4: Unstable spectra for the activation energy $\varepsilon_A^\star = 7.5$, as the reaction heat takes the values $Q_R^* = -0.1$, $Q_R^* = 0$, $Q_R^* = 0.1$. $\mathrm{Re}\, a$ is scaled by the factor 10^2 and $\mathrm{Im}\, a$ by the factor 10. Zoom at an upper-left sub-domain of $\mathcal{R}$.

the four instability modes with lower perturbation frequency shown in the instability spectrum for $Q_R^* = -0.1$ are those modes previously represented in the three-dimensional plot of Fig. 3.2. Similarly, the instability mode with the lowest perturbation frequency shown in the instability spectrum for $Q_R^* = 0$ is the one represented in Fig. 3.3 at the square labeled point. Since the lower curve corresponds to the inert case ($Q_R^* = 0$) and all the instability modes for both positive and negative reaction heat are located in the area above this curve, Fig. 3.4 suggests the idea that all other possible instability modes are located above the inert curve for $Q_R^* = 0$, and thus the region below the curve corresponds to a stability region. Since the perturbation frequency increases with the growth rate, another interesting feature of Fig. 3.4 is that, for a fixed growth rate, the perturbation frequency of the inert instability mode may be seen as the lower bound of the instability perturbation frequencies. Conversely, for a fixed perturbation frequency, the growth rate of the inert instability mode may be seen as the upper bound of the instability perturbation frequencies.

3.5 Final remarks

The one-dimensional linear stability of the steady detonation wave is here investigated, with emphasis on the influence of the reaction heat on the instability behavior. Assuming a chemical regime of slow reactive process, the Euler equations obtained with the kinetic approach incorporate explicit contributions of the reaction heat and activation energy, which result as fundamental for the stability analysis. In fact, this explicit dependence permits to obtain a rather complete description, in comparison to the previous investigations based on a kinetic approach. The numerical method of solution proposed for the stability problem allowed to present some results concerning linear stability spectra of the whole structure of the ZND solution with exothermic chemical reaction and the second branch of the pathological solution with endothermic chemical reaction. The stability boundary in the parameter plane $Q_R^* - \varepsilon_A^*$ and the migration of the fundamental instability mode with lowest perturbation frequency are just two interesting examples of these results.

We intend to extended this study to a quaternary reactive mixture, starting from the kinetic modeling and macroscopic closure procedure referred to a mixture of four constituents, in order to consider more general detonating mixtures. Another interesting extensions of the present study could be its application to the CJ idealized detonation in a reactive mixture of two or four constituents and the analysis of the complete structure and stability of the pathological detonation, by considering two consecutive chemical reactions, the former being of exothermic type describing the branch between the shock front and the pathological point and the latter being of endothermic type describing the branch between the pathological point and the final equilibrium state.

Chapter 4

SRS theory for a quaternary reactive mixture

In this chapter we present the theory of simple reacting spheres (SRS) for the chemically reactive Boltzmann equation. After mentioning some preliminary works about this theory [57, 64, 87], we explore these model's characteristics. The mathematical properties of the collisional dynamics are deduced from the physical principles, and the consistency of the theory and other mathematical properties are then investigated in detail.

The structure of this chapter is similar to that of Chapter 1, but here we built in the dynamics of the SRS theory and prove all the relevant results. In particular, we derive the linearized version of the SRS kinetic equations and give the explicit representation of the collisional kernels. To the best of our knowledge, this is the first contribution at the level of the kernel representation for a reactive kinetic system. The derivation of the kernels is rather intricate and requires some hard manipulations. The main aspects of the SRS linearized theory and the kernel representation are given in paper [16]. Representative examples, for both elastic and reactive kernels, are given in Appendixes A and B, respectively.

4.1 Introduction

In this section we briefly mention some previous contributions to the chemically reactive Boltzmann theory. Then we describe the SRS theory and explain its strong points from the mathematical point of view. The problem of polyatomic reactive mixtures, within kinetic theory, was first investigated in 1949 by Prigogine and Xhrouet [68]. They treated the reactive terms as perturbations of the elastic terms. This approach is only valid if the reactive cross sections are much smaller then the elastic cross sections. In 1959, Present gave another important contribution to this problem [66]. Although, in some aspects, different from the work by Prigogine and Xhrouet, the Present's theory is also based on the assumption that the reactive terms are small perturbations of the elastic terms. Ross and Mazur, in 1961, as well as Shizgal and Karplus, in 1970, see papers [70, 77] respectively, used the Chapman-Enskog method in the space homogeneous case with the aim of investigating the non-equilibrium effects induced by the chemical reactions and deducing, in particular, the explicit expression of the reaction rate specifying the chemical production of each constituent of the mixture. The works of Moreau [59], in 1975, and Xystris and Dahler [86], in 1978, used the method of Grad in both homogeneous and inhomogeneous cases with the objective of deducing, again, explicit expressions for the reaction rate. The generalization of the H-theorem to chemically reactive gas mixture was given by Polak and Khachoyan [63] in 1985. In 1998, Rossani and Spiga [71] constructed a kinetic model based on physical principles, namely on the conservation laws and trend to equilibrium. Polewczak proved, in his work [64] in 2000, the existence of global in time, spatially inhomogeneous, and L^1-renormalized solution for the model of simple reacting spheres, under the assumption of finite initial mass, momentum and energy. The existence result refers to a four component mixture with a chemical bimolecular reaction in which there was no mass exchange. The kinetic theories developed in papers [64, 71] were analyzed and compared in 2004, by Groppi and Polewczak, see [43].

The kinetic theory of the simple reacting spheres was first proposed by Marron [57] in 1970 and then developed by Xystris and Dahler [87] in 1978. Within this theory, both elastic and reactive collisions are of hard-sphere type. This feature reduces the micro-reversibility principle to a simpler condition that we explain in Section 4.2. Furthermore, being a natural extension of the hard-sphere collisional model, when the chemical reactions are turned off the model reduces itself to the revised Enskog theory. In the dilute-gas limit, it provides an interesting kinetic model of chemical reactions that has not yet been studied in detail.

In the present chapter, starting from the previous papers on the SRS theory, we consider the general case of a four-component mixture undergoing a bimolecular chemical reaction. A detailed analysis of the mathematical properties of the SRS theory is presented here and rigorous results about the collisional dynamics, passage to the hydrodynamics and trend to equilibrium are proved and explained in detail. Finally, in order to prove the existence and stability of close to equilibrium solutions, particular attention is devoted to the linearized version of the SRS system around the local Maxwellian equilibrium.

The content of this chapter is based on paper [65], still in preparation. Some proofs and details of the SRS theory, as well as some spectral properties of the linearized system, are explained here and omitted in paper [65].

4.2 Kinetic modeling

We consider a gas mixture with four constituents, say $A_1, ..., A_4$, with masses $m_1, ..., m_4$, and formation energies $E_1, ..., E_4$, respectively, which undergo the reversible reaction

$$A_1 + A_2 \rightleftharpoons A_3 + A_4. \tag{4.1}$$

The constituents' indexes are chosen in such a way that the reaction heat and molecular masses verify

$$Q_R = E_3 + E_4 - E_1 - E_2 > 0, \qquad m_1 < m_2 \qquad \text{and} \qquad m_4 < m_3.$$

Note 4.2.1. *The above choices do not represent any specific restriction. With the exception of a gas mixture where all the constituents have the same mass, any situation can be described using them. They are used to fix the notation. Nevertheless, they affect, formally, some results that are obtained in this chapter.*

In this Chapter, only collisions between two particles are considered. The collisions might be elastic or reactive. An elastic collision between particles A_i and A_s with velocities $\boldsymbol{c}_i$ and $\boldsymbol{c}_s$, respectively, results in a change of the velocities of both constituents, $(\boldsymbol{c}_i, \boldsymbol{c}_s) \to (\boldsymbol{c}_i', \boldsymbol{c}_s')$, with $i, s = 1, ..., 4$. A reactive collision between particles A_i and A_j with velocities $\boldsymbol{c}_i$ and $\boldsymbol{c}_j$, respectively, results in a transition of the constituents into A_k and A_l and a consequent change of velocities to $\boldsymbol{c}_k$ and $\boldsymbol{c}_l$, respectively, with $(i, j, k, l) \in \{(1, 2, 3, 4), (2, 1, 4, 3), (3, 4, 1, 2), (4, 3, 2, 1)\}$.
Concerning the elastic collisions, the mass of the colliding particles is obviously preserved, since the constituents do not change during the collision. Moreover, the physical conservation laws of linear momentum and kinetic energy of the colliding particles are specified by the following mathematical conditions

$$m_i \boldsymbol{c}_i + m_s \boldsymbol{c}_s = m_i \boldsymbol{c}_i' + m_s \boldsymbol{c}_s', \tag{4.2}$$

$$m_i \boldsymbol{c}_i^2 + m_s \boldsymbol{c}_s^2 = m_i \boldsymbol{c}_i'^2 + m_s \boldsymbol{c}_s'^2. \tag{4.3}$$

Concerning reactive collisions, the physical conservation laws of mass, linear momentum and total energy of the colliding particles are specified by the following mathematical conditions

$$m_1 + m_2 = m_3 + m_4, \tag{4.4}$$

$$m_1\boldsymbol{c}_1 + m_2\boldsymbol{c}_2 = m_3\boldsymbol{c}_3 + m_4\boldsymbol{c}_4, \tag{4.5}$$

$$E_1 + \frac{1}{2}m_1\boldsymbol{c}_1^2 + E_2 + \frac{1}{2}m_2\boldsymbol{c}_2^2 = E_3 + \frac{1}{2}m_3\boldsymbol{c}_3^2 + E_4 + \frac{1}{2}m_4\boldsymbol{c}_4^2. \tag{4.6}$$

4.2.1 Collisional dynamics

In this subsection we deduce some important relations concerning the collisional dynamics. We try to base our analysis only on classical mechanics theory and basic physical laws. Some properties are used in other important results presented here.

The hard-spheres model is one of the most important and more frequently used models for the elastic cross section, mainly due to its simplicity. The elastic cross section σ_{is}^2 associated to an elastic collision between two particles of constituents A_i and A_s is given by

$$\sigma_{is}^2 = \frac{1}{4}(d_i + d_s)^2, \tag{4.7}$$

where d_i and d_s denote the diameters of the particle constituents A_i and A_s, respectively. The natural extension of the hard-spheres model to chemically reactive gas mixtures is the SRS model, in which the chemical collisions are treated as hard-spheres-like collisions . Additionally, the reactive collision between particles A_i and A_j, with $(i, j) \in \{(1, 2), (2, 1), (3, 4), (4, 3)\}$, occurs if the kinetic energy associated with the relative motion along the line of centers exceeds the respective activation energy. The chemical reactive cross sections for the SRS model have the expressions

$$\sigma_{12}^{*2} = \begin{cases} \beta_{12}\sigma_{12}^2, & \langle \epsilon, \boldsymbol{c}_1 - \boldsymbol{c}_2 \rangle \geq \Gamma_{12}, \\ 0, & \langle \epsilon, \boldsymbol{c}_1 - \boldsymbol{c}_2 \rangle < \Gamma_{12}, \end{cases} \tag{4.8}$$

and

$$\sigma_{34}^{*2} = \begin{cases} \beta_{34}\sigma_{34}^2, & \langle \epsilon, \boldsymbol{c}_3 - \boldsymbol{c}_4 \rangle \geq \Gamma_{34}, \\ 0, & \langle \epsilon, \boldsymbol{c}_3 - \boldsymbol{c}_4 \rangle < \Gamma_{34}, \end{cases} \tag{4.9}$$

for the direct and inverse reaction, respectively. Above, β_{ij} is the steric factor for the collision between constituents A_i and A_j, with $0 \leq \beta_{ij} \leq 1$. Moreover, Γ_{ij} is a threshold velocity given by $\Gamma_{ij} = \sqrt{2\varepsilon_i/\mu_{ij}}$, where ε_i is the activation energy for the constituent A_i, and $\mu_{ij} = \frac{m_i m_j}{m_i + m_j}$ is a reduced mass. The notation $\langle \cdot, \cdot \rangle$ is used for the inner product in $\mathbb{R}^3$ and ϵ is the unit vector along the line passing through the centers of the spheres at the moment of impact,

$$\epsilon \in \{\epsilon \in \mathbb{R}^3 : \|\epsilon\| = 1 \wedge \langle \epsilon, \boldsymbol{c}_i - \boldsymbol{c}_j \rangle \geq 0\} \equiv \mathbb{S}_+^2.$$

Notice that for the chemical reaction defined in Eq. (4.1), we have $\varepsilon_2 = \varepsilon_1$, $\varepsilon_3 = \varepsilon_1 - Q_R$ and $\varepsilon_4 = \varepsilon_3$. Moreover, we have $\beta_{ij} = 0$ for $(i, j) \notin \{(1, 2), (2, 1), (3, 4), (4, 3)\}$. Furthermore, since we consider that $Q_R > 0$, we have $\varepsilon_1 > Q_R$. For other general relations between the activation energies and the reaction heat, see Chapter 9 of [51].

Note 4.2.2. *In expressions (4.8) and (4.9) that define the reactive cross sections, condition* $\langle \epsilon, \boldsymbol{c}_i - \boldsymbol{c}_j \rangle \geq \Gamma_{ij}$ *is equivalent to* $1/2\mu_{ij}(\langle \epsilon, \boldsymbol{c}_i - \boldsymbol{c}_j \rangle)^2 \geq \varepsilon_i$, *which expresses that the energy of the relative motion along the line of centers is greater or equal to the corresponding activation energy.*

Note 4.2.3. *From definition (4.7) of the elastic cross sections it is clear that elastic collisions verify the micro-reversibility principle. Moreover, the reactive cross sections defined in (4.8) and (4.9) verify the micro-reversibility principle when the steric factors are symmetric and equal for the forward and backward reactions, that is* $\beta_{ij} = \beta_{ji}$ *and* $\beta_{12} = \beta_{34}$, *and the mean collisional diameter is preserved in the reactive collisions, that is* $\sigma_{12} = \sigma_{34}$.

Now we construct the post-collisional velocities, using some physical properties of the model, such as the conservation of linear momentum (4.5) and the conservation of total energy (4.6).

Proposition 4.2.1. *In the case of elastic collisions between two particles of constituents A_i and A_s, with initial velocities $\boldsymbol{c}_i$ and $\boldsymbol{c}_s$, respectively, the post-collisional velocities are given by*

$$\boldsymbol{c}_i' = \boldsymbol{c}_i - 2\frac{\mu_{is}}{m_i}\epsilon\langle\epsilon, \boldsymbol{c}_i - \boldsymbol{c}_s\rangle \qquad \textit{and} \qquad \boldsymbol{c}_s' = \boldsymbol{c}_s + 2\frac{\mu_{is}}{m_s}\epsilon\langle\epsilon, \boldsymbol{c}_i - \boldsymbol{c}_s\rangle, \quad (4.10)$$

respectively.

Proof: From the definition of ϵ, we may write

$$\boldsymbol{c}_i' = \boldsymbol{c}_i - P\epsilon, \quad (4.11)$$

with P being an unknown scalar. Inserting expression (4.11) in the conservation equation (4.2) of linear momentum for elastic collisions, we obtain:

$$\boldsymbol{c}_s' = \boldsymbol{c}_s + \frac{m_i}{m_s}P\epsilon. \quad (4.12)$$

Using the conservation equation (4.3) of kinetic energy for elastic collisions, inserting expressions (4.11) and (4.12) and discarding the trivial null solution for P, we get

$$P = \frac{2\mu_{is}}{m_i}\langle\epsilon, \boldsymbol{c}_i - \boldsymbol{c}_s\rangle. \quad (4.13)$$

Finally, inserting expression (4.13) for the scalar P into Eqs. (4.11) and (4.12) for the post-collisional velocities, we obtain expression (4.10) and conclude the proof. □

Before deducing the expressions for the reactive post-collisional velocities we present a property that is used to prove them.

Lemma 4.2.1. *For the considered reactive collisions the following condition holds true*

$$\frac{1}{2}\mu_{12}(\boldsymbol{c}_1 - \boldsymbol{c}_2)^2 = \frac{1}{2}\mu_{34}(\boldsymbol{c}_3 - \boldsymbol{c}_4)^2 + Q_R. \quad (4.14)$$

Proof: We start by considering the conservation Eq. (4.6) of total energy written in the equivalent form

$$m_1\boldsymbol{c}_1^2 + m_2\boldsymbol{c}_2^2 = m_3\boldsymbol{c}_3^2 + m_4\boldsymbol{c}_4^2 + 2Q_R. \tag{4.15}$$

Multiplying Eq. (4.15) by M, with $M = m_1 + m_2 = m_3 + m_4$, we obtain

$$m_1^2\boldsymbol{c}_1^2+m_1m_2\boldsymbol{c}_1^2+m_1m_2\boldsymbol{c}_2^2+m_2^2\boldsymbol{c}_2^2 = m_3^2\boldsymbol{c}_3^2+m_3m_4\boldsymbol{c}_3^2+m_3m_4\boldsymbol{c}_4^2+m_4^2\boldsymbol{c}_4^2+2MQ_R,$$

or even

$$\begin{aligned}(m_1\boldsymbol{c}_1 + m_2\boldsymbol{c}_2)^2 - 2m_1m_2\boldsymbol{c}_1\boldsymbol{c}_2 + m_1m_2\boldsymbol{c}_1^2 + m_1m_2\boldsymbol{c}_2^2 \\ = (m_3\boldsymbol{c}_3 + m_4\boldsymbol{c}_4)^2 - 2m_3m_4\boldsymbol{c}_3\boldsymbol{c}_4 + m_3m_4\boldsymbol{c}_3^2 + m_3m_4\boldsymbol{c}_4^2 + 2MQ_R.\end{aligned} \tag{4.16}$$

Taking into account the conservation Eq. (4.5) of linear momentum, Eq. (4.16) transforms to

$$m_1m_2(\boldsymbol{c}_1 - \boldsymbol{c}_2)^2 = m_3m_4(\boldsymbol{c}_3 - \boldsymbol{c}_4)^2 + 2MQ_R,$$

which reproduces Eq. (4.14). □

It is known, from the theory of physical mechanics, see for instance [19], that the tangential component of the relative velocity does not change in a hard-spheres collision and, therefore,

$$\langle \xi, \tau \rangle = \langle \xi', \tau \rangle, \tag{4.17}$$

where τ is the unit vector perpendicular to ϵ and $\xi_1 = \xi_2 = \xi = \boldsymbol{c}_1 - \boldsymbol{c}_2$, $\xi_3 = \xi_4 = \xi' = \boldsymbol{c}_3 - \boldsymbol{c}_4$. Property (4.17), together with Lemma 4.2.1, is used to derive the expressions for the reactive post-collisional velocities.

Proposition 4.2.2. *In the case of reactive collisions between two particles,* *the post-collisional velocities for the direct reaction are*

$$\boldsymbol{c}_3 = \frac{1}{M}\left[m_1\boldsymbol{c}_1 + m_2\boldsymbol{c}_2 + m_4\sqrt{\frac{\mu_{12}}{\mu_{34}}}\left\{\xi - \epsilon\langle\epsilon,\xi\rangle + \epsilon\alpha^-\right\}\right] \tag{4.18}$$

and

$$\boldsymbol{c}_4 = \frac{1}{M}\left[m_1\boldsymbol{c}_1 + m_2\boldsymbol{c}_2 - m_3\sqrt{\frac{\mu_{12}}{\mu_{34}}}\left\{\xi - \epsilon\langle\epsilon,\xi\rangle + \epsilon\alpha^-\right\}\right]. \tag{4.19}$$

The post-collisional velocities for the inverse reaction are

$$\boldsymbol{c}_1 = \frac{1}{M}\left[m_3\boldsymbol{c}_3 + m_4\boldsymbol{c}_4 + m_2\sqrt{\frac{\mu_{34}}{\mu_{12}}}\left\{\xi' - \epsilon\langle\epsilon,\xi'\rangle + \epsilon\alpha^+\right\}\right] \tag{4.20}$$

and

$$\boldsymbol{c}_2 = \frac{1}{M}\left[m_3\boldsymbol{c}_3 + m_4\boldsymbol{c}_4 - m_1\sqrt{\frac{\mu_{34}}{\mu_{12}}}\left\{\xi' - \epsilon\langle\epsilon,\xi'\rangle + \epsilon\alpha^+\right\}\right]. \tag{4.21}$$

Above, $\alpha^- = \sqrt{(\langle\epsilon,\xi\rangle)^2 - 2Q_R/\mu_{12}}$ *and* $\alpha^+ = \sqrt{(\langle\epsilon,\xi'\rangle)^2 + 2Q_R/\mu_{34}}$.

Proof: Here we deduce the expression of the post-collisional velocity $\boldsymbol{c}_3$. The expressions of the other velocities are obtained following similar procedures. The relative velocities ξ and ξ' may be written as linear combination of τ and ϵ, in the following form

$$\xi' = \langle\xi',\tau\rangle\tau + \langle\xi',\epsilon\rangle\epsilon \qquad \text{and} \qquad \xi = \langle\xi,\tau\rangle\tau + \langle\xi,\epsilon\rangle\epsilon. \tag{4.22}$$

From condition (4.14), using expressions (4.22) for the relative velocities ξ and ξ', we obtain

$$\frac{1}{2}\mu_{12}(\langle\xi,\tau\rangle\tau + \langle\xi,\epsilon\rangle\epsilon)^2 = \frac{1}{2}\mu_{34}(\langle\xi',\tau\rangle\tau + \langle\xi',\epsilon\rangle\epsilon)^2 + Q_R. \tag{4.23}$$

Now, using property (4.17), we obtain

$$\mu_{12}(\langle \xi, \epsilon \rangle)^2 = \mu_{34}(\langle \xi', \epsilon \rangle)^2 + 2Q_R,$$

and therefore,

$$(\langle \xi', \epsilon \rangle)^2 = \frac{\mu_{12}}{\mu_{34}} \left[(\langle \xi, \epsilon \rangle)^2 - \frac{2Q_R}{\mu_{12}} \right]. \tag{4.24}$$

Now, taking into account the conservation of linear momentum (4.5), the first equality of (4.22) can be written as

$$\boldsymbol{c}_3 = \frac{m_1\boldsymbol{c}_1 + m_2\boldsymbol{c}_2 - m_3\boldsymbol{c}_3}{m_4} + \langle \xi', \tau \rangle \tau + \langle \xi', \epsilon \rangle \epsilon.$$

Using Eq. (4.17) to transform the tangential component of the relative velocity ξ' and Eq. (4.24) to transform the normal component, we get

$$\boldsymbol{c}_3 = \frac{m_1\boldsymbol{c}_1 + m_2\boldsymbol{c}_2 - m_3\boldsymbol{c}_3}{m_4} + \sqrt{\frac{\mu_{12}}{\mu_{34}}} \langle \xi, \tau \rangle \tau + \epsilon \sqrt{\frac{\mu_{12}}{\mu_{34}} \left[(\langle \xi, \epsilon \rangle)^2 - \frac{2Q_R}{\mu_{12}} \right]},$$

that is,

$$\frac{M\boldsymbol{c}_3}{m_4} = \frac{m_1\boldsymbol{c}_1 + m_2\boldsymbol{c}_2}{m_4} + \sqrt{\frac{\mu_{12}}{\mu_{34}}} \langle \xi, \tau \rangle \tau + \epsilon \sqrt{\frac{\mu_{12}}{\mu_{34}} \left[(\langle \xi, \epsilon \rangle)^2 - \frac{2Q_R}{\mu_{12}} \right]}.$$

Using the second equality of (4.22) and taking into account the definition of α^- we obtain the expression (4.18) for the post-collisional velocity $\boldsymbol{c}_3$. □

Note 4.2.4. *In the proof of Proposition 4.2.2, due to the reversibility of the conservation equations and other laws used in the proof, there is no need to fix wether we refer to post-collisional or pre-collisional velocities. Therefore the pre-collisional velocities can be expressed in terms of the post-collisional velocities through the same Eqs. (4.18), (4.19), (4.20) and (4.21). In particular,*

if two particles of constituents A_1 and A_2 are the result of a reactive collision between two particles of constituents A_3 and A_4, then the pre-collisional velocities $\boldsymbol{c}_3$ and $\boldsymbol{c}_4$ can be expressed in terms of the post-reactive velocities $\boldsymbol{c}_1$ and $\boldsymbol{c}_2$ through the expressions (4.18) and (4.19).
A similar statement is valid for the elastic pre-collisional and post-collisional velocities.

Lemma 4.2.2. *For a fixed vector ϵ the following equalities hold true:*

$$\langle \epsilon, \xi \rangle = \sqrt{\tfrac{\mu_{34}}{\mu_{12}}}\, \alpha^+, \tag{4.25}$$

$$\langle \epsilon, \xi' \rangle = \sqrt{\tfrac{\mu_{12}}{\mu_{34}}}\, \alpha^-, \tag{4.26}$$

$$\tfrac{1}{2}\mu_{12}(\langle \epsilon, \xi \rangle)^2 - \varepsilon_1 = \tfrac{1}{2}\mu_{34}(\langle \epsilon, \xi' \rangle)^2 - \varepsilon_3. \tag{4.27}$$

Proof: The proof follows directly from expressions (4.18), (4.19), (4.20) and (4.21) by computing the inner products $\langle \epsilon, \xi \rangle$ and $\langle \epsilon, \xi' \rangle$. □

We finish this subsection with the following lemma about the Jacobian of the transformation from the pre-collisional to the post-collisional velocities. It will be used in the next subsection.

Lemma 4.2.3. *For a fixed vector ϵ, the Jacobians of the transformations $(\boldsymbol{c}_1, \boldsymbol{c}_2) \mapsto (\boldsymbol{c}_3, \boldsymbol{c}_4)$ and $(\boldsymbol{c}_3, \boldsymbol{c}_4) \mapsto (\boldsymbol{c}_1, \boldsymbol{c}_2)$ are given by*

$$\left(\frac{\mu_{34}}{\mu_{12}}\right)^{3/2} \frac{\langle \epsilon, \xi' \rangle}{\alpha^+} \qquad \text{and} \qquad \left(\frac{\mu_{12}}{\mu_{34}}\right)^{3/2} \frac{\langle \epsilon, \xi \rangle}{\alpha^-}, \tag{4.28}$$

respectively.

Proof: We prove the first part of the lemma. The proof of the second part is similar. The Jacobian matrix of the transformation $(\boldsymbol{c}_3, \boldsymbol{c}_4) \mapsto (\boldsymbol{c}_1, \boldsymbol{c}_2)$, say

A, with elements $a_{ij}, i, j \in \{1,2,3,4,5,6\}$, is defined by

$$a_{ij} = \frac{\partial}{\partial c_j^1} c_i^3 = \begin{cases} \frac{1}{M}\left[m_1 - m_4\sqrt{\frac{\mu_{12}}{\mu_{34}}}\left\{-1+\epsilon_i^2\left(1-\frac{\langle\epsilon,\xi\rangle}{\alpha^-}\right)\right\}\right], & i=j \\ -\frac{m_4}{M}\sqrt{\frac{\mu_{12}}{\mu_{34}}}\left\{\epsilon_i\epsilon_j\left(1-\frac{\langle\epsilon,\xi\rangle}{\alpha^-}\right)\right\}, & i\neq j \end{cases}$$

for $i, j \in \{1,2,3\}$,

$$a_{ij} = \frac{\partial}{\partial c_j^2} c_i^3 = \begin{cases} \frac{1}{M}\left[m_2 + m_4\sqrt{\frac{\mu_{12}}{\mu_{34}}}\left\{-1+\epsilon_i^2\left(1-\frac{\langle\epsilon,\xi\rangle}{\alpha^-}\right)\right\}\right], & i+3=j \\ \frac{m_4}{M}\sqrt{\frac{\mu_{12}}{\mu_{34}}}\left\{\epsilon_i\epsilon_j\left(1-\frac{\langle\epsilon,\xi\rangle}{\alpha^-}\right)\right\}, & i+3\neq j \end{cases}$$

for $i \in \{1,2,3\}, j \in \{4,5,6\}$,

$$a_{ij} = \frac{\partial}{\partial c_j^1} c_i^4 = \begin{cases} \frac{1}{M}\left[m_1 + m_3\sqrt{\frac{\mu_{12}}{\mu_{34}}}\left\{-1+\epsilon_i^2\left(1-\frac{\langle\epsilon,\xi\rangle}{\alpha^-}\right)\right\}\right], & i=j+3 \\ \frac{m_3}{M}\sqrt{\frac{\mu_{12}}{\mu_{34}}}\left\{\epsilon_i\epsilon_j\left(1-\frac{\langle\epsilon,\xi\rangle}{\alpha^-}\right)\right\}, & i\neq j+3 \end{cases}$$

for $i \in \{4,5,6\}, j \in \{1,2,3\}$ and

$$a_{ij} = \frac{\partial}{\partial c_j^2} c_i^4 = \begin{cases} \frac{1}{M}\left[m_2 - m_3\sqrt{\frac{\mu_{12}}{\mu_{34}}}\left\{-1+\epsilon_i^2\left(1-\frac{\langle\epsilon,\xi\rangle}{\alpha^-}\right)\right\}\right], & i=j \\ -\frac{m_3}{M}\sqrt{\frac{\mu_{12}}{\mu_{34}}}\left\{\epsilon_i\epsilon_j\left(1-\frac{\langle\epsilon,\xi\rangle}{\alpha^-}\right)\right\}, & i\neq j \end{cases}$$

for $i \in \{4,5,6\}, j \in \{4,5,6\}$. Thus, by inspection, the determinant of the matrix is given by $\left(\frac{\mu_{12}}{\mu_{34}}\right)^{3/2} \frac{\langle\epsilon,\xi\rangle}{\alpha^-}$. □

4.2.2 Kinetic equations

In this subsection we deduce the kinetic equations of the SRS model. If we consider the absence of external forces, they are of type

$$\frac{\partial}{\partial t} f_i + \sum_{l=1}^{3} c_l^i \frac{\partial}{\partial x_l} f_i = \mathcal{Q}_i^E + \mathcal{Q}_i^R, \tag{4.29}$$

where $\mathcal{Q}_i^E$ and $\mathcal{Q}_i^R$ represent the elastic and the reactive collisional operators, respectively. The expressions of the collisional operators, both elastic and reactive, are justified in what follows.

The collisional operator of constituent A_i has a gain term and a loss term, as usual, that count the number of particles of that constituent that are gained and lost, respectively, due to collisions.
By considering the hard-sphere model for the elastic collisions and the SRS model for the reactive collisions, the elastic operator $\mathcal{Q}_i^E$ takes the form:

$$\begin{aligned} \mathcal{Q}_i^E \quad &= \quad \sum_{s=1}^{4} \left\{ \sigma_{is}^2 \int_{\mathbb{R}^3} \int_{\mathbb{S}_+^2} \left[f_i' f_s' - f_i f_s \right] \langle \epsilon, \boldsymbol{c}_i - \boldsymbol{c}_s \rangle d\epsilon d\boldsymbol{c}_s \right\} \qquad (4.30) \\ & \quad -\beta_{ij} \sigma_{ij}^2 \int_{\mathbb{R}^3} \int_{\mathbb{S}_+^2} \left[f_i' f_j' - f_i f_j \right] \Theta(\langle \epsilon, \xi_i \rangle - \Gamma_{ij}) \langle \epsilon, \xi_i \rangle d\epsilon d\boldsymbol{c}_j, \end{aligned}$$

where Θ is the Heaviside step function and $(i, j) \in \{(1, 2), (2, 1), (3, 4), (4, 3)\}$. Some collisions between particles of constituents A_1 and A_2 or A_3 and A_4 are elastic and some of them are reactive. The definition of the chemical reactive cross section, in terms of an activation energy, determines how to count each collision. The interpretation of the elastic collisional operator is similar to the one presented in Chapter 1 but here we have an additional term to avoid the double counting. In fact, the second term in (4.30) singles out those pre-collisional states that are energetic enough to result in chemical reaction, and thus preventing double counting of the events in the collisional operators.
Many works neglect the counting of reactive collisions in the elastic operator. There are some situations where this is not a serious problem but, there are others where this procedure leads to critical ones, see for instance [51]. With the elastic collisional operator defined in (4.30) this double counting does not occur.

Now we construct the reactive collisional operator $\mathcal{Q}_i^R$. We only present the construction of $\mathcal{Q}_1^R$, since the other operators $\mathcal{Q}_i^R$, with $i = 2, 3, 4$, follow a similar procedure. The number of reactive collisions between particles of constituents A_1 and A_2 that contribute to the loss of particles A_1 with velocity $\boldsymbol{c}_1$, with the hard-sphere type reactive cross section defined in (4.8), is given by

$$\beta_{12}\sigma_{12}^2 \int_{\mathbb{R}^3} \int_{\mathbb{S}_+^2} f_1 f_2 \Theta(\langle \epsilon, \xi \rangle - \Gamma_{12}) \langle \epsilon, \xi \rangle d\epsilon d\boldsymbol{c}_2. \tag{4.31}$$

To obtain $\mathcal{Q}_1^R$ we also have to count the number of particles A_1 with velocity $\boldsymbol{c}_1$ that are gained with reactive collisions between particles of constituents A_3 and A_4 with velocities $\boldsymbol{c}_3$ and $\boldsymbol{c}_4$. However, the velocities $\boldsymbol{c}_3$ and $\boldsymbol{c}_4$ must be related to the velocities $\boldsymbol{c}_1$ (corresponding to the situation that we are considering) and $\boldsymbol{c}_2$ (corresponding to the integrand of expression (4.31)) by the conservation equations of linear momentum and total energy. Thus, if we consider the micro-reversibility principle and Lemmas 4.2.2 and 4.2.3, the number of particles of constituent A_1 with velocity $\boldsymbol{c}_1$ that are gained from reactive collisions between particles of constituents A_3 and A_4 is given by

$$\begin{aligned}
&\beta_{34}\sigma_{34}^2 \int_{\mathbb{R}^3} \int_{\mathbb{S}_+^2} f_3 f_4 \Theta(\langle \epsilon, \xi' \rangle - \Gamma_{34}) \langle \epsilon, \xi' \rangle d\epsilon d\boldsymbol{c}_3 \\
&= \beta_{12}\sigma_{12}^2 \int_{\mathbb{R}^3} \int_{\mathbb{S}_+^2} f_3 f_4 \Theta(\langle \epsilon, \xi \rangle - \Gamma_{12}) \sqrt{\frac{\mu_{12}}{\mu_{34}}} \alpha^- \left(\frac{\mu_{12}}{\mu_{34}}\right)^{3/2} \frac{\langle \epsilon, \xi \rangle}{\alpha^-} d\epsilon d\boldsymbol{c}_2 \\
&= \beta_{12}\sigma_{12}^2 \int_{\mathbb{R}^3} \int_{\mathbb{S}_+^2} \left(\frac{\mu_{12}}{\mu_{34}}\right)^2 f_3 f_4 \Theta(\langle \epsilon, \xi \rangle - \Gamma_{12}) \langle \epsilon, \xi \rangle d\epsilon d\boldsymbol{c}_2. \qquad (4.32)
\end{aligned}$$

Joining the loss term (4.31) and the gain term (4.32), we obtain the following expression for the reactive operator $\mathcal{Q}_1^R$,

$$\mathcal{Q}_1^R = \beta_{12}\sigma_{12}^2 \int_{\mathbb{R}^3} \int_{\mathbb{S}_+^2} \left[\left(\frac{\mu_{12}}{\mu_{34}}\right)^2 f_3 f_4 - f_1 f_2 \right] \Theta(\langle \epsilon, \xi \rangle - \Gamma_{12}) \langle \epsilon, \xi \rangle d\epsilon d\boldsymbol{c}_2. \tag{4.33}$$

Using a similar procedure, we obtain the reactive collisional operators for all the constituents, namely

$$\mathcal{Q}_i^R = \beta_{ij}\sigma_{ij}^2 \int_{\mathbb{R}^3}\int_{\mathbb{S}_+^2} \left[\left(\frac{\mu_{ij}}{\mu_{kl}}\right)^2 f_k f_l - f_i f_j \right] \Theta(\langle \epsilon, \xi_i\rangle - \Gamma_{ij})\langle \epsilon, \xi_i\rangle d\epsilon d\boldsymbol{c}_j, \quad (4.34)$$

where $(i, j, k, l) \in \{(1, 2, 3, 4), (2, 1, 4, 3), (3, 4, 1, 2), (4, 3, 2, 1)\}$.

As known in literature, see for instance [17, 51], and described in Chapter 1, the Boltzmann equations may be used to deduce appropriate balance equations for the evolution of the macroscopic variables of the reactive gas mixture. For that purpose, one needs to define the macroscopic variables as microscopic averages of the distribution function. for brevity, we present here the definition of those macroscopic variables that will be used in later sections.
The number density n_i of constituent A_i, with $i = 1, ..., 4$, and the number density n of the gas mixture are defined by

$$n_i = \int_{\mathbb{R}^3} f_i d\mathbf{c}_i \quad \text{and} \quad n = \sum_{i=1}^{4} n_i. \qquad (4.35)$$

The gas velocity components v_l, with $l = 1, ..., 3$, of the mixture are defined by

$$v_i = \frac{\sum_{i=1}^{4} m_i n_i v_l^i}{\sum_{i=1}^{4} m_i n_i}, \quad \text{with} \quad v_l^i = \frac{\int_{\mathbb{R}^3} c_l^i f_i d\mathbf{c}_l^i}{n_i}. \qquad (4.36)$$

The temperature T of the gas mixture is defined by

$$T = \frac{\sum_{i=1}^{4} p_i}{nk}, \quad \text{with} \quad p_i = \frac{1}{3}\int_{\mathbb{R}^3} m_i (c_l^i - v_l)^2 f_i d\mathbf{c}_i, \qquad (4.37)$$

where k is the Boltzmann constant.

4.3 Properties of the collisional operators

The consistency of the model is assured when the collisional operators have some important properties. We begin with the following fundamental results, concerning the elastic and reactive operators.

Proposition 4.3.1. *If we assume that $\beta_{ij} = \beta_{ji}$ then, for ψ_i measurable on $\mathbb{R}^3$ and $f_i \in C_0(\mathbb{R}^3)$, $i = 1, 2, 3, 4$,*

$$\begin{aligned}\int_{\mathbb{R}^3}\psi_i \mathcal{Q}_i^E d\boldsymbol{c}_i = &\frac{1}{4}\sum_{s=1}^{4}\left\{\sigma_{is}^2\int_{\mathbb{R}^3}\int_{\mathbb{R}^3}\int_{\mathbb{S}_+^2}[\psi_i+\psi_s-\psi_i'-\psi_s']\,[f_i'f_s'-f_if_s]\langle\epsilon,\boldsymbol{c}_i-\boldsymbol{c}_s\rangle d\epsilon d\boldsymbol{c}_s d\boldsymbol{c}_i\right\}\\ &-\frac{1}{4}\beta_{ij}\sigma_{ij}^2\int_{\mathbb{R}^3}\int_{\mathbb{R}^3}\int_{\mathbb{S}_+^2}\left[\psi_i+\psi_j-\psi_i'-\psi_j'\right]\left[f_i'f_j'-f_if_j\right]\\ &\times\Theta(\langle\epsilon,\xi_i\rangle-\Gamma_{ij})\langle\epsilon,\xi_i\rangle d\epsilon d\boldsymbol{c}_j d\boldsymbol{c}_i. \qquad (4.38)\end{aligned}$$

Proof: Taking into account the expression (4.30) for the elastic operator $\mathcal{Q}_i^E$, we separate the proof in two parts, namely

$$\begin{aligned}&\sigma_{is}^2\int_{\mathbb{R}^3}\int_{\mathbb{R}^3}\int_{\mathbb{S}_+^2}\psi_i\,[f_i'f_s'-f_if_s]\,\langle\epsilon,\boldsymbol{c}_i-\boldsymbol{c}_s\rangle d\epsilon d\boldsymbol{c}_s d\boldsymbol{c}_i \qquad (4.39)\\ &= \frac{1}{4}\sigma_{is}^2\int_{\mathbb{R}^3}\int_{\mathbb{R}^3}\int_{\mathbb{S}_+^2}[\psi_i+\psi_s-\psi_i'-\psi_s']\,[f_i'f_s'-f_if_s]\,\langle\epsilon,\boldsymbol{c}_i-\boldsymbol{c}_s\rangle d\epsilon d\boldsymbol{c}_s d\boldsymbol{c}_i\end{aligned}$$

and

$$\begin{aligned}&-\beta_{ij}\sigma_{ij}^2\int_{\mathbb{R}^3}\int_{\mathbb{R}^3}\int_{\mathbb{S}_+^2}\psi_i\left[f_i'f_j'-f_if_j\right]\Theta(\langle\epsilon,\xi_i\rangle-\Gamma_{ij})\langle\epsilon,\xi_i\rangle d\epsilon d\boldsymbol{c}_j d\boldsymbol{c}_i \qquad (4.40)\\ &= -\frac{1}{4}\beta_{ij}\sigma_{ij}^2\int_{\mathbb{R}^3}\int_{\mathbb{R}^3}\int_{\mathbb{S}_+^2}\left[\psi_i+\psi_j-\psi_i'-\psi_j'\right]\left[f_i'f_j'-f_if_j\right]\\ &\qquad\times\Theta(\langle\epsilon,\xi_i\rangle-\Gamma_{ij})\langle\epsilon,\xi_i\rangle d\epsilon d\boldsymbol{c}_j d\boldsymbol{c}_i.\end{aligned}$$

First we prove condition (4.39). We start by taking the left-hand side of the equality and rename the velocities as follows: the pre-collisional velocities become now $\boldsymbol{c}_i'$, $\boldsymbol{c}_s'$ and the post-collisional velocities become $\boldsymbol{c}_i$, $\boldsymbol{c}_s$. Then we perform the transformation $(\boldsymbol{c}_i', \boldsymbol{c}_s') \mapsto (\boldsymbol{c}_i, \boldsymbol{c}_s)$ whose Jacobian is 1. The described steps can be represented by

$$\begin{aligned}
&\sigma_{is}^2 \int_{\mathbb{R}^3} \int_{\mathbb{R}^3} \int_{\mathbb{S}_+^2} \psi_i \left[f_i' f_s' - f_i f_s\right] \langle \epsilon, \boldsymbol{c}_i - \boldsymbol{c}_s \rangle d\epsilon d\boldsymbol{c}_s d\boldsymbol{c}_i \\
&= \sigma_{is}^2 \int_{\mathbb{R}^3} \int_{\mathbb{R}^3} \int_{\mathbb{S}_+^2} \psi_i' \left[f_i f_s - f_i' f_s'\right] \langle \epsilon, \boldsymbol{c}_i' - \boldsymbol{c}_s' \rangle d\epsilon d\boldsymbol{c}_s' d\boldsymbol{c}_i' \\
&= -\sigma_{is}^2 \int_{\mathbb{R}^3} \int_{\mathbb{R}^3} \int_{\mathbb{S}_+^2} \psi_i' \left[f_i' f_s' - f_i f_s\right] \langle \epsilon, \boldsymbol{c}_i - \boldsymbol{c}_s \rangle d\epsilon d\boldsymbol{c}_s d\boldsymbol{c}_i.
\end{aligned}$$

Thus we have

$$\begin{aligned}
&\sigma_{is}^2 \int_{\mathbb{R}^3} \int_{\mathbb{R}^3} \int_{\mathbb{S}_+^2} \psi_i \left[f_i' f_s' - f_i f_s\right] \langle \epsilon, \boldsymbol{c}_i - \boldsymbol{c}_s \rangle d\epsilon d\boldsymbol{c}_s d\boldsymbol{c}_i \\
&= \frac{1}{2} \sigma_{is}^2 \int_{\mathbb{R}^3} \int_{\mathbb{R}^3} \int_{\mathbb{S}_+^2} \left[\psi_i - \psi_i'\right] \left[f_i' f_s' - f_i f_s\right] \langle \epsilon, \boldsymbol{c}_i - \boldsymbol{c}_s \rangle d\epsilon d\boldsymbol{c}_s d\boldsymbol{c}_i. \quad (4.41)
\end{aligned}$$

Now, considering the right-hand side of Eq. (4.41), we rename the velocities $\boldsymbol{c}_i$ and $\boldsymbol{c}_s$ by changing the indices i and s of the particles. By taking into account that $\sigma_{is} = \sigma_{si}$, we have

$$\begin{aligned}
&\frac{1}{2} \sigma_{is}^2 \int_{\mathbb{R}^3} \int_{\mathbb{R}^3} \int_{\mathbb{S}_+^2} \left[\psi_i - \psi_i'\right] \left[f_i' f_s' - f_i f_s\right] \langle \epsilon, \boldsymbol{c}_i - \boldsymbol{c}_s \rangle d\epsilon d\boldsymbol{c}_s d\boldsymbol{c}_i \\
&= \frac{1}{2} \sigma_{is}^2 \int_{\mathbb{R}^3} \int_{\mathbb{R}^3} \int_{\mathbb{S}_+^2} \left[\psi_s - \psi_s'\right] \left[f_i' f_s' - f_i f_s\right] \langle \epsilon, \boldsymbol{c}_i - \boldsymbol{c}_s \rangle d\epsilon d\boldsymbol{c}_s d\boldsymbol{c}_i. \quad (4.42)
\end{aligned}$$

Therefore, combining expressions (4.41) and (4.42), we derive expression (4.39). Then, we prove condition (4.40) using a similar procedure and the conclusion comes out. □

Proposition 4.3.2. *If* $0 \leq \beta_{ij} = \beta_{ji} \leq 1$ *(*$i = 1, \ldots, 4$*) and* $\beta_{12}\sigma_{12}^2 = \beta_{34}\sigma_{34}^2$*, then we have*

$$\begin{aligned}\sum_{i=1}^{4} \int_{\mathbb{R}^3} \psi_i \mathcal{Q}_i^R d\boldsymbol{c}_i &= \beta_{12}\sigma_{12}^2 \int_{\mathbb{R}^3}\int_{\mathbb{R}^3}\int_{\mathbb{S}_+^2} [\psi_1 + \psi_2 - \psi_3 - \psi_4] \qquad (4.43)\\ &\times \left[\left(\frac{\mu_{12}}{\mu_{34}}\right)^2 f_3 f_4 - f_1 f_2\right] \Theta(\langle \epsilon, \xi\rangle - \Gamma_{12})\langle \epsilon, \xi\rangle d\epsilon d\boldsymbol{c}_2 d\boldsymbol{c}_1\\ &= \beta_{34}\sigma_{34}^2 \int_{\mathbb{R}^3}\int_{\mathbb{R}^3}\int_{\mathbb{S}_+^2} [\psi_3 + \psi_4 - \psi_1 - \psi_2] \qquad (4.44)\\ &\times \left[\left(\frac{\mu_{34}}{\mu_{12}}\right)^2 f_1 f_2 - f_3 f_4\right] \Theta(\langle \epsilon, \xi'\rangle - \Gamma_{34})\langle \epsilon, \xi'\rangle d\epsilon d\boldsymbol{c}_4 d\boldsymbol{c}_3.\end{aligned}$$

Proof: It is easy to verify, by inspection, that

$$\begin{aligned}\int_{\mathbb{R}^3} \psi_2 \mathcal{Q}_2^R d\boldsymbol{c}_2 &= \beta_{12}\sigma_{12}^2 \int_{\mathbb{R}^3}\int_{\mathbb{R}^3}\int_{\mathbb{S}_+^2} \psi_2 \left[\left(\frac{\mu_{12}}{\mu_{34}}\right)^2 f_3 f_4 - f_1 f_2\right] \qquad (4.45)\\ &\times \Theta(\langle \epsilon, \xi\rangle - \Gamma_{12})\langle \epsilon, \xi\rangle d\epsilon d\boldsymbol{c}_2 d\boldsymbol{c}_1.\end{aligned}$$

We now prove that

$$\begin{aligned}\int_{\mathbb{R}^3} \psi_3 \mathcal{Q}_3^R d\boldsymbol{c}_3 &= -\beta_{12}\sigma_{12}^2 \int_{\mathbb{R}^3}\int_{\mathbb{R}^3}\int_{\mathbb{S}_+^2} \psi_3 \left[\left(\frac{\mu_{12}}{\mu_{34}}\right)^2 f_3 f_4 - f_1 f_2\right] \qquad (4.46)\\ &\times \Theta(\langle \epsilon, \xi\rangle - \Gamma_{12})\langle \epsilon, \xi\rangle d\epsilon d\boldsymbol{c}_2 d\boldsymbol{c}_1.\end{aligned}$$

We perform the transformation $(\boldsymbol{c}_3, \boldsymbol{c}_4) \mapsto (\boldsymbol{c}_1, \boldsymbol{c}_2)$ in the integral on the left-hand side of Eq. (4.46), and the corresponding Jacobian is $\left(\frac{\mu_{12}}{\mu_{34}}\right)^{3/2} \frac{\langle \epsilon, \xi\rangle}{\alpha^-}$, see Lemma 4.2.3. By using expression (4.27) of Lemma 4.2.2 we may easily prove that

$$\langle \epsilon, \xi'\rangle - \Gamma_{34} > 0 \Leftrightarrow \langle \epsilon, \xi\rangle - \Gamma_{12} > 0,$$

and thus

$$\Theta(\langle \epsilon, \xi'\rangle - \Gamma_{34}) = \Theta(\langle \epsilon, \xi\rangle - \Gamma_{12}).$$

With this transformation we obtain

$$\int_{\mathbb{R}^3} \psi_3 \mathcal{Q}_3^R d\boldsymbol{c}_3 = \beta_{34}\sigma_{34}^2 \int_{\mathbb{R}^3}\int_{\mathbb{R}^3}\int_{\mathbb{S}_+^2} \psi_3 \left[\left(\frac{\mu_{34}}{\mu_{12}}\right)^2 f_3 f_4 - f_1 f_2 \right] \times \Theta(\langle \epsilon, \xi \rangle - \Gamma_{12}) \left(\frac{\mu_{12}}{\mu_{34}}\right)^2 \langle \epsilon, \xi \rangle d\epsilon d\boldsymbol{c}_2 d\boldsymbol{c}_1.$$

Now, performing some simplifications and taking into account the assumption $\beta_{12}\sigma_{12}^2 = \beta_{34}\sigma_{34}^2$, we obtain condition (4.46).
A similar procedure may be used to prove that

$$\int_{\mathbb{R}^3} \psi_4 \mathcal{Q}_4^R d\boldsymbol{c}_4 = -\beta_{12}\sigma_{12}^2 \int_{\mathbb{R}^3}\int_{\mathbb{R}^3}\int_{\mathbb{S}_+^2} \psi_4 \left[\left(\frac{\mu_{12}}{\mu_{34}}\right)^2 f_3 f_4 - f_1 f_2 \right] \times \Theta(\langle \epsilon, \xi \rangle - \Gamma_{12}) \langle \epsilon, \xi \rangle d\epsilon d\boldsymbol{c}_2 d\boldsymbol{c}_1. \tag{4.47}$$

Now, combining conditions (4.45), (4.46) and (4.47), we prove condition (4.43). The proof of condition (4.44) follows a similar procedure. □

Propositions 4.3.1 and 4.3.2 are fundamental for the proof of the following results.

Proposition 4.3.3. *The elastic collisional terms are such that*

$$\int_{\mathbb{R}^3} \mathcal{Q}_i^E d\boldsymbol{c}_i = 0, \qquad i = 1, ..., 4. \tag{4.48}$$

Proof: The proof comes directly from Proposition 4.3.1 by considering $\psi_i = 1$, $i = 1, ..., 4$. □

Proposition 4.3.3 states that elastic encounters do not change the number of particles of each constituent.

Proposition 4.3.4. *The reaction terms satisfy the following property:*

$$\int_{\mathbb{R}^3} \mathcal{Q}_1^R d\boldsymbol{c}_1 = \int_{\mathbb{R}^3} \mathcal{Q}_2^R d\boldsymbol{c}_2 = -\int_{\mathbb{R}^3} \mathcal{Q}_3^R d\boldsymbol{c}_3 = -\int_{\mathbb{R}^3} \mathcal{Q}_4^R d\boldsymbol{c}_4. \tag{4.49}$$

Proof: These results come directly from Proposition 4.3.2 by considering $\psi = (0,1,0,0)$, $\psi = (0,0,1,0)$ and $\psi = (0,0,0,1)$. □

Proposition 4.3.4 states that the variation of the number of particles of constituent A_1 is the same as that of constituent A_2 and symmetric to the variation of constituents A_3 and A_4.
Now we recall the definition of collisional invariants and present the definition of elastic collisional invariants.

Definition 4.3.1. *A function $\psi = (\psi_i, \psi_s, \psi_i', \psi_s')$ is an* **elastic collisional invariant** *in the velocity space if*

$$\int_{\mathbb{R}^3} \psi_i \mathcal{Q}_i^E d\boldsymbol{c}_i + \int_{\mathbb{R}^3} \psi_s \mathcal{Q}_s^E d\boldsymbol{c}_s + \int_{\mathbb{R}^3} \psi_i' \mathcal{Q}_i^E d\boldsymbol{c}_i' + \int_{\mathbb{R}^3} \psi_s' \mathcal{Q}_s^E d\boldsymbol{c}_s' = 0. \tag{4.50}$$

Definition 4.3.2. *A function $\psi = (\psi_1, \psi_2, \psi_3, \psi_4)$ is a* **collisional invariant** *in the velocity space, for the SRS model, if*

$$\sum_{i=1}^{4} \int_{\mathbb{R}^3} \psi_i \left(\mathcal{Q}_i^E + \mathcal{Q}_i^R\right) d\boldsymbol{c}_i = 0. \tag{4.51}$$

Proposition 4.3.5. *Functions $\psi = (1,1,1,1)$, $\psi = (m_i c_l^i, m_s c_l^s, m_i {c'}_l^i, m_s {c'}_l^s)$, $l = 1,2,3$, and $\psi = (\boldsymbol{c}_i^2 m_i, \boldsymbol{c}_s^2 m_s, \boldsymbol{c}'^2_i m_i, \boldsymbol{c}'^2_s m_s)$ are elastic collisional invariants, for $i, s = 1, ..., 4$.*

Proof: These results come from the direct application of Proposition 4.3.1 and conservation laws (4.2) and (4.3). □

All functions ψ which are a linear combination of the above five functions introduced in Proposition 4.3.5 are also elastic collisional invariants. They can be defined by

$$\psi_i = G_i + \mathbf{H}_i \cdot m_i \boldsymbol{c}_i + J_i \boldsymbol{c}_i^2, \tag{4.52}$$

where G_i and J_i are two scalar functions and $\mathbf{H}_i$ a vectorial function, all of them being independent of $\boldsymbol{c}_i$.

Proposition 4.3.6. *Functions $\psi = (1, 0, 1, 0)$, $\psi = (1, 0, 0, 1)$, $\psi = (0, 1, 1, 0)$, and functions $\psi = (\psi_1, \psi_2, \psi_3, \psi_4)$ defined by $\psi_i = m_i c_1^i$, $\psi_i = m_i c_2^i$, $\psi_i = m_i c_3^i$ and $\psi_i = E_i + \frac{1}{2}\boldsymbol{c}_i^2 m_i$ are collisional invariants.*

Proof: These results come directly from Propositions 4.3.1 and 4.3.2 and conservation laws (4.5) and (4.6). □

All functions ψ, which are a linear combination of the seven functions introduced in Proposition 4.3.6 are also collisional invariants. They can be defined by

$$\psi_i = G_i + \mathbf{H}_i \cdot m_i \boldsymbol{c}_i + J_i (E_i + \frac{1}{2}\boldsymbol{c}_i^2), \tag{4.53}$$

where G_i and J_i are two scalar functions, such that $G_1 + G_2 = G_3 + G_4$, and $\mathbf{H}_i$ a vectorial function, all of them being independent of $\boldsymbol{c}_i$.

4.4 Boltzmann H-theorem

In this section we prove the existence of an H-function (Liapunov functional) for the SRS system (4.29), (4.30) and (4.34). This result is related to the physical trend to equilibrium that will be presented in the next section.

Proposition 4.4.1. *If $0 \le \beta_{ij} = \beta_{ji} \le 1$ $(i = 1, \ldots, 4)$ and $\beta_{12}\sigma_{12}^2 = \beta_{34}\sigma_{34}^2$,* *the convex function* $\mathsf{H}(t)$*, defined by*

$$\mathsf{H}(t) = \sum_{i=1}^{4} \int_{\Omega} \int_{\mathbb{R}^3} f_i \log\left(\frac{f_i}{\mu_{ij}}\right) d\boldsymbol{c}_i d\boldsymbol{x}, \tag{4.54}$$

where $(i,j) \in \{(1,2),(2,1),(3,4),(4,3)\}$*,* $f_i \in L^1(\mathbb{R}^3_{\boldsymbol{x}})$ *for all* $i = 1,..,4$*, and* $\Omega = \mathbb{R}^3$*, is an H-function (Liapunov functional) for the system (4.29), (4.30) and (4.34).*

Proof: We start by multiplying Eq. (4.29) by $1+\log\left(\frac{f_i}{\mu_{ij}}\right)$, with $i = 1,...,4$ and $(i,j) \in (1,2),(2,1),(3,4),(4,3)$. Then we integrate the resulting equations over $\Omega \times \mathbb{R}$, sum over all constituents and use Propositions 4.3.1 and 4.3.2 with $\psi_i = \log\left(\frac{f_i}{\mu_{ij}}\right)$. We treat separately each term in Eq. (4.29) and then conclude the proof gathering the results and considering the complete equation.

If we multiply $\frac{\partial}{\partial t} f_i$ by $1+\log\left(\frac{f_i}{\mu_{ij}}\right)$, integrate over $\Omega \times \mathbb{R}^3$ and sum over all constituents we get

$$\begin{aligned}
&\sum_{i=1}^{4} \int_{\Omega} \int_{\mathbb{R}^3} \left[1+\log\left(\frac{f_i}{\mu_{ij}}\right)\right] \frac{\partial}{\partial t} f_i d\boldsymbol{c}_i d\boldsymbol{x} \\
&\quad = \sum_{i=1}^{4} \int_{\Omega} \int_{\mathbb{R}^3} \left[\log\left(\frac{f_i}{\mu_{ij}}\right) \frac{\partial}{\partial t} f_i + \frac{1}{f_i} f_i \frac{\partial}{\partial t} f_i\right] d\boldsymbol{c}_i d\boldsymbol{x} \\
&\quad = \sum_{i=1}^{4} \int_{\Omega} \int_{\mathbb{R}^3} \frac{\partial}{\partial t}\left[f_i \log\left(\frac{f_i}{\mu_{ij}}\right)\right] d\boldsymbol{c}_i d\boldsymbol{x},
\end{aligned}$$

therefore

$$\sum_{i=1}^{4} \int_{\Omega} \int_{\mathbb{R}^3} \left[1+\log\left(\frac{f_i}{\mu_{ij}}\right)\right] \frac{\partial}{\partial t} f_i d\boldsymbol{c}_i d\boldsymbol{x} = \frac{d}{dt} \sum_{i=1}^{4} \int_{\Omega} \int_{\mathbb{R}^3} f_i \log\left(\frac{f_i}{\mu_{ij}}\right) d\boldsymbol{c}_i d\boldsymbol{x}. \tag{4.55}$$

Now, if we multiply $\sum_{l=1}^{3} c_l^i \frac{\partial}{\partial x_l} f_i$ by $1+\log\left(\frac{f_i}{\mu_{ij}}\right)$, integrate over $\Omega \times \mathbb{R}^3$ and sum over all constituents we get

$$\sum_{i=1}^{4}\int_{\Omega}\int_{\mathbb{R}^3}\left[1+\log\left(\frac{f_i}{\mu_{ij}}\right)\right]\sum_{l=1}^{3}c_l^i\frac{\partial}{\partial x_l}f_i d\boldsymbol{c}_i d\boldsymbol{x}$$
$$= \sum_{i=1}^{4}\sum_{l=1}^{3}\int_{\mathbb{R}^3}c_l^i\int_{\Omega}\left[1+\log\left(\frac{f_i}{\mu_{ij}}\right)\right]\frac{\partial}{\partial x_l}f_i d\boldsymbol{x} d\boldsymbol{c}_i$$
$$= \sum_{i=1}^{4}\sum_{l=1}^{3}\int_{\mathbb{R}^3}c_l^i\int_{\Omega}\frac{\partial}{\partial x_l}\left[f_i\log\left(\frac{f_i}{\mu_{ij}}\right)\right]d\boldsymbol{x} d\boldsymbol{c}_i.$$

Since $\Omega=\mathbb{R}^3$, we have

$$\sum_{i=1}^{4}\int_{\Omega}\int_{\mathbb{R}^3}\left[1+\log\left(\frac{f_i}{\mu_{ij}}\right)\right]\sum_{l=1}^{3}c_l^i\frac{\partial}{\partial x_l}f_i d\boldsymbol{c}_i d\boldsymbol{x}$$
$$= \sum_{i=1}^{4}\sum_{l=1}^{3}\int_{\mathbb{R}^3}c_l^i\lim_{r\to+\infty}\int_{B(0,r)}\frac{\partial}{\partial x_l}\left[f_i\log\left(\frac{f_i}{\mu_{ij}}\right)\right]d\boldsymbol{x} d\boldsymbol{c}_i,$$

where $B(0,r)=\{\boldsymbol{x}\in\mathbb{R}^3:\|x\|<r\}$. Using the divergence theorem we obtain

$$\sum_{i=1}^{4}\int_{\Omega}\int_{\mathbb{R}^3}\left[1+\log\left(\frac{f_i}{\mu_{ij}}\right)\right]\sum_{l=1}^{3}c_l^i\frac{\partial}{\partial x_l}f_i d\boldsymbol{c}_i d\boldsymbol{x}$$
$$= \sum_{i=1}^{4}\sum_{l=1}^{3}\int_{\mathbb{R}^3}c_l^i\lim_{r\to+\infty}\oint_{\mathbb{S}_r^2}f_i\log\left(\frac{f_i}{\mu_{ij}}\right)d\boldsymbol{x} d\boldsymbol{c}_i,$$

where $\mathbb{S}_r^2=\{\boldsymbol{x}\in\mathbb{R}^3:\|x\|=r\}$. Since $f_i\in L^1(\mathbb{R}^3_{\boldsymbol{x}})$ the integral $\oint_{\mathbb{S}_r^2}f_i\log\left(\frac{f_i}{\mu_{ij}}\right)d\boldsymbol{x}$ vanishes for sufficiently large values of r, and we conclude that

$$\sum_{i=1}^{4}\int_{\Omega}\int_{\mathbb{R}^3}\left[1+\log\left(\frac{f_i}{\mu_{ij}}\right)\right]\sum_{l=1}^{3}c_l^i\frac{\partial}{\partial x_l}f_i d\boldsymbol{c}_i d\boldsymbol{x}=0. \tag{4.56}$$

If we multiply $\mathcal{Q}_i^E$ by $1+\log\left(\frac{f_i}{\mu_{ij}}\right)$, integrate over $\Omega\times\mathbb{R}^3$ and use Proposition

4.3.1 with $\psi_i = 1 + \log\left(\frac{f_i}{\mu_{ij}}\right)$, we get

$$\int_\Omega \int_{\mathbb{R}^3} \left[1 + \log\left(\frac{f_i}{\mu_{ij}}\right)\right] \mathcal{Q}_i^E d\boldsymbol{c}_i d\boldsymbol{x}$$

$$= \frac{1}{4} \int_\Omega \left\{ \sum_{s=1}^{4} \sigma_{is}^2 \int_{\mathbb{R}^3} \int_{\mathbb{R}^3} \int_{\mathbb{S}_+^2} \log\left(\frac{f_i f_s}{f_i' f_s'}\right) [f_i' f_s' - f_i f_s] \langle \epsilon, \boldsymbol{c}_i - \boldsymbol{c}_s \rangle d\epsilon d\boldsymbol{c}_s d\boldsymbol{c}_i \right.$$

$$\left. - \beta_{ij} \sigma_{ij}^2 \int_{\mathbb{R}^3} \int_{\mathbb{R}^3} \int_{\mathbb{S}_+^2} \log\left(\frac{f_i f_j}{f_i' f_j'}\right) [f_i' f_j' - f_i f_j] \Theta(\langle \epsilon, \xi_i \rangle - \Gamma_{ij}) \langle \epsilon, \xi_i \rangle d\epsilon d\boldsymbol{c}_j d\boldsymbol{c}_i \right\} d\boldsymbol{x}.$$

$$= \frac{1}{4} \int_\Omega \sum_{s=1}^{4} \sigma_{is}^2 \int_{\mathbb{R}^3} \int_{\mathbb{R}^3} \int_{\mathbb{S}_+^2} \log\left(\frac{f_i f_s}{f_i' f_s'}\right) [f_i' f_s' - f_i f_s] \langle \epsilon, \boldsymbol{c}_i - \boldsymbol{c}_s \rangle$$

$$\times \left(1 - \gamma_{is} \Theta(\langle \epsilon, \xi_i \rangle - \Gamma_{is})\right) d\epsilon d\boldsymbol{c}_s d\boldsymbol{c}_i d\boldsymbol{x},$$

where $\gamma_{is} = \beta_{is}$ for $(i, s) \in \{(1,2), (2,1), (3,4), (4,3)\}$ and zero otherwise. Since the steric factor and the Heaviside function are such that $0 \leq \beta_{ij} \leq 1$, $0 \leq \Theta(\langle \epsilon, \xi_i \rangle - \Gamma_{ij}) \leq 1$ and the integration over ϵ is performed in $\mathbb{S}_+^2$ so that $\langle \epsilon, \xi_i \rangle \geq 0$, from the well known inequality

$$\log\left(\frac{a}{b}\right) [b - a] \leq 0, \qquad a > 0, \quad b > 0, \tag{4.57}$$

we conclude that

$$\int_\Omega \int_{\mathbb{R}^3} \left[1 + \log\left(\frac{f_i}{\mu_{ij}}\right)\right] \mathcal{Q}_i^E d\boldsymbol{c}_i d\boldsymbol{x} \leq 0, \tag{4.58}$$

and thus,

$$\sum_{i=1}^{4} \int_\Omega \int_{\mathbb{R}^3} \left[1 + \log\left(\frac{f_i}{\mu_{ij}}\right)\right] \mathcal{Q}_i^E d\boldsymbol{c}_i d\boldsymbol{x} \leq 0. \tag{4.59}$$

Finally, if we multiply $\mathcal{Q}_i^R$ by $1 + \log\left(\frac{f_i}{\mu_{ij}}\right)$, integrate over $\Omega \times \mathbb{R}^3$ and use

Proposition 4.3.2 with $\psi_i = 1 + \log\left(\frac{f_i}{\mu_{ij}}\right)$, we get

$$\sum_{i=1}^{4} \int_\Omega \int_{\mathbb{R}^3} \left[1 + \log\left(\frac{f_i}{\mu_{ij}}\right)\right] \mathcal{Q}_i^R d\boldsymbol{c}_i d\boldsymbol{x}$$
$$= \beta_{12}\sigma_{12}^2 \int_\Omega \int_{\mathbb{R}^3} \int_{\mathbb{S}_+^2} \log\left(\frac{f_1 f_2}{\left(\frac{\mu_{12}}{\mu_{34}}\right)^2 f_3 f_4}\right) \left[\left(\frac{\mu_{12}}{\mu_{34}}\right)^2 f_3 f_4 - f_1 f_2\right]$$
$$\times \Theta(\langle\epsilon,\xi\rangle - \Gamma_{12})\langle\epsilon,\xi\rangle d\epsilon d\boldsymbol{c}_2 d\boldsymbol{c}_1.$$

Since the steric factor and the Heaviside function are such that $0 \le \beta_{12} \le 1$, $0 \le \Theta(\langle\epsilon,\xi\rangle - \Gamma_{12}) \le 1$ and the integration over ϵ is performed in $\mathbb{S}_+^2$ so that $\langle\epsilon,\xi\rangle \ge 0$, from the well known inequality (4.57) we conclude that

$$\sum_{i=1}^{4} \int_\Omega \int_{\mathbb{R}^3} \left[1 + \log\left(\frac{f_i}{\mu_{ij}}\right)\right] \mathcal{Q}_i^R d\boldsymbol{c}_i d\boldsymbol{x} \le 0. \tag{4.60}$$

Now, if we consider all terms in Eq. (4.29) and take into account the partial results (4.55), (4.56), (4.59) and (4.60) we have

$$\frac{d}{dt} \sum_{i=1}^{4} \int_\Omega \int_{\mathbb{R}^3} f_i \log\left(\frac{f_i}{\mu_{ij}}\right) d\boldsymbol{c}_i d\boldsymbol{x} \le 0, \tag{4.61}$$

which concludes the proof. □

Note 4.4.1. *When we consider the case of a spatial homogeneous evolution, the domain* Ω *is irrelevant for the result stated in Proposition 4.4.1. In the general case considered in the proposition, there exists a limited range of known situations, for which the result is still valid. Some of them correspond to consider* Ω *as a box with boundary conditions of periodic type or boundary conditions of specular reflection at the walls, see for instance [17, 19, 85].*

4.5 Equilibrium distributions

In this section we characterize the mechanical and the thermodynamical equilibrium states of the reactive gas mixture, in particular we define the Maxwellian distribution and introduce the appropriate mass action law.

Proposition 4.5.1. *The following expressions are equivalent:*

1) $$f_i = n_i \left(\frac{m_i}{2\pi kT}\right)^{3/2} \exp\left[-\frac{m_i(\boldsymbol{c}_i - v)^2}{2kT}\right], \quad i = 1, .., 4 \tag{4.62}$$

and

$$n_1 n_2 = n_3 n_4 \sqrt{\frac{\mu_{12}}{\mu_{34}}} \exp\left[Q_R/kT\right]; \tag{4.63}$$

2) $\mathcal{Q}_i^E = 0$ *and* $\mathcal{Q}_i^R = 0$, *for* $i = 1, ..., 4$;

3) $$\sum_{i=1}^{4} \int_{\mathbb{R}^3} \left[\mathcal{Q}_i^E + \mathcal{Q}_i^R\right] \log\left(\frac{f_i}{\mu_{ij}}\right) d\boldsymbol{c}_i = 0.$$

Proof: We prove that *1)* $\Rightarrow$ *2)* $\Rightarrow$ *3)* $\Rightarrow$ *1)*. For the first implication we introduce the expression (4.62) of f_i in the elastic operator $\mathcal{Q}_i^E$ defined in Eq. (4.30), obtaining

$$\begin{aligned} f_i' f_s' - f_i f_s \quad = \quad & n_i n_s \frac{(m_i m_s)^{3/2}}{(2\pi kT)^3} \left\{ \exp\left[-\frac{m_i(\boldsymbol{c}_i' - v)^2 + m_s(\boldsymbol{c}_s' - v)^2}{2kT}\right] \right. \\ & \left. - \exp\left[-\frac{m_i(\boldsymbol{c}_i - v)^2 + m_s(\boldsymbol{c}_s - v)^2}{2kT}\right] \right\}. \end{aligned}$$

Now, using the conservation equations of linear momentum and total energy for elastic collisions, namely Eqs. (4.2) and (4.3), we notice that

$$(\boldsymbol{c}_i' - v)^2 + m_s(\boldsymbol{c}_s' - v)^2 = (\boldsymbol{c}_i - v)^2 + m_s(\boldsymbol{c}_s - v)^2,$$

and we get $f_i' f_s' - f_i f_s = 0$ for all $i, s = 1, ..., 4$. Thus $\mathcal{Q}_i^E = 0$ for all $i = 1, ..., 4$. We proceed similarly with the reactive operator $\mathcal{Q}_i^R$ defined in Eq. (4.34).

In particular, when $i = 3$, we have

$$\left(\frac{\mu_{34}}{\mu_{12}}\right)^2 f_1 f_2 - f_3 f_4$$

$$= \left(\frac{\mu_{34}}{\mu_{12}}\right)^2 n_1 n_2 \frac{(m_1 m_2)^{3/2}}{(2\pi kT)^3} \exp\left[-\frac{m_1(\boldsymbol{c}_1 - v)^2 + m_2(\boldsymbol{c}_2 - v)^2}{2kT}\right]$$
$$- n_3 n_4 \frac{(m_3 m_4)^{3/2}}{(2\pi kT)^3} \exp\left[-\frac{m_3(\boldsymbol{c}_3 - v)^2 + m_4(\boldsymbol{c}_4 - v)^2}{2kT}\right].$$

By using the conservation laws of mass, linear momentum and total energy for reactive collisions, namely Eqs. (4.4), (4.5) and (4.6), we conclude that

$$\left(\frac{\mu_{34}}{\mu_{12}}\right)^2 f_1 f_2 - f_3 f_4$$

$$= \exp\left[-\frac{m_3(\boldsymbol{c}_3 - v)^2 + m_4(\boldsymbol{c}_4 - v)^2}{2kT}\right] \exp\left[-\frac{Q_R}{kT}\right] \left(\frac{\mu_{34}}{\mu_{12}}\right)^2 (m_1 m_2)^{3/2}$$
$$\times \left\{ n_1 n_2 - n_3 n_4 \sqrt{\frac{\mu_{12}}{\mu_{34}}} \exp\left[Q_R/kT\right] \right\}.$$

Taking into account condition (4.63), we conclude that

$$\left(\frac{\mu_{34}}{\mu_{12}}\right)^2 f_1 f_2 - f_3 f_4 = 0,$$

and thus $\mathcal{Q}_3^R = 0$. A similar procedure can also be used to prove that $\mathcal{Q}_1^R = \mathcal{Q}_2^R = \mathcal{Q}_4^R = 0$. Therefore the proof of the first implication is concluded.

The second implication, *2)* $\Rightarrow$ *3)*, is trivially verified.

We now prove the implication *3)* $\Rightarrow$ *1)*. First, using Propositions 4.3.1 and 4.3.2, we have

$$\sum_{i=1}^{4} \int_{\mathbb{R}^3} \left[\mathcal{Q}_i^E + \mathcal{Q}_i^R\right] \log\left(\frac{f_i}{\mu_{ij}}\right) d\boldsymbol{c}_i = 0,$$

if and only if,

$$
\begin{aligned}
&\frac{1}{4}\sum_{i=1}^{4}\left[\sum_{s=1}^{4}\sigma_{is}^2\int_{\mathbb{R}^3}\int_{\mathbb{R}^3}\int_{\mathbb{S}_+^2}\log\left(\frac{f_if_s}{f_i'f_s'}\right)[f_i'f_s'-f_if_s]\langle\epsilon,\boldsymbol{c}_i-\boldsymbol{c}_s\rangle d\epsilon d\boldsymbol{c}_j d\boldsymbol{c}_i\right.\\
&\qquad\left.-\beta_{ij}\sigma_{ij}^2\int_{\mathbb{R}^3}\int_{\mathbb{R}^3}\int_{\mathbb{S}_+^2}\log\left(\frac{f_if_j}{f_i'f_j'}\right)[f_i'f_j'-f_if_j]\Theta(\langle\epsilon,\xi_i\rangle-\Gamma_{ij})\langle\epsilon,\xi_i\rangle d\epsilon d\boldsymbol{c}_j d\boldsymbol{c}_i\right]\\
&\qquad+\beta_{12}\sigma_{12}^2\int_{\mathbb{R}^3}\int_{\mathbb{R}^3}\int_{\mathbb{S}_+^2}\log\left[\left(\frac{\mu_{34}}{\mu_{12}}\right)^2\frac{f_1f_2}{f_3f_4}\right]\left[\left(\frac{\mu_{12}}{\mu_{34}}\right)^2 f_3f_4-f_1f_2\right]\\
&\qquad\times\Theta(\langle\epsilon,\xi\rangle-\Gamma_{12})\langle\epsilon,\xi\rangle d\epsilon d\boldsymbol{c}_2 d\boldsymbol{c}_1=0,
\end{aligned}
$$

that is

$$
\begin{aligned}
&\frac{1}{4}\sum_{i=1}^{4}\sum_{s=1}^{4}\sigma_{is}^2\int_{\mathbb{R}^3}\int_{\mathbb{R}^3}\int_{\mathbb{S}_+^2}\log\left(\frac{f_if_s}{f_i'f_s'}\right)[f_i'f_s'-f_if_s]\langle\epsilon,\boldsymbol{c}_i-\boldsymbol{c}_s\rangle\\
&\qquad\qquad\qquad\qquad\times\left(1-\gamma_{is}\Theta(\langle\epsilon,\xi_i\rangle-\Gamma_{is})\right)d\epsilon d\boldsymbol{c}_s d\boldsymbol{c}_i\\
&\quad+\beta_{12}\sigma_{12}^2\int_{\mathbb{R}^3}\int_{\mathbb{R}^3}\int_{\mathbb{S}_+^2}\log\left[\left(\frac{\mu_{34}}{\mu_{12}}\right)^2\frac{f_1f_2}{f_3f_4}\right]\left[\left(\frac{\mu_{12}}{\mu_{34}}\right)^2 f_3f_4-f_1f_2\right]\\
&\qquad\qquad\qquad\qquad\times\Theta(\langle\epsilon,\xi\rangle-\Gamma_{12})\langle\epsilon,\xi\rangle d\epsilon d\boldsymbol{c}_2 d\boldsymbol{c}_1=0,
\end{aligned}
$$

where $\gamma_{is}=\beta_{is}$ for $(i,s)\in\{(1,2),(2,1),(3,4),(4,3)\}$ and zero otherwise. Since the steric factor and the Heaviside function are such that $0\leq\beta_{ij}\leq 1$, $0\leq\Theta(\langle\epsilon,\xi_i\rangle-\Gamma_{ij})\leq 1$, and the integration over ϵ is performed in $\mathbb{S}_+^2$, so that $\langle\epsilon,\xi_i\rangle\geq 0$, the previous equality is verified only if

$$\log\left(\frac{f_if_s}{f_i'f_s'}\right)[f_i'f_s'-f_if_s]=0, \tag{4.64}$$

almost everywhere in $(c_i,c_s)\in\mathbb{R}^3\times\mathbb{R}^3$, for $i,s=1,...,4$, and

$$\log\left[\left(\frac{\mu_{34}}{\mu_{12}}\right)^2\frac{f_1f_2}{f_3f_4}\right]\left[\left(\frac{\mu_{12}}{\mu_{34}}\right)^2 f_3f_4-f_1f_2\right]=0, \tag{4.65}$$

almost everywhere in $(c_1, c_2) \in \mathbb{R}^3 \times \mathbb{R}^3$. Since, for $a > 0$ and $b > 0$, we have $\log(a/b)(b-a) = 0$ if and only if $a = b$, we conclude that conditions (4.64) and (4.65) are verified if and only if

$$f_i' f_s' = f_i f_s \tag{4.66}$$

and

$$\left(\frac{\mu_{12}}{\mu_{34}}\right)^2 f_3 f_4 = f_1 f_2 \tag{4.67}$$

almost everywhere.

Now, from Eq. (4.66) we obtain

$$\log f_i' + \log f_s' = \log f_i + \log f_s. \tag{4.68}$$

Thus function $\psi = (\log f_i, \log f_s, \log f_i', \log f_s')$ is an elastic collisional invariant and from Eq. (4.52), we may write

$$\log f_i = G_i + \mathbf{H}_i \cdot m_i \boldsymbol{c}_i + J_i \boldsymbol{c}_i^2, \tag{4.69}$$

or even

$$f_i = \exp[G_i + \mathbf{H}_i \cdot m_i \boldsymbol{c}_i + J_i \boldsymbol{c}_i^2]. \tag{4.70}$$

If we now introduce expression (4.70) in the definition of the number density, velocity and pressure of the constituents and of the mixture we obtain, see [64],

$$f_i = n_i \left(\frac{m_i}{2\pi kT}\right)^{3/2} \exp\left[-\frac{m_i(\boldsymbol{c}_i - v)^2}{2kT}\right]. \tag{4.71}$$

Now, introducing expression (4.71) in Eq. (4.67) and using the conservation of the total energy for reactive collisions (4.6), we obtain

$$n_1 n_2 = n_3 n_4 \sqrt{\frac{\mu_{12}}{\mu_{34}}} \exp\left[Q_R/kT\right], \tag{4.72}$$

which concludes the proof of the third implication. □

In the proof of Proposition 4.5.1 we introduced expressions (4.62) of the distributions f_i into the elastic operators $\mathcal{Q}_i^E$ defined in Eq. (4.30), and obtained $\mathcal{Q}_i^E = 0$, for all $i = 1, ..., 4$. This vanishing of the elastic operators motivates the following definition.

Definition 4.5.1. *The Maxwellian distribution functions of mechanical equilibrium are defined by*

$$f_i^M = n_i \left(\frac{m_i}{2\pi kT}\right)^{3/2} \exp\left[-\frac{m_i(\boldsymbol{c}_i - v)^2}{2kT}\right], \quad i = 1, .., 4. \tag{4.73}$$

On the other hand, to vanish also the reactive operator, it was necessary to include also condition (4.63). This condition represents the mass action law and imposes a relation between the equilibrium number densities and temperature. This feature motivates the following definition

Definition 4.5.2. *The Maxwellian distribution functions of thermodynamical equilibrium are given by*

$$M_i(\boldsymbol{c}_i) = n_i \left(\frac{m_i}{2\pi kT}\right)^{3/2} \exp\left[-\frac{m_i(\boldsymbol{c}_i - v)^2}{2kT}\right], \tag{4.74}$$

with number densities satisfying the mass action law (4.63).

In what follows, we will use the reference frame moving with the gas mixture, in order to simplify the expression of the Maxwellian distribution functions of thermodynamical equilibrium and subsequent calculations.

4.6 Linearized SRS kinetic equations

In this section we construct the linearized SRS kinetic system. The gas mixture is considered to be close to the thermodynamical equilibrium and the distribution function f_i is expanded around the Maxwellian distribution M_i, in the form

$$f_i(\boldsymbol{x}, \boldsymbol{c}_i, t) = M_i(\boldsymbol{x}, \boldsymbol{c}_i, t)\Big[1 + h_i(\boldsymbol{x}, \boldsymbol{c}_i, t)\Big], \qquad i = 1, ..., 4, \tag{4.75}$$

where h_i represents the deviation from the equilibrium. In the sequel we will use the following result.

Lemma 4.6.1. *The Maxwellian distribution functions M_i, defined in expression (4.74), are such that*

1. *for $i = 1, ..., 4$, if $\boldsymbol{c}_i$ and $\boldsymbol{c}'_s$ are the elastic pre-collisional velocities of species A_i and A_s, respectively, and $\boldsymbol{c}'_i$ and $\boldsymbol{c}'_s$ are the corresponding elastic post-collisional velocities, we have*

$$M'_i M'_s = M_i M_s; \tag{4.76}$$

2. *for $(i, j, k, l) \in \{(1, 2, 3, 4), (2, 1, 4, 3), (3, 4, 1, 2), (4, 3, 2, 1)\}$, if $\boldsymbol{c}_i$ and $\boldsymbol{c}_j$ are the pre-collisional velocities of species A_i and A_j, respectively, and $\boldsymbol{c}_k$ and $\boldsymbol{c}_l$ are the corresponding reactive post-collisional velocities, we have*

$$\left(\frac{\mu_{ij}}{\mu_{kl}}\right)^2 M_k M_l = M_i M_j. \tag{4.77}$$

Proof: Using the conservation of total energy (4.3) for elastic collisions, we prove condition (4.76).
Now, we prove condition (4.77) for $(i, j) \in \{(1, 2), (2, 1)\}$. Using conservation equation total energy for reactive collisions (4.6), as well as the mass action

law (4.63), we have

$$
\begin{aligned}
\left(\frac{\mu_{12}}{\mu_{34}}\right)^2 M_3 M_4 = & \left(\frac{\mu_{12}}{\mu_{34}}\right)^2 n_3 n_4 \left(\frac{m_3 m_4}{(2\pi kT)^2}\right)^{3/2} \exp\left[-\frac{m_3 \boldsymbol{c}_3^2 + m_4 \boldsymbol{c}_4^2}{2kT}\right] \\
= & \left(\frac{\mu_{12}}{\mu_{34}}\right)^2 \left(\frac{\mu_{12}}{\mu_{34}}\right)^{1/2} n_1 n_2 \exp\left[-\frac{Q_R}{kT}\right] \left(\frac{m_3 m_4}{(2\pi kT)^2}\right)^{3/2} \\
& \times \exp\left[-\frac{m_1 \boldsymbol{c}_1^2 + m_2 \boldsymbol{c}_2^2 - 2Q_R}{2kT}\right] \\
= & \; n_1 n_2 \left(\frac{m_1 m_2}{(2\pi kT)^2}\right)^{3/2} \exp\left[-\frac{m_1 \boldsymbol{c}_1^2 + m_2 \boldsymbol{c}_2^2}{2kT}\right] \\
= & \; M_1 M_2.
\end{aligned}
$$

The proof of condition (4.77) for $(i, j) \in \{(3, 4), (4, 3)\}$ is similar. □

We proceed now with the derivation of the linearized SRS system.

Proposition 4.6.1. *If we neglect quadratic terms in the deviations h_i, the linearized SRS system takes the form*

$$
\frac{\partial}{\partial t} h_i + \sum_{l=1}^{3} \boldsymbol{c}_l^i \frac{\partial}{\partial x_l} h_i = \mathcal{L}_i^E(\underline{h}) + \mathcal{L}_i^R(\underline{h}) \equiv \mathcal{L}_i(\underline{h}), \qquad i = 1, ..., 4, \tag{4.78}
$$

with

$$
\begin{aligned}
\mathcal{L}_i^E(\underline{h}) = & \sum_{s=1}^{4} \sigma_{is}^2 \int_{\mathbb{R}^3} \int_{\mathbb{S}_+^2} M_s \Big[h_i' + h_s' - h_i - h_s\Big] \langle \epsilon, \boldsymbol{c}_i - \boldsymbol{c}_s \rangle \, d\epsilon \, d\boldsymbol{c}_s \\
& - \beta_{ij} \sigma_{ij}^2 \int_{\mathbb{R}^3} \int_{\mathbb{S}_+^2} M_j \Big[h_i' + h_j' - h_i - h_j\Big] \Theta(\langle \epsilon, \xi_i \rangle - \Gamma_{ij}) \, \langle \epsilon, \xi_i \rangle \, d\epsilon \, d\boldsymbol{c}_j
\end{aligned} \tag{4.79}
$$

and

$$
\mathcal{L}_i^R(\underline{h}) = \beta_{ij} \sigma_{ij}^2 \int_{\mathbb{R}^3} \int_{\mathbb{S}_+^2} M_j \left[h_k + h_l - h_i - h_j\right] \Theta(\langle \epsilon, \xi_i \rangle - \Gamma_{ij}) \langle \epsilon, \xi_i \rangle d\epsilon d\boldsymbol{c}_j, \tag{4.80}
$$

where $(i, j, k, l) \in \{(1, 2, 3, 4), (2, 1, 4, 3), (3, 4, 1, 2), (4, 3, 2, 1)\}$.

Proof: To obtain the linearized SRS system, we introduce expansions (4.75) in Eqs. (4.29), (4.30) and (4.34), and neglect quadratic terms in the deviations h_i. First we work on the left-hand side of Eq. (4.29), obtaining

$$\begin{aligned}
&\frac{\partial}{\partial t} f_i + \sum_{l=1}^{3} \boldsymbol{c}_l^i \frac{\partial}{\partial x_l} f_i \\
&= \frac{\partial}{\partial t}\Big(M_i\Big[1+h_i\Big]\Big) + \sum_{l=1}^{3} \boldsymbol{c}_l^i \frac{\partial}{\partial x_l}\Big(M_i\Big[1+h_i\Big]\Big) \\
&= \Big[1+h_i\Big]\left(\frac{\partial}{\partial t} M_i + \sum_{l=1}^{3} \boldsymbol{c}_l^i \frac{\partial}{\partial x_l} M_i\right) + M_i\left(\frac{\partial}{\partial t} h_i + \sum_{l=1}^{3} \boldsymbol{c}_l^i \frac{\partial}{\partial x_l} h_i\right).
\end{aligned}$$

Since M_i is a Maxwellian, we have

$$\frac{\partial}{\partial t} M_i + \sum_{l=1}^{3} \boldsymbol{c}_l^i \frac{\partial}{\partial x_l} M_i = 0,$$

so that,

$$\frac{\partial}{\partial t} f_i + \sum_{l=1}^{3} \boldsymbol{c}_l^i \frac{\partial}{\partial x_l} f_i = M_i\left(\frac{\partial}{\partial t} h_i + \sum_{l=1}^{3} \boldsymbol{c}_l^i \frac{\partial}{\partial x_l} h_i\right). \tag{4.81}$$

Now we linearize the elastic collisional term $\mathcal{Q}_i^E$ given in Eq. (4.30). Using Lemma 4.6.1, part 1, and neglecting quadratic terms in the deviation h_i, we obtain

$$f_i' f_s' - f_i f_s = M_i M_s\Big[h_i' + h_s' - h_i - h_s\Big].$$

Therefore the linearized elastic operator takes the form

$$\begin{aligned}
&M_i \sum_{s=1}^{4} \sigma_{is}^2 \int_{\mathbb{R}^3}\int_{\mathbb{S}^2_+} M_s\Big[h_i' + h_s' - h_i - h_s\Big]\langle \epsilon, \boldsymbol{c}_i - \boldsymbol{c}_s\rangle \, d\epsilon \, d\boldsymbol{c}_s \qquad (4.82)\\
&\quad -\beta_{ij}\sigma_{ij}^2 M_i \int_{\mathbb{R}^3}\int_{\mathbb{S}^2_+} M_j\Big[h_i' + h_j' - h_i - h_j\Big]\Theta(\langle \epsilon, \xi_i\rangle - \Gamma_{ij})\,\langle \epsilon, \xi_i\rangle \, d\epsilon \, d\boldsymbol{c}_j.
\end{aligned}$$

Now we linearize the reactive collisional term $\mathcal{Q}_i^R$ given in Eq. (4.34). Using Lemma 4.6.1, part 2, and neglecting quadratic terms in the deviation h_i, we obtain

$$\left(\frac{\mu_{ij}}{\mu_{kl}}\right)^2 f_k f_l - f_i f_j = M_i M_j \left[h_k + h_l - h_i - h_j\right].$$

Therefore, the linearized reactive operator takes the form

$$M_i \beta_{ij} \sigma_{ij}^2 \int_{\mathbb{R}^3} \int_{\mathbb{S}_+^2} M_j \left[h_k + h_l - h_i - h_j\right] \Theta(\langle \epsilon, \xi_i \rangle - \Gamma_{ij}) \langle \epsilon, \xi_i \rangle d\epsilon d\boldsymbol{c}_j. \tag{4.83}$$

At last, we insert expressions (4.81), (4.82) and (4.83) into Eq. (4.29) and divide it by M_i, obtaining the linearized SRS system in the form (4.78), (4.79) and (4.80). □

Some basic properties of the linearized SRS system will be studied in the next subsection.

4.6.1 Mathematical properties of the linearized SRS system

In order to easily compare our results with previous ones in literature, we will consider the following weighted distribution function

$$\hat{f}_i = M_i^{1/2} f_i, \qquad \text{with} \quad i = 1, ..., 4, \tag{4.84}$$

and the following weighted operator,

$$\hat{\mathcal{L}}_i(\underline{\hat{h}}) = M_i^{1/2} \mathcal{L}_i(\underline{h}), \qquad \text{with} \quad i = 1, ..., 4. \tag{4.85}$$

Just as the collisional operator $\mathcal{L}_i$, the weighted collisional operator $\hat{\mathcal{L}}_i$ may be separated in two parts, the elastic weighted collisional operator $\hat{\mathcal{L}}_i^E$ and the reactive weighted collisional operator $\hat{\mathcal{L}}_i^R$, which expressions read

$$\begin{aligned}
\hat{\mathcal{L}}_i^E(\underline{\hat{h}}) &= M_i^{1/2}\mathcal{L}_i^E(\underline{h}) \qquad (4.86)\\
&= \sum_{s=1}^{4}\sigma_{is}^2\int_{\mathbb{R}^3}\int_{\mathbb{S}_+^2}(-M_s\hat{h}_i - M_i^{1/2}M_s^{1/2}\hat{h}_s)\langle\epsilon,\boldsymbol{c}_i-\boldsymbol{c}_s\rangle\, d\epsilon\, d\boldsymbol{c}_s\\
&+ \sum_{s=1}^{4}\sigma_{is}^2\int_{\mathbb{R}^3}\int_{\mathbb{S}_+^2}M_i^{1/2}M_s\left(M_i'^{-1/2}\hat{h}_i{}' + M_s'^{-1/2}\hat{h}_s{}'\right)\langle\epsilon,\boldsymbol{c}_i-\boldsymbol{c}_s\rangle\, d\epsilon\, d\boldsymbol{c}_s\\
&- \beta_{ij}\sigma_{ij}^2\int_{\mathbb{R}^3}\int_{\mathbb{S}_+^2}(-M_j\hat{h}_i - M_i^{1/2}M_j^{1/2}\hat{h}_j)\Theta(\langle\epsilon,\xi_i\rangle-\Gamma_{ij})\,\langle\epsilon,\xi_i\rangle\, d\epsilon\, d\boldsymbol{c}_j\\
&- \beta_{ij}\sigma_{ij}^2\int_{\mathbb{R}^3}\int_{\mathbb{S}_+^2}M_i^{1/2}M_j\left(M_i'^{-1/2}\hat{h}_i{}' + M_j'^{-1/2}\hat{h}_j{}'\right)\Theta(\langle\epsilon,\xi_i\rangle-\Gamma_{ij})\,\langle\epsilon,\xi_i\rangle\, d\epsilon\, d\boldsymbol{c}_j
\end{aligned}$$

and

$$\begin{aligned}
\hat{\mathcal{L}}_i^R(\underline{\hat{h}}) &= M_i^{1/2}\mathcal{L}_i^R(\underline{h}) \qquad (4.87)\\
&= -\beta_{ij}\sigma_{ij}^2\int_{\mathbb{R}^3}\int_{\mathbb{S}_+^2}(M_j\hat{h}_i + M_i^{1/2}M_j^{1/2}\hat{h}_j)\Theta(\langle\epsilon,\xi_i\rangle-\Gamma_{ij})\,\langle\epsilon,\xi_i\rangle\, d\epsilon\, d\boldsymbol{c}_j\\
&+ \beta_{ij}\sigma_{ij}^2\int_{\mathbb{R}^3}\int_{\mathbb{S}_+^2}M_i^{1/2}M_j\left(M_k{}^{-1/2}\hat{h}_k + M_l{}^{-1/2}\hat{h}_l\right)\Theta(\langle\epsilon,\xi_i\rangle-\Gamma_{ij})\,\langle\epsilon,\xi_i\rangle\, d\epsilon\, d\boldsymbol{c}_j.
\end{aligned}$$

Note 4.6.1. *We can verify that h_i defines a solution of the linearized SRS system if and only if $\hat{h}_i$ defines a solution of the weighted linearized system*

$$\frac{\partial}{\partial t}\hat{h}_i + \sum_{l=1}^{3}\boldsymbol{c}_l^i\frac{\partial}{\partial x_l}\hat{h}_i = \hat{\mathcal{L}}_i(\underline{\hat{h}}), \qquad (4.88)$$

since Eqs. (4.88) are obtained from (4.78), multiplying by $M_i^{1/2}$.

In what follows we consider velocity L^2-space, endowed with the inner product defined by

$$\langle\underline{F},\underline{G}\rangle = \sum_{i=1}^{4}\int_{\mathbb{R}^3}F_iG_i d\boldsymbol{c}_i. \qquad (4.89)$$

The weighted linearized collisional operator satisfies the following property.

Proposition 4.6.2. *If we consider that for* $(i,j) \in \{(1,2),(2,1),(3,4),(4,3)\}$ *we have* $0 < \beta_{ij} = \beta_{ji} \leq 1$ *and* $\beta_{12}\sigma_{12}^2 = \beta_{34}\sigma_{34}^2$*, the weighted linearized collisional operator* $\hat{\mathcal{L}}$ *is symmetric and non-positive semi-definite, that is:*

1) $\langle \hat{\underline{g}}, \hat{\mathcal{L}}(\hat{\underline{h}})\rangle = \langle \hat{\underline{h}}, \hat{\mathcal{L}}(\hat{\underline{g}})\rangle$ *for all* $\underline{g}, \underline{h} \in Y^4$*;*

2) $\langle \hat{\underline{h}}, \hat{\mathcal{L}}(\hat{\underline{h}})\rangle \leq 0$*, for all* $\underline{h} \in Y^4$ *and* $\langle \hat{\underline{h}}, \hat{\mathcal{L}}(\hat{\underline{h}})\rangle = 0$ *if and only if* $\underline{h}$ *is a collisional invariant.*

Above, $Y = L^2(\mathbb{R}^3 \times \mathbb{R}^3)$*.*

Proof: With the considered inner product, if we use a procedure similar to the one employed to prove Propositions 4.3.1 and 4.3.2, we may write

$$\begin{aligned}\langle \hat{\underline{g}}, \hat{\mathcal{L}}(\hat{\underline{h}})\rangle = -\frac{1}{4}\sum_{i=1}^{4}\sum_{s=1}^{4}\sigma_{is}^2 \int_{\mathbb{R}^3}\int_{\mathbb{R}^3}\int_{\mathbb{S}_+^2} & M_i M_s \Big[g_i' + g_s' - g_i - g_s\Big]\Big[h_i' + h_s' - h_i - h_s\Big] \\ & \times \langle \epsilon, \boldsymbol{c}_i - \boldsymbol{c}_s\rangle (1 - \gamma_{is}\Theta(\langle \epsilon, \xi_i\rangle - \Gamma_{is})\,\langle \epsilon, \boldsymbol{c}_i - \boldsymbol{c}_s\rangle\, d\epsilon\, d\boldsymbol{c}_s d\boldsymbol{c}_i \\ - \sum_{i=1}^{4}\beta_{ij}\sigma_{ij}^2 \int_{\mathbb{R}^3}\int_{\mathbb{R}^3}\int_{\mathbb{S}_+^2} & M_i M_j \Big[g_k + g_l - g_i - g_j\Big]\Big[h_k + h_l - h_i - h_j\Big] \\ & \times \Theta(\langle \epsilon, \xi_i\rangle - \Gamma_{ij})\,\langle \epsilon, \xi_i\rangle\, d\epsilon\, d\boldsymbol{c}_j, \end{aligned} \tag{4.90}$$

where $\gamma_{is} = \beta_{is}$ for $(i,s) \in \{(1,2),(2,1),(3,4),(4,3)\}$ and $\gamma_{is} = 0$ otherwise. The symmetry property, part 1, of the Proposition is easily verified using condition (4.90). For the non-positivity, part 2, if we use condition (4.90) and consider $\hat{\underline{g}} = \hat{\underline{h}}$, we get

$$\begin{aligned}\langle \hat{\underline{h}}, \hat{\mathcal{L}}(\hat{\underline{h}})\rangle = -\frac{1}{4}\sum_{i=1}^{4}\sum_{s=1}^{4}\sigma_{is}^2 \int_{\mathbb{R}^3}\int_{\mathbb{R}^3}\int_{\mathbb{S}_+^2} & M_i M_s \Big[h_i' + h_s' - h_i - h_s\Big]^2 \\ & \times \langle \epsilon, \boldsymbol{c}_i - \boldsymbol{c}_s\rangle (1 - \gamma_{is}\Theta(\langle \epsilon, \xi_i\rangle - \Gamma_{is})\,\langle \epsilon, \boldsymbol{c}_i - \boldsymbol{c}_s\rangle\, d\epsilon\, d\boldsymbol{c}_s d\boldsymbol{c}_i \\ - \sum_{i=1}^{4}\beta_{ij}\sigma_{ij}^2 \int_{\mathbb{R}^3}\int_{\mathbb{R}^3}\int_{\mathbb{S}_+^2} & M_i M_j \Big[h_k + h_l - h_i - h_j\Big]^2 \\ & \times \Theta(\langle \epsilon, \xi_i\rangle - \Gamma_{ij})\,\langle \epsilon, \xi_i\rangle\, d\epsilon\, d\boldsymbol{c}_j. \end{aligned} \tag{4.91}$$

Since the steric factor and the Heaviside function are such that $0 \leq \beta_{ij} \leq 1$, $0 \leq \Theta(\langle \epsilon, \xi_i \rangle - \Gamma_{ij}) \leq 1$ and the integration over ϵ is performed in $\mathbb{S}^2_+$ so that $\langle \epsilon, \xi_i \rangle \geq 0$, we conclude that $\langle \underline{\hat{h}}, \hat{\mathcal{L}}(\underline{\hat{h}}) \rangle$ is non positive and vanishes if and only if the following two equalities

$$h_i' + h_s' - h_i - h_j = 0, \qquad \text{for} \quad i, s = 1, ..., 4, \tag{4.92}$$

and

$$h_k + h_l - h_i - h_j = 0, \tag{4.93}$$

hold almost everywhere for $(i, j, k, l) \in \{(1, 2, 3, 4), (2, 1, 4, 3), (3, 4, 1, 2), (4, 3, 2, 1)\}$. From conditions (4.92) and (4.93) we can conclude that $\underline{h}$ is a collisional invariant. □

4.6.2 Kernels of the linearized integral operators

In this subsection we present the kernels of the weighted linearized collisional operators.

Starting from the weighted linearized operators (4.86) and (4.87), we introduce the following notation

$$\begin{aligned} Q_i(\underline{\hat{h}}) = & \sum_{s=1}^{4} \sigma_{is}^2 \int_{\mathbb{R}^3} \int_{\mathbb{S}^2_+} -M_s \hat{h}_i \langle \epsilon, \boldsymbol{c}_i - \boldsymbol{c}_s \rangle \, d\epsilon \, d\boldsymbol{c}_s \\ + & \sum_{s=1}^{4} \sigma_{is}^2 \int_{\mathbb{R}^3} \int_{\mathbb{S}^2_+} -M_i^{1/2} M_s^{1/2} \hat{h}_s \langle \epsilon, \boldsymbol{c}_i - \boldsymbol{c}_s \rangle \, d\epsilon \, d\boldsymbol{c}_s \\ + & \sum_{s=1}^{4} \sigma_{is}^2 \int_{\mathbb{R}^3} \int_{\mathbb{S}^2_+} M_i^{1/2} M_s \left({M_i'}^{-1/2} \hat{h}_i' + {M_s'}^{-1/2} \hat{h}_s' \right) \langle \epsilon, \boldsymbol{c}_i - \boldsymbol{c}_s \rangle \, d\epsilon \, d\boldsymbol{c}_s, \end{aligned} \tag{4.94}$$

$$
\begin{aligned}
R_i(\underline{\hat{h}}) = & -\beta_{ij}\sigma_{ij}^2 \int_{\mathbb{R}^3}\int_{\mathbb{S}_+^2} M_j \hat{h}_i \Theta(\langle \epsilon, \xi_i\rangle - \Gamma_{ij})\,\langle \epsilon, \xi_i\rangle\, d\epsilon\, d\boldsymbol{c}_j \\
& - \beta_{ij}\sigma_{ij}^2 \int_{\mathbb{R}^3}\int_{\mathbb{S}_+^2} M_i^{1/2} M_j \hat{h}_j \Theta(\langle \epsilon, \xi_i\rangle - \Gamma_{ij})\,\langle \epsilon, \xi_i\rangle\, d\epsilon\, d\boldsymbol{c}_j \\
& + \beta_{ij}\sigma_{ij}^2 \int_{\mathbb{R}^3}\int_{\mathbb{S}_+^2} M_i^{1/2} M_j \left(M_k{}^{-1/2}\hat{h}_k + M_l{}^{-1/2}\hat{h}_l \right) \Theta(\langle \epsilon, \xi_i\rangle - \Gamma_{ij})\,\langle \epsilon, \xi_i\rangle\, d\epsilon\, d\boldsymbol{c}_j,
\end{aligned}
\tag{4.95}
$$

$$
\begin{aligned}
T_i(\underline{\hat{h}}) = & \beta_{ij}\sigma_{ij}^2 \int_{\mathbb{R}^3}\int_{\mathbb{S}_+^2} M_j \hat{h}_i \Theta(\langle \epsilon, \xi_i\rangle - \Gamma_{ij})\,\langle \epsilon, \xi_i\rangle\, d\epsilon\, d\boldsymbol{c}_j \\
& + \beta_{ij}\sigma_{ij}^2 \int_{\mathbb{R}^3}\int_{\mathbb{S}_+^2} M_i^{1/2} M_j \hat{h}_j \Theta(\langle \epsilon, \xi_i\rangle - \Gamma_{ij})\,\langle \epsilon, \xi_i\rangle\, d\epsilon\, d\boldsymbol{c}_j \\
& - \beta_{ij}\sigma_{ij}^2 \int_{\mathbb{R}^3}\int_{\mathbb{S}_+^2} M_i^{1/2} M_j \left(M_i'^{-1/2}\hat{h}_i{}' + M_j'^{-1/2}\hat{h}_j{}' \right) \Theta(\langle \epsilon, \xi_i\rangle - \Gamma_{ij})\,\langle \epsilon, \xi_i\rangle\, d\epsilon\, d\boldsymbol{c}_j.
\end{aligned}
\tag{4.96}
$$

The operator $Q_i(\underline{\hat{h}})$ represents the elastic contributions and $R_i(\underline{\hat{h}})$ the reactive ones. Moreover, $T_i(\underline{\hat{h}})$ stands for the "hybrid" operator. Now we treat separately these operators.

Kernels of the elastic operators

We split the operator Q_i of Eq. (4.94) in the form

$$
Q_i(\underline{\hat{h}}) = -\nu_i \hat{h}_i - Q_i^{(1)}(\underline{\hat{h}}) + Q_i^{(2)}(\underline{\hat{h}}) + Q_i^{(3)}(\underline{\hat{h}}), \tag{4.97}
$$

where

$$\nu_i \hat{h}_i = \hat{h}_i \sum_{s=1}^{4} \sigma_{is}^2 \int_{\mathbb{R}^3} \int_{\mathbb{S}_+^2} M_s \langle \epsilon, \boldsymbol{c}_i - \boldsymbol{c}_s \rangle \, d\epsilon \, d\boldsymbol{c}_s, \tag{4.98}$$

$$Q_i^{(1)}(\underline{\hat{h}}) = \sum_{s=1}^{4} \sigma_{is}^2 \int_{\mathbb{R}^3} \int_{\mathbb{S}_+^2} M_i^{1/2} M_s^{1/2} \hat{h}_s \langle \epsilon, \boldsymbol{c}_i - \boldsymbol{c}_s \rangle \, d\epsilon \, d\boldsymbol{c}_s, \tag{4.99}$$

$$Q_i^{(2)}(\underline{\hat{h}}) = \sum_{s=1}^{4} \sigma_{is}^2 \int_{\mathbb{R}^3} \int_{\mathbb{S}_+^2} M_i^{1/2} M_s M_i'^{-1/2} \hat{h}_i{}' \langle \epsilon, \boldsymbol{c}_i - \boldsymbol{c}_s \rangle \, d\epsilon \, d\boldsymbol{c}_s, \tag{4.100}$$

$$Q_i^{(3)}(\underline{\hat{h}}) = \sum_{s=1}^{4} \sigma_{is}^2 \int_{\mathbb{R}^3} \int_{\mathbb{S}_+^2} M_i^{1/2} M_s M_s'^{-1/2} \hat{h}_s{}' \langle \epsilon, \boldsymbol{c}_i - \boldsymbol{c}_s \rangle \, d\epsilon \, d\boldsymbol{c}_s. \tag{4.101}$$

Now, using Lemma 4.6.1, part 1, $Q_i^{(2)}(\underline{\hat{h}})$ simplifies to

$$Q_i^{(2)}(\underline{\hat{h}}) = \sum_{s=1}^{4} \sigma_{is}^2 \int_{\mathbb{R}^3} \int_{\mathbb{S}_+^2} M_s^{1/2} M_s'^{1/2} \hat{h}_i' \langle \epsilon, \boldsymbol{c}_i - \boldsymbol{c}_s \rangle \, d\epsilon d\boldsymbol{c}_s, \tag{4.102}$$

while $Q_i^{(3)}(\underline{\hat{h}})$ simplifies to

$$Q_i^{(3)}(\underline{\hat{h}}) = \sum_{s=1}^{4} \sigma_{is}^2 \int_{\mathbb{R}^3} \int_{\mathbb{S}_+^2} M_s^{1/2} M_i'^{1/2} \hat{h}_s' \langle \epsilon, \boldsymbol{c}_i - \boldsymbol{c}_s \rangle \, d\epsilon d\boldsymbol{c}_s. \tag{4.103}$$

The factor ν_i can be identified as a collisional operator. In what follows we present the kernels of the operators defined in expressions (4.99), (4.102) and (4.134). Here, we do not present their deduction that is long and very technical. Two representative calculations are presented in Appendix A and Appendix B. After some manipulations we have obtained the expression listed in the following Eqs. (4.104), (4.105) and (4.106).

$$N(Q_i^{(1)})(u,w) = \sum_{s=1}^{4} \sigma_{is}^2 \|u-w\| (n_i n_s)^{1/2} \left(\frac{m_i m_s}{(2\pi kT)^2} \right)^{3/4} \times \exp\left[-\frac{m_i u^2 + m_s w^2}{4kT} \right], \tag{4.104}$$

$$N(Q_i^{(2)})(u,w) = \sum_{s=1}^{4} \sigma_{is}^2\, n_s \left(\frac{m_i}{2\mu_{is}} \right)^2 \left(\frac{m_s}{2\pi kT} \right)^{1/2} \frac{1}{\|u-w\|} \times \exp\left[-\frac{m_s}{8kT} \frac{(u^2-w^2)^2}{\|u-w\|^2} - \frac{m_s}{4kT} \left(\frac{m_i}{2\mu_{is}} - \frac{1}{2} \right) (u-w)^2 \right], \tag{4.105}$$

$$\begin{aligned} N(Q_i^{(3)})(u,w) & \qquad \qquad (4.106) \\ = & \sum_{s\in I^-} \sigma_{is}^2 (n_i n_s)^{1/2} \left(\frac{m_i m_s}{(2\pi kT)^2} \right)^{\frac{3}{4}} \int_{D_{L_2^-}} \int_{D_{L_1^-}} \frac{1}{\sqrt{\|u-w\|^2 - (\frac{2\mu_{is}}{m_s} - 1)^2 \|L\|^2}} \\ & \times \exp\left[-\frac{1}{4kT} \left\{ m_s \left(w - \frac{2\mu_{is}}{m_s} L \right)^2 + m_i \left(u \left(1 - \frac{2\mu_{is}}{m_i} \right) \right.\right.\right. \\ & \left.\left.\left. + \frac{2\mu_{is}}{m_i} w - \frac{2\mu_{is}}{m_i} \left(\frac{2\mu_{is}}{m_s} - 1 \right) L \right)^2 \right\} \right] dL_1 dL_2 \\ + & \sum_{s\in I^+} \sigma_{is}^2 (n_i n_s)^{1/2} \left(\frac{m_i m_s}{(2\pi kT)^2} \right)^{\frac{3}{4}} \int_{D_{L_2^+}} \int_{D_{L_1^+}} \frac{1}{\sqrt{\|u-w\|^2 - (\frac{2\mu_{is}}{m_s} - 1)^2 \|L\|^2}} \\ & \times \exp\left[-\frac{1}{4kT} \left\{ m_s \left(w - \frac{2\mu_{is}}{m_s} L \right)^2 + m_i \left(u \left(1 - \frac{2\mu_{is}}{m_i} \right) \right.\right.\right. \\ & \left.\left.\left. + \frac{2\mu_{is}}{m_i} w - \frac{2\mu_{is}}{m_i} \left(\frac{2\mu_{is}}{m_s} - 1 \right) L \right)^2 \right\} \right] dL_1 dL_2 \\ + & \sum_{s\in I^0} \frac{\sigma_{is}^2}{\|u-w\|} (n_i n_s)^{1/2} \left(\frac{m_s}{2\pi kT} \right)^{1/2} \exp\left[-\frac{m_s}{8kT} (u-w)^2 - \frac{m_s}{8kT} \frac{(u^2-w^2)^2}{\|u-w\|^2} \right]. \end{aligned}$$

In the above expression (4.106), the symbols I^-, I^+ and I^0 represent sets of indices defined by

$$I^- = \{s \in I: \; m_s < m_i\}, I^+ = \{s \in I: \; m_s > m_i\}, I^0 = \{s \in I: \; m_s = m_i\},$$

where $I = \{1, 2, 3, 4\}$. The integration domains $D_{L_1^-}$ and $D_{L_2^-}$ on the first summation term on the right-hand-side of Eq. (4.106) are characterized by

$$\frac{w_1 - u_1 - \sqrt{(u_1 - w_1)^2 + (u_3 - w_3)^2 - 4\left(\frac{2\mu_{is}}{m_s} - 1\right) L_2 \left(u_2 - w_2 + L_2\left(\frac{2\mu_{is}}{m_s} - 1\right)\right)}}{2\left(\frac{2\mu_{is}}{m_s} - 1\right)}$$

$$\leq L_1 \leq \tag{4.107}$$

$$\frac{w_1 - u_1 + \sqrt{(u_1 - w_1)^2 + (u_3 - w_3)^2 - 4\left(\frac{2\mu_{is}}{m_s} - 1\right) L_2 \left(u_2 - w_2 + L_2\left(\frac{2\mu_{is}}{m_s} - 1\right)\right)}}{2\left(\frac{2\mu_{is}}{m_s} - 1\right)}$$

$$\frac{w_2 - u_2 - \|u - w\|}{2\left(\frac{2\mu_{is}}{m_s} - 1\right)} \leq L_2 \leq \frac{w_2 - u_2 + \|u - w\|}{2\left(\frac{2\mu_{is}}{m_s} - 1\right)} \tag{4.108}$$

whereas the domains $D_{L_1^+}$ and $D_{L_2^+}$ on the second summation term are characterized by

$$\frac{w_1-u_1+\sqrt{(u_1-w_1)^2+(u_3-w_3)^2-4\left(\dfrac{2\mu_{is}}{m_s}-1\right)L_2\left(u_2-w_2+L_2\left(\dfrac{2\mu_{is}}{m_s}-1\right)\right)}}{2\left(\frac{2\mu_{is}}{m_s}-1\right)}$$

$$\leq L_1 \leq \tag{4.109}$$

$$\frac{w_1-u_1-\sqrt{(u_1-w_1)^2+(u_3-w_3)^2-4\left(\dfrac{2\mu_{is}}{m_s}-1\right)L_2\left(u_2-w_2+L_2\left(\dfrac{2\mu_{is}}{m_s}-1\right)\right)}}{2\left(\frac{2\mu_{is}}{m_s}-1\right)}$$

$$\frac{w_2-u_2+\|u-w\|}{2\left(\frac{2\mu_{is}}{m_s}-1\right)} \leq \ L_2 \leq \frac{w_2-u_2-\|u-w\|}{2\left(\frac{2\mu_{is}}{m_s}-1\right)} \tag{4.110}$$

Note 4.6.2. *We should notice that if we simplify the kernels of the elastic operators here obtained for the inert case of a single gas constituent, we obtain expressions similar to those presented by Grad in [40]. The differences between our's and Grad's expressions are due to the fact that he used a dimensionless normalized Maxwellian and we use a regular Maxwellian.*

Kernels of the reactive operators

We split the operator R_i of Eq. (4.95) in the form

$$R_i(\underline{\hat{h}}) = -\,\nu_R^i(u)\hat{h}_i(u) - R_i^{(1)}(\underline{\hat{h}}) + R_i^{(2)}(\underline{\hat{h}}) + R_i^{(3)}(\underline{\hat{h}}),$$

where

$$\nu_R^i(u)\hat{h}_i(u) = \hat{h}_i\beta_{ij}\sigma_{ij}^2\int_{\mathbb{R}^3}\int_{\mathbb{S}_+^2} M_j\Theta(\langle\epsilon,\xi_i\rangle - \Gamma_{ij})\,\langle\epsilon,\xi_i\rangle\, d\epsilon\, d\boldsymbol{c}_j, \tag{4.111}$$

$$R_i^{(1)}(\underline{\hat{h}}) = \beta_{ij}\sigma_{ij}^2\int_{\mathbb{R}^3}\int_{\mathbb{S}_+^2} M_i^{1/2}M_j\hat{h}_j\Theta(\langle\epsilon,\xi_i\rangle - \Gamma_{ij})\,\langle\epsilon,\xi_i\rangle\, d\epsilon\, d\boldsymbol{c}_j, \tag{4.112}$$

$$R_i^{(2)}(\underline{\hat{h}}) = \beta_{ij}\sigma_{ij}^2\int_{\mathbb{R}^3}\int_{\mathbb{S}_+^2} M_i^{1/2}M_jM_k^{-1/2}\hat{h}_k\Theta(\langle\epsilon,\xi_i\rangle - \Gamma_{ij})\,\langle\epsilon,\xi_i\rangle\, d\epsilon\, d\boldsymbol{c}_j, \tag{4.113}$$

$$R_i^{(3)}(\underline{\hat{h}}) = \beta_{ij}\sigma_{ij}^2\int_{\mathbb{R}^3}\int_{\mathbb{S}_+^2} M_i^{1/2}M_jM_l^{-1/2}\hat{h}_l\Theta(\langle\epsilon,\xi_i\rangle - \Gamma_{ij})\,\langle\epsilon,\xi_i\rangle\, d\epsilon\, d\boldsymbol{c}_j. \tag{4.114}$$

Now, using 2) of Lemma 4.6.1, $R_i^{(2)}(\underline{\hat{h}})$ simplifies to

$$R_i^{(2)}(\underline{\hat{h}}) = \beta_{ij}\sigma_{ij}^2\int_{\mathbb{R}^3}\int_{\mathbb{S}_+^2}\left(\frac{\mu_{ij}}{\mu_{kl}}\right)M_j^{1/2}M_l^{1/2}\hat{h}_k\Theta(\langle\epsilon,\xi_i\rangle - \Gamma_{ij})\,\langle\epsilon,\xi_i\rangle\, d\epsilon\, d\boldsymbol{c}_j, \tag{4.115}$$

while $R_i^{(3)}(\underline{\hat{h}})$ simplifies to

$$R_i^{(3)}(\underline{\hat{h}}) = \beta_{ij}\sigma_{ij}^2\int_{\mathbb{R}^3}\int_{\mathbb{S}_+^2}\left(\frac{\mu_{ij}}{\mu_{kl}}\right)M_j^{1/2}M_k^{1/2}\hat{h}_l\Theta(\langle\epsilon,\xi_i\rangle - \Gamma_{ij})\,\langle\epsilon,\xi_i\rangle\, d\epsilon\, d\boldsymbol{c}_j. \tag{4.116}$$

We work separately on the integral operators (4.112), (4.115) and (4.116). We note that the assumptions $Q_R > 0$, $m_1 < m_2$ and $m_4 < m_3$, already presented, are used to derive the expressions for the reactive kernels.

A) Kernel of $\boldsymbol{R_i^{(1)}}$ The kernel of $R_i^{(1)}$, $i = 1, ..., 4$, is

$$N(R_i^{(1)})(u,w) = \beta_{ij}\sigma_{ij}^2\|u-w\|(n_in_j)^{1/2}\left(\frac{m_im_j}{(2\pi kT)^2}\right)^{3/4}\exp\left[-\frac{m_iu^2+m_jw^2}{4kT}\right]$$
$$\times\int_0^{\frac{\pi}{2}}\cos\theta\sin\theta\Theta(\|u-w\|\cos\theta - \Gamma_{ij})d\theta. \tag{4.117}$$

B) Kernel of $\boldsymbol{R_i^{(2)}}$ The kernel of $R_i^{(2)}$, $i = 1, ..., 4$, has been obtained separately for each value of the index i.

B1) For $i = 1$, the kernel is

$$N(R_1^{(2)})(u,w) = \int_0^{2\pi} \Bigg[\int_0^{\frac{\|w-u\|M}{m_2}} \Delta_1^{(2)}\, d\|L\| + \int_{\|L\|_{12}^-}^{\|L\|_{12}^+} \Delta_1^{(2)}\, d\|L\| \tag{4.118}$$

$$\times \Theta\left(\|w-u\| - \sqrt{\left(m_2^2 - m_4^2 \frac{\mu_{12}}{\mu_{34}} \right) \frac{2Q_R}{M^2}} \right) \Theta\left(\sqrt{\frac{2m_2^2 E}{M^2 \mu_{12}}} - \|w-u\| \right)$$

$$+ \int_{\frac{\|w-u\|M}{m_2}}^{\|L\|_{12}^+} \Delta_1^{(2)}\, d\|L\| \Theta\left(\|w-u\| - \sqrt{\frac{2m_2^2 E}{M^2 \mu_{12}}} \right) \Bigg] \times \left(\frac{M}{m_4 \sqrt{\frac{\mu_{12}}{\mu_{34}}} - m_2} \right)^3 d\varphi,$$

where $\|L\|_{12}^+$ and $\|L\|_{12}^-$ are defined by

$$\|L\|_{12}^+ = \frac{m_2 \|w-u\| M + \sqrt{\left(m_4^2 \frac{\mu_{12}}{\mu_{34}} - m_2^2 \right) \frac{2Q_R m_4^2}{\mu_{34}} + m_4^2 \frac{\mu_{12}}{\mu_{34}} \|w-u\|^2 M^2}}{m_2^2 - m_4^2 \frac{\mu_{12}}{\mu_{34}}},$$

$$\|L\|_{12}^- = \frac{m_2 \|w-u\| M - \sqrt{\left(m_4^2 \frac{\mu_{12}}{\mu_{34}} - m_2^2 \right) \frac{2Q_R m_4^2}{\mu_{34}} + m_4^2 \frac{\mu_{12}}{\mu_{34}} \|w-u\|^2 M^2}}{m_2^2 - m_4^2 \frac{\mu_{12}}{\mu_{34}}}$$

and $\Delta_1^{(2)}$ is given by

$$
\begin{aligned}
\Delta_1^{(2)} &= \beta_{12}\sigma_{12}^2 (n_2 n_4)^{1/2} \left(\frac{m_2 m_4}{(2\pi kT)^2}\right)^{3/4} \frac{\mu_{12}}{\mu_{34}} \\
&\quad \times \exp\left[-\frac{m_2}{2kT} \left(u - \frac{w - u - \frac{1}{M}\left(m_4\sqrt{\frac{\mu_{12}}{\mu_{34}} - \frac{2Q_R}{\mu_{34}\|L\|^2}} - m_2\right) L}{\frac{1}{M}\left(m_4\sqrt{\frac{\mu_{12}}{\mu_{34}}} - m_2\right)} - L \right)^2 \right. \\
&\quad -\frac{m_4}{2kT} \left(u + \frac{1}{M}\left(-m_3\sqrt{\frac{\mu_{12}}{\mu_{34}} - \frac{2Q_R}{\mu_{34}\|L\|^2}} - m_2\right) L \right. \\
&\quad \left.\left. -\frac{1}{M}\left(m_3\sqrt{\frac{\mu_{12}}{\mu_{34}}} + m_2\right) \frac{w - u - \frac{1}{M}\left(m_4\sqrt{\frac{\mu_{12}}{\mu_{34}} - \frac{2Q_R}{\mu_{34}\|L\|^2}} - m_2\right) L}{\frac{1}{M}\left(m_4\sqrt{\frac{\mu_{12}}{\mu_{34}}} - m_2\right)} \right)^2 \right] \\
&\quad \times \Theta(\|L\| - \Gamma_{12}) \left\| \frac{\frac{1}{M}\left(m_4\sqrt{\frac{\mu_{12}}{\mu_{34}}} - m_2\right)}{w - u - \frac{1}{M}\left(m_4\sqrt{\frac{\mu_{12}}{\mu_{34}} - \frac{2Q_R}{\mu_{34}\|L\|^2}} - m_2\right) L} \right\| \|L\|^2 \sin\theta,
\end{aligned}
$$

with

$$
\begin{aligned}
L &= (\|L\|\cos\theta, \|L\|\sin\theta\cos\varphi, \|L\|\sin\theta\sin\varphi), \\
\cos\theta &= \frac{1}{M}\left(m_4\sqrt{\frac{\mu_{12}}{\mu_{34}} - \frac{2Q_R}{\mu_{34}\|L\|^2}} - m_2\right) \frac{\|L\|}{\|w - u\|}, \\
\sin\theta &= \sqrt{1 - \cos^2\theta}.
\end{aligned}
$$

B2) For $i = 2$, the kernel is

$$N(R_2^{(2)})(u,w) = \int_0^{2\pi} \left[\int_0^{\frac{\|w-u\|M}{m_1}} \Delta_2^{(2)}\, d\|L\| + \int_{\|L\|_{22}^+}^{\|L\|_{22b}^+} \Delta_2^{(2)}\, d\|L\| \right. \tag{4.119}$$

$$\times \Theta\left(\sqrt{\left(-m_1^2 + m_3^2 \frac{\mu_{12}}{\mu_{34}}\right) \frac{2Q_R}{M^2 \mu_{12} \left(\frac{m_2 m_3}{m_1 m_4} - 1\right)}} - \|w-u\| \right)$$

$$\left. + \int_0^{\|L\|_{22b}^+} \Delta_2^{(2)}\, d\|L\| \Theta\left(\|w-u\| - \sqrt{\left(-m_1^2 + m_3^2 \frac{\mu_{12}}{\mu_{34}}\right) \frac{2Q_R}{M^2 \mu_{12} \left(\frac{m_2 m_3}{m_1 m_4} - 1\right)}} \right) \right]$$

$$\times \left(\frac{M}{m_1 - m_3 \sqrt{\frac{\mu_{12}}{\mu_{34}}}} \right)^3 d\varphi,$$

where $\|L\|_{22}^+$ and $\|L\|_{22b}^+$ are defined by

$$\|L\|_{22}^+ = \frac{-m_1\|w-u\|M + \sqrt{\left(m_3^2 \frac{\mu_{12}}{\mu_{34}} - m_1^2\right) \frac{2Q_R m_3^2}{\mu_{34}} + m_3^2 \frac{\mu_{12}}{\mu_{34}} \|w-u\|^2 M^2}}{-m_1^2 + m_3^2 \frac{\mu_{12}}{\mu_{34}}},$$

$$\|L\|_{22b}^+ = \frac{m_1\|w-u\|M + \sqrt{\left(m_3^2 \frac{\mu_{12}}{\mu_{34}} - m_1^2\right) \frac{2Q_R m_3^2}{\mu_{34}} + m_3^2 \frac{\mu_{12}}{\mu_{34}} \|w-u\|^2 M^2}}{-m_1^2 + m_3^2 \frac{\mu_{12}}{\mu_{34}}},$$

and $\Delta_2^{(2)}$ is given by

$$\Delta_2^{(2)} = \beta_{21}\sigma_{21}^2(n_1n_3)^2\left(\frac{m_1m_3}{(2\pi kT)^2}\right)^{3/4}\frac{\mu_{12}}{\mu_{34}}$$

$$\times\exp\left[-\frac{m_1}{2kT}\left(w+\frac{u-w-\frac{1}{M}\left(m_1-m_3\sqrt{\frac{\mu_{12}}{\mu_{34}}-\frac{2Q_R}{\mu_{34}\|L\|^2}}\right)L}{m_1-m_3\sqrt{\frac{\mu_{12}}{\mu_{34}}}}+L\right)^2\right.$$

$$-\frac{m_3}{2kT}\left(w+\frac{1}{M}\left(m_1+m_4\sqrt{\frac{\mu_{12}}{\mu_{34}}-\frac{2Q_R}{\mu_{34}\|L\|^2}}\right)L\right.$$

$$\left.\left.\frac{1}{M}\left(m_1+m_4\sqrt{\frac{\mu_{12}}{\mu_{34}}}\right)\frac{u-w-\frac{1}{M}\left(m_1-m_3\sqrt{\frac{\mu_{12}}{\mu_{34}}-\frac{2Q_R}{\mu_{34}\|L\|^2}}\right)L}{m_1-m_3\sqrt{\frac{\mu_{12}}{\mu_{34}}}}\right)^2\right]$$

$$\times\Theta(\|L\|-\Gamma_{21})\left\|\frac{m_1-m_3\sqrt{\frac{\mu_{12}}{\mu_{34}}}}{u-w-\frac{1}{M}\left(m_1-m_3\sqrt{\frac{\mu_{12}}{\mu_{34}}-\frac{2Q_R}{\mu_{34}\|L\|^2}}\right)L}\right\|\|L\|^2\sin\theta,$$

with

$$L = (\|L\|\cos\theta, \|L\|\sin\theta\cos\varphi, \|L\|\sin\theta\sin\varphi),$$

$$\cos\theta = \frac{1}{M}\left(m_1-m_3\sqrt{\frac{\mu_{12}}{\mu_{34}}-\frac{2Q_R}{\mu_{34}\|L\|^2}}\right)\frac{\|L\|}{\|w-u\|},$$

$$\sin\theta = \sqrt{1-\cos^2\theta}.$$

B3) For $i = 3$ the kernel is

$$N(R_3^{(2)})(u,w) = \int_0^{2\pi} \left[\int_{\|L\|_{32}^-}^{\|L\|_{32}^+} \Delta_3^{(2)}\, d\|L\| \right. \tag{4.120}$$

$$\times \Theta\left(\|w-u\| - \sqrt{\left(m_2^2 \frac{\mu_{34}}{\mu_{12}} - m_4^2 \right) \frac{2Q_R}{\mu_{34} M^2}} \right) \Theta\left(\sqrt{\frac{2Q_R m_2^2}{\mu_{12} M^2}} - \|w-u\| \right)$$

$$\left. + \int_0^{\|L\|_{32}^+} \Delta_3^{(2)}\, d\|L\| \Theta\left(\|w-u\| - \sqrt{\frac{2Q_R m_2^2}{\mu_{12} M^2}} \right) \right] \times \left(\frac{M}{m_2 \sqrt{\frac{\mu_{34}}{\mu_{12}}} - m_4} \right)^3 d\varphi,$$

where $\|L\|_{32}^-$ and $\|L\|_{32}^+$ are defined by

$$\|L\|_{32}^+ = \frac{m_4 \|w-u\| M + \sqrt{-\left(m_2^2 \frac{\mu_{34}}{\mu_{12}} - m_4^2 \right) \frac{2Q_R m_2^2}{\mu_{12}} + m_2^2 \frac{\mu_{34}}{\mu_{12}} \|w-u\|^2 M^2}}{m_2^2 \frac{\mu_{34}}{\mu_{12}} - m_4^2}$$

$$\|L\|_{32}^- = \frac{m_4 \|w-u\| M - \sqrt{-\left(m_2^2 \frac{\mu_{34}}{\mu_{12}} - m_4^2 \right) \frac{2Q_R m_2^2}{\mu_{12}} + m_2^2 \frac{\mu_{34}}{\mu_{12}} \|w-u\|^2 M^2}}{m_2^2 \frac{\mu_{34}}{\mu_{12}} - m_4^2}$$

and $\Delta_3^{(2)}$ is given by

$$\Delta_3^{(2)} = \beta_{34}\sigma_{34}^2(n_2 n_4)^{1/2}\left(\frac{m_2 m_4}{(2\pi kT)^2}\right)^{3/4}\frac{\mu_{34}}{\mu_{12}}$$
$$\times\exp\left[-\frac{m_4}{2kT}\left(u-\frac{w-u-\frac{1}{M}\left(m_2\sqrt{\frac{\mu_{34}}{\mu_{12}}+\frac{2Q_R}{\mu_{12}\|L\|^2}}-m_4\right)L}{\frac{1}{M}\left(m_2\sqrt{\frac{\mu_{34}}{\mu_{12}}}-m_4\right)}-L\right)^2\right.$$
$$-\frac{m_2}{2kT}\left(u+\frac{1}{M}\left(-m_1\sqrt{\frac{\mu_{34}}{\mu_{12}}+\frac{2Q_R}{\mu_{12}\|L\|^2}}-m_4\right)L\right.$$
$$\left.\left.+\frac{1}{M}\left(-m_1\sqrt{\frac{\mu_{34}}{\mu_{12}}}-m_4\right)\frac{w-u-\frac{1}{M}\left(m_2\sqrt{\frac{\mu_{34}}{\mu_{12}}+\frac{2Q_R}{\mu_{12}\|L\|^2}}-m_4\right)L}{\frac{1}{M}\left(m_2\sqrt{\frac{\mu_{34}}{\mu_{12}}}-m_4\right)}\right)^2\right]$$
$$\times\Theta(\|L\|-\Gamma_{34})\left\|\frac{\frac{1}{M}\left(m_2\sqrt{\frac{\mu_{34}}{\mu_{12}}}-m_4\right)}{w-u-\frac{1}{M}\left(m_2\sqrt{\frac{\mu_{34}}{\mu_{12}}+\frac{2Q_R}{\mu_{12}\|L\|^2}}-m_4\right)L}\right\|\|L\|^2\sin\theta,$$

with

$$L = (\|L\|\cos\theta, \|L\|\sin\theta\cos\varphi, \|L\|\sin\theta\sin\varphi),$$

$$\cos\theta = \frac{1}{M}\left(m_2\sqrt{\frac{\mu_{34}}{\mu_{12}}-\frac{2Q_R}{\mu_{12}\|L\|^2}}-m_4\right)\frac{\|L\|}{\|w-u\|},$$

$$\sin\theta = \sqrt{1-\cos^2\theta}.$$

B4) For $i = 4$ the kernel is

$$N(R_4^{(2)})(u,w) = \int_0^{2\pi} \left[\int_{\|L\|_{42b}^+}^{\|L\|_{42}^+} \Delta_4^{(2)} \, d\|L\| \Theta\left(\sqrt{\frac{2Q_R m_1^2}{\mu_{12} M^2}} - \|w-u\| \right) \right. \tag{4.121}$$

$$\left. + \int_0^{\|L\|_{42}^+} \Delta_4^{(2)} \, d\|L\| \Theta\left(\|w-u\| - \sqrt{\frac{2Q_R m_1^2}{\mu_{12} M^2}} \right) \right] \left(\frac{M}{m_3 - m_1 \sqrt{\frac{\mu_{34}}{\mu_{12}}}} \right)^3 d\varphi,$$

where $\|L\|_{42}^+$ and $\|L\|_{42b}^+$ are defined by

$$\|L\|_{42}^+ = \frac{m_3\|w-u\|M + \sqrt{\left(m_1^2\frac{\mu_{34}}{\mu_{12}} + m_3^2\right)\frac{2Q_R m_1^2}{\mu_{12}} + m_1^2\frac{\mu_{34}}{\mu_{12}}\|w-u\|^2 M^2}}{m_3^2 - m_1^2\frac{\mu_{34}}{\mu_{12}}},$$

$$\|L\|_{42b}^+ = \frac{-m_3\|w-u\|M + \sqrt{\left(-m_1^2\frac{\mu_{34}}{\mu_{12}} + m_3^2\right)\frac{2Q_R m_1^2}{\mu_{12}} + m_1^2\frac{\mu_{34}}{\mu_{12}}\|w-u\|^2 M^2}}{m_3^2 - m_1^2\frac{\mu_{34}}{\mu_{12}}},$$

and $\Delta_4^{(2)}$ is given by

$$\Delta_4^{(2)} = \beta_{43}\sigma_{43}^2(n_1n_3)^{1/2}\left(\frac{m_1m_3}{(2\pi kT)^2}\right)^{3/4}\frac{\mu_{34}}{\mu_{12}}$$
$$\times\exp\left[-\frac{m_3}{2kT}\left(w+\frac{u-w-\frac{1}{M}\left(m_3-m_1\sqrt{\frac{\mu_{34}}{\mu_{12}}+\frac{2Q_R}{\mu_{12}\|L\|^2}}\right)L}{\frac{1}{M}\left(m_3-m_1\sqrt{\frac{\mu_{34}}{\mu_{12}}}\right)}+L\right)^2\right.$$
$$-\frac{m_1}{2kT}\left(w+\frac{1}{M}\left(m_3+m_2\sqrt{\frac{\mu_{34}}{\mu_{12}}+\frac{2Q_R}{\mu_{12}\|L\|^2}}\right)L\right.$$
$$\left.\left.+\frac{1}{M}\left(m_3+m_2\sqrt{\frac{\mu_{34}}{\mu_{12}}}\right)\frac{u-w-\frac{1}{M}\left(m_3-m_1\sqrt{\frac{\mu_{34}}{\mu_{12}}+\frac{2Q_R}{\mu_{12}\|L\|^2}}\right)L}{\frac{1}{M}\left(m_3-m_1\sqrt{\frac{\mu_{34}}{\mu_{12}}}\right)}\right)^2\right]$$
$$\times\Theta(\|L\|-\Gamma_{34})\left\|\frac{\frac{1}{M}\left(m_3-m_1\sqrt{\frac{\mu_{34}}{\mu_{12}}}\right)}{u-w-\frac{1}{M}\left(m_3-m_1\sqrt{\frac{\mu_{34}}{\mu_{12}}+\frac{2Q_R}{\mu_{12}\|L\|^2}}\right)L}\right\|\|L\|^2\sin\theta,$$

with

$$L = (\|L\|\cos\theta, \|L\|\sin\theta\cos\varphi, \|L\|\sin\theta\sin\varphi),$$

$$\cos\theta = \frac{1}{M}\left(-m_1\sqrt{\frac{\mu_{34}}{\mu_{12}}+\frac{2Q_R}{\mu_{12}\|L\|^2}}+m_2\right)\frac{\|L\|}{\|w-u\|},$$

$$\sin\theta = \sqrt{1-\cos^2\theta}.$$

C) Kernel of $\boldsymbol{R_i^{(3)}}$ The kernel of $R_i^{(3)}$, $i = 1, ..., 4$, has been obtained for each value of the index i as follows.

C1) For $i = 1$ we have two different situations.

Situation 1. If $m_2 > m_3$ the kernel of $R_1^{(3)}$ has the form

$$
\begin{aligned}
N(R_1^{(3)})(u,w) = & \int_0^{2\pi} \left[\int_0^{\frac{\|w-u\|M}{m_2}} \Delta_1^{(3)} d\|L\| \right. \\
& \times \Theta\left(\sqrt{\left(m_2^2 - m_3^2 \frac{\mu_{12}}{\mu_{34}} \right) \frac{2Q_R}{M^2}} - \|w-u\| \right) + \int_0^{\frac{\|w-u\|M}{m_2}} \Delta_1^{(3)} \, d\|L\| \\
& \times \Theta\left(\|w-u\| - \sqrt{\left(m_2^2 - m_3^2 \frac{\mu_{12}}{\mu_{34}} \right) \frac{2Q_R}{M^2}} \right) \Theta\left(\sqrt{\frac{2m_2^2 Q_R}{M^2 \mu_{12}}} - \|w-u\| \right) \\
& \left. + \int_0^{\|L\|_{13}^-} \Delta_1^{(3)} \, d\|L\| \Theta\left(\|w-u\| - \sqrt{\frac{2m_2^2 Q_R}{M^2 \mu_{12}}} \right) \right] \left(\frac{M}{-m_3 \sqrt{\frac{\mu_{12}}{\mu_{34}}} - m_2} \right)^3 d\varphi,
\end{aligned}
\tag{4.122}
$$

where

$$
\|L\|_{13}^- = \frac{m_2 \|w-u\| M - \sqrt{\left(m_3^2 \frac{\mu_{12}}{\mu_{34}} - m_2^2 \right) \frac{2Q_R m_3^2}{\mu_{34}} + m_3^2 \frac{\mu_{12}}{\mu_{34}} \|w-u\|^2 M^2}}{m_2^2 - m_3^2 \frac{\mu_{12}}{\mu_{34}}}
$$

and

$$\Delta_1^{(3)} = \beta_{12}\sigma_{12}^2(n_2n_3)^{1/2}\left(\frac{m_2m_3}{(2\pi kT)^2}\right)^{3/4}\frac{\mu_{12}}{\mu_{34}}$$

$$\times\exp\left[-\frac{m_2}{2kT}\left(u-\frac{w-u-\frac{1}{M}\left(-m_3\sqrt{\frac{\mu_{12}}{\mu_{34}}-\frac{2Q_R}{\mu_{34}\|L\|^2}}-m_2\right)L}{\frac{1}{M}\left(-m_3\sqrt{\frac{\mu_{12}}{\mu_{34}}}-m_2\right)}-L\right)^2\right.$$

$$-\frac{m_3}{2kT}\left(u+\frac{1}{M}\left(m_4\sqrt{\frac{\mu_{12}}{\mu_{34}}-\frac{2Q_R}{\mu_{34}\|L\|^2}}-m_2\right)L\right.$$

$$\left.\left.+\frac{1}{M}\left(m_4\sqrt{\frac{\mu_{12}}{\mu_{34}}}-m_2\right)\frac{w-u-\frac{1}{M}\left(-m_3\sqrt{\frac{\mu_{12}}{\mu_{34}}-\frac{2Q_R}{\mu_{34}\|L\|^2}}-m_2\right)L}{\frac{1}{M}\left(-m_3\sqrt{\frac{\mu_{12}}{\mu_{34}}}-m_2\right)}\right)^2\right]$$

$$\times\Theta(\|L\|-\Gamma_{12})\left\|\frac{\frac{1}{M}\left(-m_3\sqrt{\frac{\mu_{12}}{\mu_{34}}}-m_2\right)}{w-u-\frac{1}{M}\left(-m_3\sqrt{\frac{\mu_{12}}{\mu_{34}}-\frac{2Q_R}{\mu_{34}\|L\|^2}}-m_2\right)L}\right\|\|L\|^2\sin\theta,$$

with

$$L = (\|L\|\cos\theta, \|L\|\sin\theta\cos\varphi, \|L\|\sin\theta\sin\varphi),$$

$$\cos\theta = \frac{1}{M}\left(-m_3\sqrt{\frac{\mu_{12}}{\mu_{34}}-\frac{2Q_R}{\mu_{34}\|L\|^2}}-m_2\right)\frac{\|L\|}{\|w-u\|},$$

$$\sin\theta = \sqrt{1-\cos^2\theta}.$$

Situation 2. If $m_2 < m_3$ the kernel of $R_1^{(3)}$ has the form

$$N(R_1^{(3)})(u,w) = \int_0^{2\pi} \left[\int_0^{\frac{\|w-u\|M}{m_2}} \Delta_1^{(3)} \, d\|L\| \Theta\left(\sqrt{\frac{2m_2^2 Q_R}{M^2 \mu_{12}}} - \|w-u\| \right) \right. \tag{4.123}$$

$$\left. + \int_0^{\|L\|_{13}^-} \Delta_1^{(3)} \, d\|L\| \, \Theta\left(\|w-u\| - \sqrt{\frac{2m_2^2 Q_R}{M^2 \mu_{12}}} \right) \right] \left(\frac{M}{-m_3\sqrt{\frac{\mu_{12}}{\mu_{34}}} - m_2} \right)^3 d\varphi,$$

where $\|L\|_{13}^-$ and $\Delta_1^{(3)}$ are already defined in **Situation 1**.

C2) For $i = 2$ we have two situations.

Situation 1. If $m_2 > m_3$ the kernel of $R_2^{(3)}$ has the form

$$N(R_2^{(3)})(u,w) = \int_0^{2\pi} \left[\int_0^{\frac{\|w-u\|M}{m_1}} \Delta_2^{(3)} \, d\|L\| \, \Theta\left(\sqrt{\frac{2Q_R m_1}{M^2 \mu_{12}}} - \|w-u\| \right) \right. \tag{4.124}$$

$$\left. + \int_0^{\|L\|_{23}^+} \Delta_2^{(3)} d\|L\| \, \Theta\left(\|w-u\| - \sqrt{\frac{2Q_R m_1}{M^2 \mu_{12}}} \right) \right] \left(\frac{M}{m_4\sqrt{\frac{\mu_{12}}{\mu_{34}}} + m_1} \right)^3 d\varphi,$$

where $\|L\|_{23}^+$ is defined by

$$\|L\|_{23}^+ = \frac{-m_1\|w-u\|M + \sqrt{\left(m_4^2\frac{\mu_{12}}{\mu_{34}} - m_1^2\right)\frac{2Q_R m_4^2}{\mu_{34}} + m_4^2\frac{\mu_{12}}{\mu_{34}}\|w-u\|^2 M^2}}{-m_1^2 + m_4^2\frac{\mu_{12}}{\mu_{34}}}$$

and

$$
\begin{aligned}
\Delta_2^{(3)} &= \beta_{12}\sigma_{12}^2(n_1 n_4)^{1/2}\left(\frac{m_1 m_4}{(2\pi kT)^2}\right)^{3/4}\frac{\mu_{12}}{\mu_{34}} \\
&\times \exp\left[-\frac{m_1}{2kT}\left(w+\frac{u-w-\frac{1}{M}\left(m_1+m_4\sqrt{\frac{\mu_{12}}{\mu_{34}}-\frac{2Q_R}{\mu_{34}\|L\|^2}}\right)L}{\frac{1}{M}\left(m_1+m_4\sqrt{\frac{\mu_{12}}{\mu_{34}}}\right)}+L\right)^2\right. \\
&-\frac{m_4}{2kT}\left(w+\frac{1}{M}\left(m_1-m_3\sqrt{\frac{\mu_{12}}{\mu_{34}}-\frac{2Q_R}{\mu_{34}\|L\|^2}}\right)L\right. \\
&\left.\left.+\frac{1}{M}\left(m_1-m_3\sqrt{\frac{\mu_{12}}{\mu_{34}}}\right)\frac{u-w-\frac{1}{M}\left(m_1+m_4\sqrt{\frac{\mu_{12}}{\mu_{34}}-\frac{2Q_R}{\mu_{34}\|L\|^2}}\right)L}{\frac{1}{M}\left(m_1+m_4\sqrt{\frac{\mu_{12}}{\mu_{34}}}\right)}\right)^2\right] \\
&\times\Theta(\|L\|-\Gamma_{12})\left\|\frac{\frac{1}{M}\left(m_1+m_4\sqrt{\frac{\mu_{12}}{\mu_{34}}}\right)}{u-w-\frac{1}{M}\left(m_1+m_4\sqrt{\frac{\mu_{12}}{\mu_{34}}-\frac{2Q_R}{\mu_{34}\|L\|^2}}\right)L}\right\|\|L\|\sin\theta,
\end{aligned}
$$

with

$$
\begin{aligned}
L &= (\|L\|\cos\theta, \|L\|\sin\theta\cos\varphi, \|L\|\sin\theta\sin\varphi), \\
\cos\theta &= \frac{1}{M}\left(m_1+m_4\sqrt{\frac{\mu_{12}}{\mu_{34}}-\frac{2Q_R}{\mu_{34}\|L\|^2}}\right)\frac{\|L\|}{\|w-u\|}, \\
\sin\theta &= \sqrt{1-\cos^2\theta}.
\end{aligned}
$$

Situation 2. If $m_2 < m_3$ the kernel of $R_2^{(3)}$ has the form

$$N(R_2^{(3)})(u,w) = \int_0^{2\pi} \left[\int_0^{\frac{\|w-u\|M}{m_1}} \Delta_2^{(3)}\, d\|L\|\, \Theta\left(\sqrt{\frac{2Q_R m_1}{M^2 \mu_{12}}} - \|w-u\| \right) + \int_0^{\|L\|_{23b}^-} \Delta_2^{(3)} d\|L\|\, \Theta\left(\|w-u\| - \sqrt{\frac{2Q_R m_1}{M^2 \mu_{12}}} \right) \right] \left(\frac{M}{m_4 \sqrt{\frac{\mu_{12}}{\mu_{34}}} + m_1} \right)^3 d\varphi, \tag{4.125}$$

where $\|L\|_{23b}^-$ is defined by

$$\|L\|_{23b}^- = \frac{m_1 \|w-u\| M - \sqrt{-\left(-m_4^2 \frac{\mu_{12}}{\mu_{34}} + m_1^2 \right) \frac{2Q_R m_4^2}{\mu_{34}} + m_4^2 \frac{\mu_{12}}{\mu_{34}} \|w-u\|^2 M^2}}{m_1^2 - m_4^2 \frac{\mu_{12}}{\mu_{34}}}$$

and $\Delta_2^{(3)}$ is already defined in **Situation 1**.

C3) For $i = 3$ we have

$$N(R_3^{(3)})(u,w) = \int_0^{2\pi} \int_0^{\|L\|_{33}^+} \Delta_3^{(3)} d\|L\| \times \Theta\left(\|w-u\| - \sqrt{\frac{2Q_R m_1^2}{\mu_{12} M^2}} \right) \left(\frac{M}{-m_1 \sqrt{\frac{\mu_{34}}{\mu_{12}}} - m_4} \right)^3 d\varphi, \tag{4.126}$$

where

$$\|L\|_{33}^+ = \frac{-m_4 \|w-u\| M + \sqrt{-\left(m_1^2 \frac{\mu_{34}}{\mu_{12}} - m_4^2 \right) \frac{2Q_R m_1^2}{\mu_{12}} + m_1^2 \frac{\mu_{34}}{\mu_{12}} \|w-u\|^2 M^2}}{m_1^2 \frac{\mu_{34}}{\mu_{12}} - m_4^2}$$

and $\Delta_3^{(3)}$ is defined by

$$\Delta_3^{(3)} = \beta_{34}\sigma_{34}^2(n_1n_4)^{1/2}\left(\frac{m_1m_4}{(2\pi kT)^2}\right)^{3/4}\frac{\mu_{34}}{\mu_{12}}$$
$$\times\exp\left[-\frac{m_4}{2kT}\left(u-\frac{w-u-\frac{1}{M}\left(-m_1\sqrt{\frac{\mu_{34}}{\mu_{12}}+\frac{2Q_R}{\mu_{12}\|L\|^2}}-m_4\right)L}{\frac{1}{M}\left(-m_1\sqrt{\frac{\mu_{34}}{\mu_{12}}}-m_4\right)}-L\right)^2\right.$$
$$-\frac{m_1}{2kT}\left(u+\frac{1}{M}\left(m_2\sqrt{\frac{\mu_{34}}{\mu_{12}}+\frac{2Q_R}{\mu_{12}\|L\|^2}}-m_4\right)L\right.$$
$$\left.\left.+\frac{1}{M}\left(m_2\sqrt{\frac{\mu_{34}}{\mu_{12}}}-m_4\right)\frac{w-u-\frac{1}{M}\left(-m_1\sqrt{\frac{\mu_{34}}{\mu_{12}}+\frac{2Q_R}{\mu_{12}\|L\|^2}}-m_4\right)L}{\frac{1}{M}\left(-m_1\sqrt{\frac{\mu_{34}}{\mu_{12}}}-m_4\right)}\right)^2\right]$$
$$\times\Theta(\|L\|-\Gamma_{34})\left\|\frac{\frac{1}{M}\left(-m_1\sqrt{\frac{\mu_{34}}{\mu_{12}}}-m_4\right)}{w-u-\frac{1}{M}\left(-m_1\sqrt{\frac{\mu_{34}}{\mu_{12}}+\frac{2Q_R}{\mu_{12}\|L\|^2}}-m_4\right)L}\right\|\|L\|^2\sin\theta,$$

with

$$L = (\|L\|\cos\theta, \|L\|\sin\theta\cos\varphi, \|L\|\sin\theta\sin\varphi),$$

$$\cos\theta = -\frac{1}{M}\left(m_1\sqrt{\frac{\mu_{34}}{\mu_{12}}+\frac{2Q_R}{\mu_{12}\|L\|^2}}+m_4\right)\frac{\|L\|}{\|w-u\|},$$

$$\sin\theta = \sqrt{1-\cos^2\theta}.$$

C4) For $i = 4$ we have

$$N(R_4^{(3)})(u,w) = \int_0^{2\pi} \left[\int_0^{\frac{\|w-u\|M}{m_3}} \Delta_4^{(3)} d\|L\| \Theta\left(\sqrt{\frac{2Q_R m_3^2}{\mu_{34} M^2}} - \|w-u\| \right) \right. \tag{4.127}$$

$$\left. + \int_0^{\|L\|_{43}^+} \Delta_4^{(3)}\, d\|L\| \Theta\left(\|w-u\| - \sqrt{\frac{2Q_R m_3^2}{\mu_{34} M^2}} \right) \right] \left(\frac{M}{m_2\sqrt{\frac{\mu_{34}}{\mu_{12}}} + m_3} \right)^3 d\varphi.$$

where $\|L\|_{43}^+$ is defined by

$$\|L\|_{43}^+ = \frac{-m_3\|w-u\|M + \sqrt{\left(m_2^2\frac{\mu_{34}}{\mu_{12}} - m_3^2\right)\frac{2Q_R m_2^2}{\mu_{12}} + m_2^2\frac{\mu_{34}}{\mu_{12}}\|w-u\|^2 M^2}}{-m_3^2 + m_2^2\frac{\mu_{34}}{\mu_{12}}}$$

and $\Delta_4^{(3)}$ is defined by

$$\Delta_4^{(3)} = \beta_{43}\sigma_{43}^2 (n_2 n_3)^{1/2} \left(\frac{m_2 m_3}{(2\pi kT)^2} \right)^{3/4} \frac{\mu_{34}}{\mu_{12}}$$

$$\times \exp\left[-\frac{m_3}{2kT} \left(w + \frac{u - w - \frac{1}{M}\left(m_2\sqrt{\frac{\mu_{34}}{\mu_{12}} + \frac{2Q_R}{\mu_{12}\|L\|^2}} + m_3\right)L}{\frac{1}{M}\left(m_2\sqrt{\frac{\mu_{34}}{\mu_{12}}} + m_3\right)} + L \right)^2 \right.$$

$$-\frac{m_2}{2kT} \left(w + \frac{1}{M}\left(-m_1\sqrt{\frac{\mu_{34}}{\mu_{12}} + \frac{2Q_R}{\mu_{12}\|L\|^2}} + m_3 \right) L \right.$$

$$\left.\left. + \frac{1}{M}\left(-m_1\sqrt{\frac{\mu_{34}}{\mu_{12}}} + m_3\right) \frac{u - w - \frac{1}{M}\left(m_2\sqrt{\frac{\mu_{34}}{\mu_{12}} + \frac{2Q_R}{\mu_{12}\|L\|^2}} + m_3\right)L}{\frac{1}{M}\left(m_2\sqrt{\frac{\mu_{34}}{\mu_{12}}} + m_3\right)} \right)^2 \right]$$

$$\times \Theta(\|L\| - \Gamma_{43}) \left\| \frac{\frac{1}{M}\left(m_2\sqrt{\frac{\mu_{34}}{\mu_{12}}} + m_3\right)}{u - w - \frac{1}{M}\left(m_2\sqrt{\frac{\mu_{34}}{\mu_{12}} + \frac{2Q_R}{\mu_{12}\|L\|^2}} + m_3\right)L} \right\| \|L\|^2 \sin\theta,$$

with

$$\begin{aligned} L &= (\|L\|\cos\theta, \|L\|\sin\theta\cos\varphi, \|L\|\sin\theta\sin\varphi), \\ \cos\theta &= \frac{1}{M}\left(m_2\sqrt{\frac{\mu_{34}}{\mu_{12}} + \frac{2Q_R}{\mu_{12}\|L\|^2}} + m_3\right)\frac{\|L\|}{\|w-u\|}, \\ \sin\theta &= \sqrt{1-\cos^2\theta}. \end{aligned}$$

Kernels of the "hybrid" operators

We split the operator T_i of Eq. (4.96) in the form

$$T_i(\underline{\hat{h}}) = \nu_i\hat{h_i} + T_i^{(1)}(\underline{\hat{h}}) - T_i^{(2)}(\underline{\hat{h}}) - T_i^{(3)}(\underline{\hat{h}}), \tag{4.128}$$

where

$$\nu_i\hat{h_i} = \hat{h}_i\beta_{ij}\sigma_{ij}^2\int_{\mathbb{R}^3}\int_{\mathbb{S}^2_+} M_j\Theta(\langle\epsilon,\xi_i\rangle - \Gamma_{ij})\,\langle\epsilon,\xi_i\rangle\,d\epsilon\,d\boldsymbol{c}_j, \tag{4.129}$$

$$T_i^{(1)}(\underline{\hat{h}}) = \beta_{ij}\sigma_{ij}^2\int_{\mathbb{R}^3}\int_{\mathbb{S}^2_+} M_i^{1/2}M_j\hat{h_j}\Theta(\langle\epsilon,\xi_i\rangle - \Gamma_{ij})\,\langle\epsilon,\xi_i\rangle\,d\epsilon\,d\boldsymbol{c}_j, \tag{4.130}$$

$$T_i^{(2)}(\underline{\hat{h}}) = \beta_{ij}\sigma_{ij}^2\int_{\mathbb{R}^3}\int_{\mathbb{S}^2_+} M_i^{1/2}M_j{M'_i}^{-1/2}\hat{h_i}'\Theta(\langle\epsilon,\xi_i\rangle - \Gamma_{ij})\,\langle\epsilon,\xi_i\rangle\,d\epsilon\,d\boldsymbol{c}_j, \tag{4.131}$$

$$T_i^{(3)}(\underline{\hat{h}}) = \beta_{ij}\sigma_{ij}^2\int_{\mathbb{R}^3}\int_{\mathbb{S}^2_+} M_i^{1/2}M_j{M'_j}^{-1/2}\hat{h_j}'\Theta(\langle\epsilon,\xi_i\rangle - \Gamma_{ij})\,\langle\epsilon,\xi_i\rangle\,d\epsilon\,d\boldsymbol{c}_j. \tag{4.132}$$

Now using 1) of Lemma 4.6.1, $T_i^{(2)}(\underline{\hat{h}})$ simplifies to

$$T_i^{(2)}(\underline{\hat{h}}) = \beta_{ij}\sigma_{ij}^2\int_{\mathbb{R}^3}\int_{\mathbb{S}^2_+} M_j^{1/2}{M'_j}^{1/2}\hat{h_i}'\Theta(\langle\epsilon,\xi_i\rangle - \Gamma_{ij})\,\langle\epsilon,\xi_i\rangle\,d\epsilon\,d\boldsymbol{c}_j, \tag{4.133}$$

while $T_i^{(3)}(\underline{\hat{h}})$ simplifies to

$$T_i^{(3)}(\underline{\hat{h}}) = \beta_{ij}\sigma_{ij}^2 \int_{\mathbb{R}^3} \int_{\mathbb{S}_+^2} M_j^{1/2} M_i'^{1/2} \hat{h}_j{}' \Theta(\langle \epsilon, \xi_i \rangle - \Gamma_{ij}) \langle \epsilon, \xi_i \rangle \, d\epsilon \, d\boldsymbol{c}_j. \quad (4.134)$$

The factor ν_i can be identified as a collisional operator. The operator $T_i^{(1)}(\underline{\hat{h}})$ of Eq. (4.130) coincides with the operator $R_i^{(1)}(\underline{\hat{h}})$ of Eq. (4.112), so that its kernel is equal to the one of $R_i^{(1)}(\underline{\hat{h}})$ given in Eq. (4.117). Moreover, the representation of the kernels of the operators $T_i^{(2)}(\underline{\hat{h}})$ and $T_i^{(3)}(\underline{\hat{h}})$ is obtained with a procedure similar to the one used for the elastic operators $Q_i^{(2)}(\underline{\hat{h}})$ and $Q_i^{(3)}(\underline{\hat{h}})$. The kernels are the following.

$$\begin{aligned} N(T_i^{(1)})(u,w) &= \beta_{ij}\sigma_{ij}^2 \|u-w\| (n_i n_j)^{1/2} \left(\frac{m_i m_j}{(2\pi kT)^2}\right)^{3/4} \exp\left[-\frac{m_i u^2 + m_j w^2}{4kT}\right] \\ &\times \int_0^{\frac{\pi}{2}} \cos\theta \sin\theta \Theta(\|u-w\|\cos\theta - \Gamma_{ij}) d\theta, \end{aligned} \quad (4.135)$$

$$\begin{aligned} N(T_i^{(2)})(u,w) &= \beta_{ij}\sigma_{ij}^2 \, n_j \left(\frac{m_i}{2\mu_{ij}}\right)^2 \left(\frac{m_j}{2\pi kT}\right)^{1/2} \frac{1}{\|u-w\|} \exp\left[-\frac{m_s}{8kT}\frac{(u^2-w^2)^2}{\|u-w\|^2}\right. \\ &\left. -\frac{m_s}{4kT}\left(\frac{m_i}{2\mu_{is}} - \frac{1}{2}\right)(u-w)^2\right] \Theta\Big(\frac{m_i\|u-w\|}{2\mu_{ij}} - \Gamma_{ij}\Big), \end{aligned} \quad (4.136)$$

If $m_j < m_i$ then

$$
\begin{aligned}
& N(T_i^{(3)})(u,w) && (4.137)\\
&= \beta_{ij}\sigma_{ij}^2(n_in_j)^{1/2}\left(\frac{m_im_j}{(2\pi kT)^2}\right)^{\frac{3}{4}}\int_{D_{L_2^-}}\int_{D_{L_1^-}}\frac{1}{\sqrt{\|u-w\|^2-(\frac{2\mu_{ij}}{m_j}-1)^2\|L\|^2}}\\
&\times\exp\left[-\frac{1}{4kT}\left\{m_j\left(w-\frac{2\mu_{ij}}{m_j}L\right)^2+m_i\left(u\left(1-\frac{2\mu_{ij}}{m_i}\right)\right.\right.\right.\\
&\left.\left.\left.+\frac{2\mu_{ij}}{m_i}w-\frac{2\mu_{ij}}{m_i}\left(\frac{2\mu_{ij}}{m_j}-1\right)L\right)^2\right\}\right]\\
&\times\Theta\left(\sqrt{\|u-w\|^2-\left(\frac{2\mu_{ij}}{m_j}-1\right)^2\|L\|^2}-\Gamma_{ij}\right)dL_1dL_2.
\end{aligned}
$$

If $m_j > m_i$ then

$$
\begin{aligned}
& N(T_i^{(3)})(u,w) && (4.138)\\
&= \beta_{ij}\sigma_{ij}^2(n_in_j)^{1/2}\left(\frac{m_im_j}{(2\pi kT)^2}\right)^{\frac{3}{4}}\int_{D_{L_2^+}}\int_{D_{L_1^+}}\frac{1}{\sqrt{\|u-w\|^2-(\frac{2\mu_{ij}}{m_j}-1)^2\|L\|^2}}\\
&\times\exp\left[-\frac{1}{4kT}\left\{m_j\left(w-\frac{2\mu_{ij}}{m_j}L\right)^2+m_i\left(u\left(1-\frac{2\mu_{ij}}{m_i}\right)\right.\right.\right.\\
&\left.\left.\left.+\frac{2\mu_{ij}}{m_i}w-\frac{2\mu_{ij}}{m_i}\left(\frac{2\mu_{ij}}{m_j}-1\right)L\right)^2\right\}\right]\\
&\times\Theta\left(\sqrt{\|u-w\|^2-\left(\frac{2\mu_{ij}}{m_j}-1\right)^2\|L\|^2}-\Gamma_{ij}\right)dL_1dL_2.
\end{aligned}
$$

If $m_j = m_i$ then

$$N(T_i^{(3)})(u,w) = \frac{\beta_{ij}\sigma_{is}^2}{\|u-w\|}\,(n_i n_s)^{1/2}\left(\frac{m_s}{2\pi kT}\right)^{1/2}\Theta\Big(\|u-w\|-\Gamma_{ij}\Big)$$
$$\times\exp\left[-\frac{m_s}{8kT}(u-w)^2-\frac{m_s}{8kT}\frac{\left(u^2-w^2\right)^2}{\|u-w\|^2}\right]. \tag{4.139}$$

In the above expression (4.137) the integration domains $D_{L_1^-}$ and $D_{L_2^-}$ are characterized by

$$\frac{w_1-u_1-\sqrt{(u_1-w_1)^2+(u_3-w_3)^2-4\left(\dfrac{2\mu_{ij}}{m_j}-1\right)L_2\left(u_2-w_2+L_2\left(\dfrac{2\mu_{ij}}{m_j}-1\right)\right)}}{2\left(\frac{2\mu_{ij}}{m_j}-1\right)}$$
$$\leq L_1 \leq \tag{4.140}$$
$$\frac{w_1-u_1+\sqrt{(u_1-w_1)^2+(u_3-w_3)^2-4\left(\dfrac{2\mu_{ij}}{m_j}-1\right)L_2\left(u_2-w_2+L_2\left(\dfrac{2\mu_{ij}}{m_j}-1\right)\right)}}{2\left(\frac{2\mu_{ij}}{m_j}-1\right)}$$
$$\frac{w_2-u_2-\|u-w\|}{2\left(\frac{2\mu_{ij}}{m_j}-1\right)} \;\leq\; L_2 \leq \frac{w_2-u_2+\|u-w\|}{2\left(\frac{2\mu_{ij}}{m_j}-1\right)} \tag{4.141}$$

In expression (4.138) the integration domains $D_{L_1^+}$ and $D_{L_2^+}$ are characterized by

$$\frac{w_1-u_1+\sqrt{(u_1-w_1)^2+(u_3-w_3)^2-4\left(\frac{2\mu_{ij}}{m_j}-1\right)L_2\left(u_2-w_2+L_2\left(\frac{2\mu_{ij}}{m_j}-1\right)\right)}}{2\left(\frac{2\mu_{ij}}{m_j}-1\right)}$$

$$\leq L_1 \leq \tag{4.142}$$

$$\frac{w_1-u_1-\sqrt{(u_1-w_1)^2+(u_3-w_3)^2-4\left(\frac{2\mu_{ij}}{m_j}-1\right)L_2\left(u_2-w_2+L_2\left(\frac{2\mu_{ij}}{m_j}-1\right)\right)}}{2\left(\frac{2\mu_{ij}}{m_j}-1\right)}$$

$$\frac{w_2-u_2+\|u-w\|}{2\left(\frac{2\mu_{ij}}{m_j}-1\right)} \leq L_2 \leq \frac{w_2-u_2-\|u-w\|}{2\left(\frac{2\mu_{ij}}{m_j}-1\right)} \tag{4.143}$$

4.7 Discussion

In this chapter we have presented the theory of simple reacting spheres (SRS), to describe the evolution of a chemically reactive mixture in the kinetic theory of gases. The model is a natural extension of the well-known hard-sphere collisional model within inert gases, see [69]. The particles behave as if they were single mass points and both elastic and reactive collisions are of hard-sphere type. In particular, reactive collisions modify the internal state of the particles and occur when the kinetic energy of the colliding particles exceeds the activation energy.

We did not take into consideration the particles shape and the intermolecular forces are considered to be instantaneous. Notwithstanding, these choices allow the construction of a consistent kinetic model verifying the fundamental basic properties from both the mathematical and physical point of view.

The Boltzmann collisional operators are nonlinear and therefore the task of finding solutions or analyzing the SRS equations is extremely difficult. It

is important to proceed with some simplifications to obtain more handling mathematical problems. The linearized formulation of the SRS equations arises as a simplification of the full system, which is valid when the reactive mixture is close to the thermodynamical equilibrium. Although simpler, the linearized SRS system retains the more relevant properties and information of the original equation. Regarding the Boltzmann equation for a single component gas, Cercignani [17], stated that the linearized Boltzmann equation is important since, under specific conditions, its results are appropriate to properly describe physical conditions and may constitute a preliminary step in the resolution of the full Boltzmann equation.
There are several works on the linearized Boltzmann equation, in particular [12, 18, 39, 40, 41], and on linear integral operators in general [48, 88]. In this chapter, we presented some properties of the linearized collisional operators such as their symmetry and non-positivity. In addition, the representation of the kernels and the expressions of the collisional frequency were computed, for the first time in literature, in the case of a chemically reactive gas mixture. Notice that, for a one component gas, the explicit expressions of the kernels and collisional frequencies of the linearized collisional operator, as well as the techniques to compute them, are presented in many works, namely in [12, 18, 40, 80]. However, this is not the case for a reactive gas mixture. Some of the adopted procedures are similar to those used in the case of one constituent gas. Since these computations are long and very technical, we decided to present only two representative cases. The complete results and the detailed calculations will be published in a detailed paper about this subject.

We would like to finish this chapter by discussing interesting developments for future works. We are interested in studying existence and asymptotic stability of close to equilibrium solutions for the simple reacting spheres system, within the kinetic theory of reactive mixtures. The properties of the linearized collisional operators around the thermodynamical equilibrium state and the explicit representation of the kernels play a crucial role in this study. Another interesting subject is the spectral analysis of the linearized collisional operator. As it is known, this can be used to characterize the solutions of the linearized Boltzmann equations and, under specific conditions [41], obtain approximations for the full Boltzmann equation solutions.

Conclusions

Since the first time it was presented, the Boltzmann equation has been the subject of several works. Some of the contents we studied here, have already been treated by other authors. However, considering the nature of this work, we think that it is of the utmost importance to present explicitly our main contributions to the kinetic theory.

The goal of Chapter 1 was to explain, in general, both the concepts and main properties of the Boltzmann equation. Although this chapter did not present any new contribution to the theme, we consider it of great importance on understanding the work presented thereafter.

In Chapter 2, we described the steady detonation wave on one space dimension. Again, other authors have studied the wave propagation in kinetic theory and the detonation wave, in particular. Our main contribution lies on the inclusion of the reaction heat effect on the detonation wave's profile. In classical theory, the results concerning this influence are already known, but in this work they were presented for the first time from a microscopic point of view.

The hydrodynamic stability of the detonation wave was studied in Chapter 3. It is a rather complex subject. This is not the first work which studies it on the scope of the kinetic theory. Nevertheless, we consider that our study is more complete as it includes certain non-equilibrium effects, such as the contribution of the reaction heat and the activation theory on the stability spectrum.

The search for the stability solutions is often a complex and slow process. To overcome these difficulties we developed a numerical method which takes into account the ideas of several authors. With this method we were able to reduce significantly the time required to find the stability solutions. We firmly believe that this method can be applied on other problems and that there is room for improving it. The results presented in Chapter 3 gave the first detailed investigation of the stability problem, obtained on the kinetic theory context, and were in qualitative accordance with the previous results known from the classical theory.

Finally, in Chapter 4, we constructed the so called SRS model, step by step, starting from basic mechanical and chemical concepts. The development of the model was described in such a detail that is not frequent in literature. We chose to do so in order to allow a greater understanding of the model. Since both the kinetic modeling and its properties are well known, besides the detail we used in describing the models' development, we stress our contribution on how we organized concepts and properties scattered throughout the literature. In addition, we also deduced the collisional frequency and the kernels' of the integral operator of the Boltzmann linearized equation explicit representation.

Appendix A

Calculation of an elastic kernel

In this appendix we include the detailed computations of the kernels of the linearized elastic integral operators $Q_i^{(2)}$. Let us re-write the integral operator $Q_i^{(2)}$ defined by expression (4.102), namely

$$Q_i^{(2)}(\underline{\hat{h}}) = \sum_{s=1}^{4} \sigma_{is}^2 \int_{\mathbb{R}^3} \int_{\mathbb{S}_+^2} M_s^{1/2} {M'_s}^{1/2} h'_i \langle \epsilon, \boldsymbol{c}_i - \boldsymbol{c}_s \rangle \, d\epsilon \, d\boldsymbol{c}_s, \tag{A.1}$$

We introduce a new notation $\boldsymbol{c}_i = u$, $\boldsymbol{c}_s = w$ and perform the transformation $w \mapsto \xi$, with $\xi = u - w$, in the external integral of expression (A.1). The Jacobian of this transformation is given by $J(\xi; w) = -1$. Since

$$\boldsymbol{c}_3 = u - \frac{2\mu_{is}}{m_i} \langle \epsilon, \xi \rangle \epsilon \qquad \text{and} \qquad \boldsymbol{c}_4 = w + \frac{2\mu_{is}}{m_s} \langle \epsilon, \xi \rangle \epsilon,$$

we get

$$\begin{aligned} Q_i^{(2)}(\underline{\hat{h}}) \;=\; & \sum_{s=1}^{4} \sigma_{is}^2 \int_{\mathbb{R}^3} \int_{\mathbb{S}_+^2} \hat{h}_i \Big(u - \frac{2\mu_{is}}{m_i} \langle \epsilon, \xi \rangle \epsilon \Big) \\ & \times M_s^{1/2} \left(u - \xi + \frac{2\mu_{is}}{m_s} \langle \epsilon, \xi \rangle \epsilon \right) M_s^{1/2}(u - \xi) \langle \epsilon, \xi \rangle \, d\epsilon \, d\xi. \end{aligned} \tag{A.2}$$

Now, in Eq. (A.2), we first change the order of integration. Then we split the vector ξ in the form $\xi = l + L$, with l and L such that $l // \epsilon$ and $L \perp \epsilon$. Therefore, we have

$$\langle \epsilon, \xi \rangle = \langle \epsilon, l \rangle + \langle \epsilon, L \rangle = \|l\|,$$

and

$$l = \langle \epsilon, \xi \rangle \epsilon = \|l\| \epsilon \qquad \text{and} \qquad L = \xi - \langle \epsilon, \xi \rangle \epsilon = \xi - \|l\| \epsilon.$$

Finally, we observe that the integration in expression (A.2), for $\epsilon \in \mathbb{S}^2_+$ and $\xi \in \mathbb{R}^3$, can be transformed to an integration over $(L, \|l\|, \epsilon)$, with $L \perp \epsilon$, $\|l\| \in [0, +\infty[$ and $\epsilon \in \mathbb{S}^2$. Consequently, from Eq. (A.2), we obtain

$$\begin{aligned} Q_i^{(2)}(\underline{\hat{h}}) = \sum_{s=1}^{4} \sigma_{is}^2 \int_{\mathbb{S}^2} \int_0^{+\infty} \int_{L \perp \epsilon} \hat{h}_i\Big(u - \frac{2\mu_{is}}{m_i}\, l\Big) \\ \times M_s^{1/2} \left(u - L + \left(\frac{2\mu_{is}}{m_s} - 1 \right) l \right) M_s^{1/2}(u - l - L)\, dL\, \|l\|\, d\|l\|\, d\epsilon. \end{aligned} \tag{A.3}$$

Now, we transform the external integral to spherical coordinates, getting

$$\begin{aligned} Q_i^{(2)}(\underline{\hat{h}}) = \sum_{s=1}^{4} \sigma_{is}^2 \int_0^{2\pi} \int_0^{\pi} \int_0^{+\infty} \int_{L \perp \epsilon} h_i\Big(u - \frac{2\mu_{is}}{m_i} l\Big) \\ \times M_s^{1/2} \left(u - L + \left(\frac{2\mu_{is}}{m_s} - 1 \right) l \right) M_s^{1/2}(u - l - L)\, dL\, \|l\|\, d\|l\| \sin\theta\, d\theta\, d\varphi. \end{aligned} \tag{A.4}$$

Then, we express the vector l in spherical coordinates, that is

$$l = (\|l\| \cos\theta, \|l\| \sin\theta \cos\varphi, \|l\| \sin\theta \sin\varphi),$$

and transform the triple integral over $[0, +\infty[\times [0, \pi] \times [0, 2\pi[$ according to $(\|l\|, \theta, \varphi) \mapsto l$. The corresponding Jacobian is given by $J(l; \|l\|, \theta, \varphi) =$

$\dfrac{1}{\|l\|^2 \sin\theta}$ and Eq. (A.4) becomes

$$Q_i^{(2)}(\underline{\hat{h}}) = \sum_{s=1}^{4} \sigma_{is}^2 \int_{\mathbb{R}^3} \frac{1}{\|l\|} \int_{L\perp l} h_i\Big(u - \frac{2\mu_{is}}{m_i} l\Big) \times M_s^{1/2}\left(u - L + \left(\frac{2\mu_{is}}{m_s} - 1\right) l\right) M_s^{1/2}(u - l - L)\, dL\, dl. \tag{A.5}$$

Introducing, in the external integral, the transformation $l \mapsto \eta$ with $\eta = u - \dfrac{2\mu_{is}}{m_i} l$, whose Jacobian is $J(\eta; l) = -\left(\dfrac{m_i}{2\mu_{is}}\right)^3$, we obtain

$$\begin{aligned} Q_i^{(2)}(\underline{\hat{h}}) &= \sum_{s=1}^{4} \sigma_{is}^2 \int_{\mathbb{R}^3} \Big|\Big| \frac{2\mu_{is}}{m_i(u-\eta)} \Big|\Big| \left(\frac{m_i}{2\mu_{is}}\right)^3 \int_{L\perp u-\eta} M_s^{1/2}\Big(u - \frac{m_i(u-\eta)}{2\mu_{is}} - L\Big) \\ &\quad \times M_s^{1/2}\left(u - L + \left(\frac{2\mu_i s}{m_s} - 1\right)\left(\frac{m_i}{2\mu_{is}}\right)(u-\eta)\right) \hat{h}_i(\eta)\, dL\, d\eta \\ &= \sum_{s=1}^{4} \sigma_{is}^2 \int_{\mathbb{R}^3} \frac{1}{\|u-\eta\|} \left(\frac{m_i}{2\mu_{is}}\right)^2 \hat{h}_i(\eta)\, n_s \left(\frac{m_s}{2\pi kT}\right)^{\frac{3}{2}} \qquad \text{(A.6)} \\ &\quad \times \int_{L\perp u-\eta} \exp\left[-\frac{m_s}{4kT}\left\{\left(u - \frac{m_i(u-\eta)}{2\mu_{is}} - L\right)^2 \right.\right. \\ &\quad \left.\left. + \left(u - L + \left(\frac{2\mu_i s}{m_s} - 1\right)\left(\frac{m_i}{2\mu_{is}}\right)(u-\eta)\right)^2\right\}\right] dL d\eta. \end{aligned}$$

Taking into account that

$$\begin{aligned} &\left(u - \frac{m_i(u-\eta)}{2\mu_{is}} - L\right)^2 + \left(u - L + \left(\frac{2\mu_i s}{m_s} - 1\right)\left(\frac{m_i}{2\mu_{is}}\right)(u-\eta)\right)^2 \\ &\qquad = 2\left(L - \frac{u+\eta}{2}\right)^2 + \left(\frac{m_i}{2\mu_{is}} - \frac{1}{2}\right)(u-\eta)^2, \end{aligned}$$

the expression (A.6) takes the form

$$\sum_{s=1}^{4} \sigma_{is}^2 \int_{\mathbb{R}^3} \frac{n_s}{\|u-\eta\|} \left(\frac{m_i}{2\mu_{is}}\right)^2 \hat{h}_i(\eta) \left(\frac{m_s}{2\pi kT}\right)^{\frac{3}{2}} \exp\left[-\frac{m_s}{2kT}\left(\frac{m_i}{2\mu_{is}} - \frac{1}{2}\right)(u-\eta)^2\right]$$
$$\times \int_{L \perp u-\eta} \exp\left[-\frac{m_s}{2kT}\left(L - \frac{u+\eta}{2}\right)^2\right] dL d\eta.$$

Now we consider the vector $\varphi = \frac{u+\eta}{2}$ and split it in the form $\varphi = \varphi_p + \varphi_n$, with $\varphi_p // L$ and $\varphi_n \perp L$. With these transformations we obtain

$$\int_{L \perp u-\eta} \exp\left[-\frac{m_s}{2kT}\left(L - \frac{u+\eta}{2}\right)^2\right] dL$$
$$= \exp\left[-\frac{m_s}{2kT}\varphi_n^2\right] \int_{L \perp u-\eta} \exp\left[-\frac{m_s}{2kT}(L-\varphi_p)^2\right] dL,$$

where

$$\varphi_n^2 = \left\langle \varphi, \frac{l}{\|l\|} \right\rangle^2 = \frac{(u^2-\eta^2)^2}{4\|u-\eta\|^2}.$$

Finally, coming back to the expression (A.7) of the integral operator $Q_i^{(2)}$ we have

$$Q_i^{(2)}(\underline{\hat{h}}) = \int_{\mathbb{R}^3} \sum_{s=1}^{4} \sigma_{is}^2 \frac{n_s}{\|u-\eta\|} \left(\frac{m_i}{2\mu_{is}}\right)^2 \left(\frac{m_s}{2\pi kT}\right)^{1/2} \hat{h}_i(\eta) \tag{A.7}$$
$$\times \exp\left[-\frac{m_s}{8kT}\frac{(u^2-\eta^2)^2}{\|u-\eta\|^2} - \frac{m_s}{4kT}\left(\frac{m_i}{2\mu_{is}} - \frac{1}{2}\right)(u-\eta)^2\right] d\eta.$$

Therefore the kernel of the operator $Q_i^{(2)}$ can be identified as

$$N(Q_i^{(2)})(u,w) = \sum_{s=1}^{4} \sigma_{is}^2 \frac{n_s}{\|u-w\|} \left(\frac{m_i}{2\mu_{is}}\right)^2 \left(\frac{m_s}{2\pi kT}\right)^{1/2}$$
$$\times \exp\left[-\frac{m_s}{8kT}\frac{(u^2-w^2)^2}{\|u-w\|^2} - \frac{m_s}{4kT}\left(\frac{m_i}{2\mu_{is}} - \frac{1}{2}\right)(u-w)^2\right]$$

and this is the expression listed in Eq. (4.105) of Subsection 4.6.2.

Appendix B

Calculation of a reactive kernel

In this appendix we include the detailed computations of the kernel of the linearized elastic integral operators $R_3^{(2)}$. The integral operator $R_3^{(2)}$ defined by expression (4.115) for the case $i = 3$ ($j = 4$, $k = 1$, $l = 2$) is given by

$$R_3^{(2)}(\underline{\hat{h}}) = \beta_{34}\sigma_{34}^2 \int_{\mathbb{R}^3} \int_{\mathbb{S}_+^2} \frac{\mu_{34}}{\mu_{12}} M_4^{1/2} M_2^{1/2} \hat{h}_1 \Theta(\langle \epsilon, \xi' \rangle - \Gamma_{34}) \langle \epsilon, \xi' \rangle \, d\epsilon \, d\boldsymbol{c}_4, \quad \text{(B.1)}$$

where

$$\boldsymbol{c}_1 = \frac{1}{M} \left[m_3 \boldsymbol{c}_3 + m_4 \boldsymbol{c}_4 + m_2 \sqrt{\frac{\mu_{34}}{\mu_{12}}} \left\{ \xi' - \epsilon \langle \epsilon, \xi' \rangle + \epsilon \alpha^+ \right\} \right] \quad \text{(B.2)}$$

and

$$\boldsymbol{c}_2 = \frac{1}{M} \left[m_3 \boldsymbol{c}_3 + m_4 \boldsymbol{c}_4 - m_1 \sqrt{\frac{\mu_{34}}{\mu_{12}}} \left\{ \xi' - \epsilon \langle \epsilon, \xi' \rangle + \epsilon \alpha^+ \right\} \right]. \quad \text{(B.3)}$$

Above, $\alpha^+ = \sqrt{(\langle \epsilon, \xi' \rangle)^2 + 2Q_R/\mu_{12}}$.

In order to simplify further calculations, we introduce the new variable β defined as follows

$$\beta = \frac{\xi' - \langle \xi', \epsilon \rangle \epsilon}{\| \xi' \times \epsilon \|}.$$

The following properties hold

(a) $\|\beta\| = 1$;

(b) $\langle \beta, \epsilon \rangle = 0$;

(c) $\langle \beta, \xi' \rangle = \|\epsilon \times \xi'\| \quad$ (assuming $\langle \beta, \xi' \rangle \geq 0$);

(d) $\langle \epsilon, \xi' \rangle = \|\beta \times \xi'\| \quad$ (assuming $\langle \epsilon, \xi' \rangle \geq 0$);

(e) $\epsilon = \dfrac{\xi' - \langle \xi', \beta \rangle \beta}{\|\xi' \times \beta\|}$.

We introduce a new notation $\boldsymbol{c}_3 = u$, $\boldsymbol{c}_4 = w$ and write the vectors $\boldsymbol{c}_1$ and $\boldsymbol{c}_2$ in expressions (B.2) and (B.3) in terms of the variable β in the form

$$\boldsymbol{c}_1 = \frac{1}{M}\left[m_3 u + m_4 w + m_2 \sqrt{\frac{\mu_{34}}{\mu_{12}}}\left\{\langle \xi', \beta \rangle \beta + \frac{\xi' - \langle \xi', \beta \rangle \beta}{\|\xi' \times \beta\|}\sqrt{\|\beta \times \xi'\|^2 + \frac{2Q_R}{\mu_{34}}}\right\}\right] \tag{B.4}$$

and

$$\boldsymbol{c}_2 = \frac{1}{M}\left[m_3 u + m_4 w - m_1 \sqrt{\frac{\mu_{34}}{\mu_{12}}}\left\{\langle \xi', \beta \rangle \beta + \frac{\xi' - \langle \xi', \beta \rangle \beta}{\|\xi' \times \beta\|}\sqrt{\|\beta \times \xi'\|^2 + \frac{2Q_R}{\mu_{34}}}\right\}\right] \tag{B.5}$$

respectively. Now we consider the transformation $(\epsilon, w) \mapsto (\beta, \xi')$. The corresponding Jacobian is given by

$$J(\beta, \xi'; \epsilon, w) = \frac{\langle \xi', \beta \rangle}{\|\xi' \times \beta\|}.$$

Accordingly, the integral in expression (B.1) transforms to

$$R_3^{(2)} = \int_{\mathbb{R}^3}\int_{\mathbb{S}^2_+} \beta_{34}\sigma_{34}^2 \frac{\mu_{34}}{\mu_{12}} M_4^{1/2}(u-\xi')M_2^{1/2}\Bigg(\frac{1}{M}[m_3u{+}m_4w \tag{B.6}$$

$$-m_1\sqrt{\frac{\mu_{34}}{\mu_{12}}}\left\{\langle\xi',\beta\rangle\beta+\frac{\xi'-\langle\xi',\beta\rangle\beta}{\|\xi'\times\beta\|}\sqrt{\|\beta\times\xi'\|^2+\frac{2Q_R}{\mu_{34}}}\right\}\Bigg]\Bigg)$$

$$\times h_1\left(\frac{1}{M}\left[m_3u{+}m_4w{+}m_2\sqrt{\frac{\mu_{34}}{\mu_{12}}}\,\{\langle\xi',\beta\rangle\beta\right.\right.$$

$$\left.\left.+\frac{\xi'-\langle\xi',\beta\rangle\beta}{\|\xi'\times\beta\|}\sqrt{\|\beta\times\xi'\|^2+\frac{2Q_R}{\mu_{34}}}\right\}\right]\right)\Theta\Big(\|\xi'\times\beta\|-\Gamma_{34}\Big)\langle\beta,\xi'\rangle\,d\beta\,d\xi'.$$

We now split the vector ξ' in the form $\xi'=l+L$, with l and L such that $l//\beta$ and $L\perp\beta$. Therefore, we have

$$\langle\beta,\xi'\rangle=\langle\beta,l\rangle+\langle\beta,L\rangle=\|l\|,$$

$$l=\langle\beta,\xi'\rangle\beta=\|l\|\beta,\qquad L=\xi'-\langle\beta,\xi'\rangle\beta=\xi'-\|l\|\beta,$$

$$\frac{\xi'-\langle\xi',\beta\rangle\beta}{\|\xi'\times\beta\|}=\frac{L}{\|L\|}.$$

Using this decomposition, we can compute the vector appearing in the argument of h_1 in the previous integral of expression (B.6), as follows

$$u+\frac{1}{M}\left[-m_4\xi'+m_2\sqrt{\frac{\mu_{34}}{\mu_{12}}}\left\{\langle\xi',\beta\rangle\beta+\frac{\xi'-\langle\xi',\beta\rangle\beta}{\|\xi'\times\beta\|}\sqrt{\|\beta\times\xi'\|^2+\frac{2Q_R}{\mu_{34}}}\right\}\right]$$

$$=u+\frac{1}{M}\left[-m_4(l+L)+m_2\sqrt{\frac{\mu_{34}}{\mu_{12}}}\left\{l+\frac{L}{\|L\|}\sqrt{\|L\|^2+\frac{2Q_R}{\mu_{34}}}\right\}\right]$$

$$=u+\frac{1}{M}\left(m_2\sqrt{\frac{\mu_{34}}{\mu_{12}}}-m_4\right)l+\frac{1}{M}\left(m_2\sqrt{\frac{\mu_{34}}{\mu_{12}}}\sqrt{1+\frac{2Q_R}{\mu_{34}\|L\|^2}}-m_4\right)L$$

$$=u+\frac{1}{M}\left(m_2\sqrt{\frac{\mu_{34}}{\mu_{12}}}-m_4\right)l+\frac{1}{M}\left(m_2\sqrt{\frac{\mu_{34}}{\mu_{12}}+\frac{2Q_R}{\mu_{12}\|L\|^2}}-m_4\right)L. \tag{B.7}$$

Finally, we observe that the integration in expression (B.6), for $\epsilon \in \mathbb{S}^2_+$ and $\xi' \in \mathbb{R}^3$, can be transformed into an integration over $(L, \|l\|, \beta)$, with $L \perp \beta$, $\|l\| \in [0, +\infty[$ and $\beta \in \mathbb{S}^2$. Consequently, from Eq. (B.6), we obtain

$$
\begin{aligned}
R_3^{(2)} = & \int_{\mathbb{S}^2} \int_0^{+\infty} \int_{L \perp \beta} \beta_{34} \sigma_{34}^2 \frac{\mu_{34}}{\mu_{12}} M_4^{1/2}(u - l - L) \\
& \times M_2^{1/2}\left(u - \frac{1}{M}\left(m_1 \sqrt{\frac{\mu_{34}}{\mu_{12}}} - m_4\right) l + \frac{1}{M}\left(-m_1 \sqrt{\frac{\mu_{34}}{\mu_{12}} + \frac{2Q_R}{\mu_{12}}} - m_4\right) L\right) \\
& \times h_1\left(u + \frac{1}{M}\left(m_2 \sqrt{\frac{\mu_{34}}{\mu_{12}}} - m_4\right) l + \frac{1}{M}\left(m_2 \sqrt{\frac{\mu_{34}}{\mu_{12}} + \frac{2Q_R}{\mu_{12}\|L\|^2}} - m_4\right) L\right) \\
& \times \Theta(\|L\| - \Gamma_{34}) \, \|l\| \, dL \, d\|l\| \, d\beta.
\end{aligned}
\tag{B.8}
$$

Now, we transform the external integral in expression (B.8) to spherical coordinates, getting

$$
\begin{aligned}
R_3^{(2)} = & \int_0^{2\pi} \int_0^{\pi} \int_0^{+\infty} \int_{L \perp \beta} \beta_{34} \sigma_{34}^2 \frac{\mu_{34}}{\mu_{12}} M_4^{1/2}(u - l - L) \\
& \times M_2^{1/2}\left(u - \frac{1}{M}\left(m_1 \sqrt{\frac{\mu_{34}}{\mu_{12}}} - m_4\right) l + \frac{1}{M}\left(-m_1 \sqrt{\frac{\mu_{34}}{\mu_{12}} + \frac{2Q_R}{\mu_{12}}} - m_4\right) L\right) \\
& \times h_1\left(u + \frac{1}{M}\left(m_2 \sqrt{\frac{\mu_{34}}{\mu_{12}}} - m_4\right) l + \frac{1}{M}\left(m_2 \sqrt{\frac{\mu_{34}}{\mu_{12}} + \frac{2Q_R}{\mu_{12}\|L\|^2}} - m_4\right) L\right) \\
& \times \Theta(\|L\| - \Gamma_{34}) \, \|l\| \, dL \, d\|l\| \sin\theta d\theta d\varphi.
\end{aligned}
\tag{B.9}
$$

Then, we express the vector l in spherical coordinates, that is

$$
l = (\|l\| \cos\theta, \|l\| \sin\theta \cos\varphi, \|l\| \sin\theta \sin\varphi),
$$

and transform the triple integral, over $[0, +\infty[\times [0, \pi] \times [0, 2\pi[$, according to $(\|l\|, \theta, \varphi) \mapsto l$, with $l \in \mathbb{R}^3$. The corresponding Jacobian is given by

$J(l;\|l\|,\theta,\varphi)=\dfrac{1}{\|l\|^2\sin\theta}$. Thus, Eq. (B.9) becomes

$$\begin{aligned}R_3^{(2)} =& \int_{\mathbb{R}^3}\int_{L\perp l} \beta_{34}\sigma_{34}^2\frac{\mu_{34}}{\mu_{12}}M_4^{1/2}(u-l-L) \qquad \text{(B.10)}\\ &\times M_2^{1/2}\!\left(u-\frac{1}{M}\left(m_1\sqrt{\frac{\mu_{34}}{\mu_{12}}}-m_4\right)l+\frac{1}{M}\left(-m_1\sqrt{\frac{\mu_{34}}{\mu_{12}}+\frac{2Q_R}{\mu_{12}}}-m_4\right)L\right)\\ &\times h_1\!\left(u+\frac{1}{M}\left(m_2\sqrt{\frac{\mu_{34}}{\mu_{12}}}-m_4\right)l+\frac{1}{M}\left(m_2\sqrt{\frac{\mu_{34}}{\mu_{12}}+\frac{2Q_R}{\mu_{12}\|L\|^2}}-m_4\right)L\right)\\ &\times\Theta(\|L\|-\Gamma_{34})\,\frac{1}{\|l\|}\,dL\,dl.\end{aligned}$$

Now we introduce the transformation $l\mapsto\eta$, with η defined by

$$\eta=u+\frac{1}{M}\left(m_2\sqrt{\frac{\mu_{34}}{\mu_{12}}}-m_4\right)l+\frac{1}{M}\left(m_2\sqrt{\frac{\mu_{34}}{\mu_{12}}+\frac{2Q_R}{\mu_{12}\|L\|^2}}-m_4\right)L, \quad \text{(B.11)}$$

in the external integral. The corresponding Jacobian is

$$J(\eta;l)=\left(\frac{M}{m_2\sqrt{\frac{\mu_{34}}{\mu_{12}}}-m_4}\right)^3.$$

Expression (B.10) takes the following form

$$R_3^{(2)} = \int_{\mathbb{R}^3}\int_{D_L} \beta_{34}\sigma_{34}^2 \frac{\mu_{34}}{\mu_{12}} \left(\frac{M}{m_2\sqrt{\frac{\mu_{34}}{\mu_{12}}} - m_4} \right)^3 \tag{B.12}$$

$$\times M_4^{1/2} \left(u - \frac{\eta - u - \frac{1}{M}\left(m_2\sqrt{\frac{\mu_{34}}{\mu_{12}} + \frac{2Q_R}{\mu_{12}\|L\|^2}} - m_4\right) L}{\frac{1}{M}\left(m_2\sqrt{\frac{\mu_{34}}{\mu_{12}}} - m_4\right)} - L \right)$$

$$\times M_2^{1/2} \left(u + \frac{1}{M}\left(-m_1\sqrt{\frac{\mu_{34}}{\mu_{12}} + \frac{2Q_R}{\mu_{12}}} - m_4\right) L \right.$$

$$\left. - \frac{1}{M}\left(m_1\sqrt{\frac{\mu_{34}}{\mu_{12}}} - m_4\right) \frac{\eta - u - \frac{1}{M}\left(m_2\sqrt{\frac{\mu_{34}}{\mu_{12}} + \frac{2Q_R}{\mu_{12}\|L\|^2}} - m_4\right) L}{\frac{1}{M}\left(m_2\sqrt{\frac{\mu_{34}}{\mu_{12}}} - m_4\right)} \right)$$

$$\times h_1(\eta)\Theta(\|L\| - \Gamma_{34}) \left\| \frac{\frac{1}{M}\left(m_2\sqrt{\frac{\mu_{34}}{\mu_{12}}} - m_4\right)}{\eta - u - \frac{1}{M}\left(m_2\sqrt{\frac{\mu_{34}}{\mu_{12}} + \frac{2Q_R}{\mu_{12}\|L\|^2}} - m_4\right) L} \right\| dL\, d\eta.$$

In order to extract the kernel of $R_3^{(2)}$ from expression (B.12), we have to specify the domain D_L and simplify the expression in the integrand. In order to do so, we transform the internal integral to spherical coordinates, introducing the angle θ between L and $\eta - u$. Using condition $\langle L, l \rangle = 0$ and expression (B.11), we can write

$$\left\langle L, \frac{\eta - u - \frac{1}{M}\left(m_2\sqrt{\frac{\mu_{34}}{\mu_{12}} + \frac{2Q_R}{\mu_{12}\|L\|^2}} - m_4\right) L}{\frac{1}{M}\left(m_2\sqrt{\frac{\mu_{34}}{\mu_{12}}} - m_4\right)} \right\rangle = 0$$

or

$$\left\langle L, \eta - u - \frac{1}{M}\left(m_2\sqrt{\frac{\mu_{34}}{\mu_{12}} + \frac{2Q_R}{\mu_{12}\|L\|^2}} - m_4\right) L \right\rangle = 0,$$

that is

$$\langle L, \eta - u \rangle = \frac{1}{M} \left(m_2 \sqrt{\frac{\mu_{34}}{\mu_{12}} + \frac{2Q_R}{\mu_{12}\|L\|^2}} - m_4 \right) \|L\|^2, \tag{B.13}$$

and we obtain

$$\cos\theta = \frac{1}{M} \left(m_2 \sqrt{\frac{\mu_{34}}{\mu_{12}} + \frac{2Q_R}{\mu_{12}\|L\|^2}} - m_4 \right) \frac{\|L\|}{\|\eta - u\|}, \tag{B.14}$$

provided that

$$-1 \leq \frac{1}{M} \left(m_2 \sqrt{\frac{\mu_{34}}{\mu_{12}} + \frac{2Q_R}{\mu_{12}\|L\|^2}} - m_4 \right) \frac{\|L\|}{\|\eta - u\|} \leq 1. \tag{B.15}$$

The conditions (B.15) are crucial for the characterization of the domain D_L. First we consider the second inequality in condition (B.15), that is

$$\frac{1}{M} \left(m_2 \sqrt{\frac{\mu_{34}}{\mu_{12}} + \frac{2Q_R}{\mu_{12}\|L\|^2}} - m_4 \right) \frac{\|L\|}{\|\eta - u\|} \leq 1, \tag{B.16}$$

or equivalently

$$m_2 \sqrt{\frac{\mu_{34}}{\mu_{12}} + \frac{2Q_R}{\mu_{12}\|L\|^2}} \leq \frac{\|\eta - u\|M}{\|L\|} + m_4. \tag{B.17}$$

Since the quantities in both sides of Eq. (B.17) are positive, we obtain

$$m_2^2 \left(\frac{\mu_{34}}{\mu_{12}} + \frac{2Q_R}{\mu_{12}\|L\|^2} \right) \leq \frac{\|\eta - u\|^2 M^2}{\|L\|^2} + m_4^2 + 2m_4 \frac{\|\eta - u\|M}{\|L\|}, \tag{B.18}$$

that is

$$\left(m_2^2 \frac{\mu_{34}}{\mu_{12}} - m_4^2 \right) \|L\|^2 - 2m_4\|\eta - u\|M\|L\| + \frac{2Q_R m_2^2}{\mu_{12}} - \|\eta - u\|^2 M^2 \leq 0, \tag{B.19}$$

where the coefficient of $\|L\|^2$ is positive, thanks to the assumptions $m_1 < m_2$ and $m_4 < m_3$. In fact,

$$\begin{aligned}
m_2^2 \frac{\mu_{34}}{\mu_{12}} - m_4^2 &= m_2^2 \frac{m_3 m_4}{m_1 m_2} - m_4^2 \\
&= \frac{m_4}{m_1} (m_2 m_3 - m_1 m_4) \\
&= \frac{m_4}{m_1} \Big(m_2(M - m_4) - (M - m_2) m_4 \Big) \\
&= \frac{m_4 M}{m_1} (m_2 - m_4) > 0. \qquad \text{(B.20)}
\end{aligned}$$

Therefore, condition (B.19) is verified in a certain domain if, and only if, its discriminant is positive, that is

$$4m_4^2 \|\eta - u\|^2 M^2 + 4 \left(m_2^2 \frac{\mu_{34}}{\mu_{12}} - m_4^2 \right) \left(-\frac{2Q_R m_2^2}{\mu_{12}} + \|\eta - u\|^2 M^2 \right) > 0,$$

or simply

$$m_2^2 \frac{\mu_{34}}{\mu_{12}} \|\eta - u\|^2 M^2 > \left(m_2^2 \frac{\mu_{34}}{\mu_{12}} - m_4^2 \right) \frac{2Q_R m_2^2}{\mu_{12}}. \qquad \text{(B.21)}$$

Since the terms in both sides of this inequality are positive, see Eq. (B.20), we get

$$\|\eta - u\| > \sqrt{\left(m_2^2 \frac{\mu_{34}}{\mu_{12}} - m_4^2 \right) \frac{2Q_R}{\mu_{34} M^2}}. \qquad \text{(B.22)}$$

The two zeros of the quadratic polynomial on the left-hand side of (B.19) are

$$\|L\|_{32}^{+} = \frac{m_4 \|\eta - u\| M + \sqrt{-\left(m_2^2 \frac{\mu_{34}}{\mu_{12}} - m_4^2 \right) \frac{2Q_R m_2^2}{\mu_{12}} + m_2^2 \frac{\mu_{34}}{\mu_{12}} \|\eta - u\|^2 M^2}}{m_2^2 \frac{\mu_{34}}{\mu_{12}} - m_4^2} \qquad \text{(B.23)}$$

and

$$\|L\|_{32}^{-} = \frac{m_4\|\eta-u\|M - \sqrt{-\left(m_2^2\frac{\mu_{34}}{\mu_{12}} - m_4^2\right)\frac{2Q_R m_2^2}{\mu_{12}} + m_2^2\frac{\mu_{34}}{\mu_{12}}\|\eta-u\|^2M^2}}{m_2^2\frac{\mu_{34}}{\mu_{12}} - m_4^2}, \tag{B.24}$$

where $\|L\|_{32}^{+} > 0$, and $\|L\|_{32}^{-} > 0$ if and only if $\|\eta-u\| < \sqrt{\frac{2Q_R m_2^2}{M^2\mu_{12}}}$. Therefore, it is convenient to compare $\sqrt{\left(m_2^2\frac{\mu_{34}}{\mu_{12}} - m_4^2\right)\frac{2Q_R}{\mu_{34}M^2}}$ with $\sqrt{\frac{2Q_R m_2^2}{M^2\mu_{12}}}$. It is immediate that

$$\sqrt{\left(m_2^2\frac{\mu_{34}}{\mu_{12}} - m_4^2\right)\frac{2Q_R}{\mu_{34}M^2}} < \sqrt{\frac{2Q_R m_2^2}{M^2\mu_{12}}}, \tag{B.25}$$

since

$$\begin{aligned}
&\sqrt{\left(m_2^2\frac{\mu_{34}}{\mu_{12}} - m_4^2\right)\frac{2Q_R}{\mu_{34}M^2}} < \sqrt{\frac{2Q_R m_2^2}{\mu_{12}M^2}} \\
&\qquad\Leftrightarrow \left(m_2^2\frac{\mu_{34}}{\mu_{12}} - m_4^2\right)\frac{2Q_R}{\mu_{34}M^2} < \frac{2Q_R m_2^2}{\mu_{12}M^2} \\
&\qquad\Leftrightarrow \left(m_2^2\frac{m_3m_4}{m_1m_2} - m_4^2\right)\frac{1}{m_3m_4} < \frac{m_2}{m_1} \\
&\qquad\Leftrightarrow \frac{m_2^2}{m_1m_2} - \frac{m_4}{m_3} < \frac{m_2}{m_1} \\
&\qquad\Leftrightarrow -\frac{m_4}{m_3} < 0.
\end{aligned}$$

The previous analysis of the second inequality in condition (B.15) leads to the following conclusion about the domain D_L in the internal integral of expression (B.12):

(i) If $\sqrt{\left(m_2^2\frac{\mu_{34}}{\mu_{12}} - m_4^2\right)\frac{2Q_R}{\mu_{34}M^2}} < \|\eta - u\| < \sqrt{\frac{2Q_R m_2^2}{M^2\mu_{12}}}$, then

$$|L\|_{32}^{-} \leq \|L\| \leq \|L\|_{32}^{+}, \tag{B.26}$$

provided that condition (B.22) holds.

(ii) If $\|\eta - u\| > \sqrt{\frac{2Q_R m_2^2}{M^2\mu_{12}}}$, then

$$\|L\|_{32}^{-} < 0 \leq \|L\| \leq \|L\|_{32}^{+}, \tag{B.27}$$

provided that condition (B.22) holds.

Observe that condition (B.27) is more restrictive than condition (B.26). However, in both cases (i) and (ii), condition (B.26) is verified. This fact is used in the sequel.

The next step is to work on the first inequality in condition (B.15), and then combine the resulting conclusions with those stated above in items (i) and (ii) for the second inequality in condition (B.15). We consider two cases, namely *Case A* and *Case B*, each one with four sub-cases, namely situations first, second, third and fourth. The results obtained for these cases and sub-cases are first combined with the above condition (B.26). In a further step, the results of both *Cases A* and *B* are gathered and simplified. Finally, the above restrictive condition (B.27) is taken into account and the analysis of the domain D_L is concluded.

Accordingly, let us consider the first inequality in condition (B.15), that is

$$\frac{1}{M}\left(m_2\sqrt{\frac{\mu_{34}}{\mu_{12}} + \frac{2Q_R}{\mu_{12}\|L\|^2}} - m_4\right)\frac{\|L\|}{\|\eta - u\|} \geq -1 \tag{B.28}$$

or

$$m_2\sqrt{\frac{\mu_{34}}{\mu_{12}} + \frac{2Q_R}{\mu_{12}\|L\|^2}} \;\geq\; m_4 - \frac{\|\eta - u\|M}{\|L\|}. \tag{B.29}$$

Now we consider two different cases.

<u>*Case A*</u> - If the term on the right-hand-side of condition (B.29) is non-positive, that is

$$m_4 - \frac{\|\eta - u\|M}{\|L\|} \leq 0, \tag{B.30}$$

or equivalently

$$\|L\| \leq \frac{\|\eta - u\|M}{m_4}, \tag{B.31}$$

then condition (B.28) is trivially verified. In this case, we have to combine condition (B.31) with those previously obtained in items (i) and (ii), see Eqs. (B.22), (B.26) and (B.27). We start with the comparison of the quantities $\|L\|_{32}^{-}$, $\|L\|_{32}^{+}$ and $\frac{\|\eta-u\|M}{m_4}$, considering the following situations.

First. $m_2m_3 \leq 2m_1m_4$ and $(m_2m_3 - 2m_1m_4)^2 < m_1m_2m_3m_4$
In this situation we have

$$\|L\|_{32}^{+} \geq \frac{\|\eta - u\|M}{m_4}, \tag{B.32}$$

since

$$\begin{aligned}
\|L\|_{32}^{+} &= \frac{m_4\|\eta - u\|M + \sqrt{-\left(m_2^2\frac{\mu_{34}}{\mu_{12}} - m_4^2\right)\frac{2Q_R m_2^2}{\mu_{12}} + m_2^2\frac{\mu_{34}}{\mu_{12}}\|\eta - u\|^2M^2}}{m_2^2\frac{\mu_{34}}{\mu_{12}} - m_4^2} \\
&\geq \frac{m_4\|\eta - u\|M}{m_2^2\frac{\mu_{34}}{\mu_{12}} - m_4^2},
\end{aligned}$$

where

$$m_2^2\frac{\mu_{34}}{\mu_{12}}-m_4^2=\frac{m_2m_3m_4}{m_1}-m_4^2=\frac{m_4}{m_1}(m_2m_3-m_1m_4)\leq\frac{m_4}{m_1}(2m_1m_4-m_1m_4)=m_4^2. \tag{B.33}$$

Therefore,

$$\|L\|_{32}^{+}\geq\frac{m_4\|\eta-u\|M}{m_4^2}=\frac{\|\eta-u\|M}{m_4}.$$

Moreover, for what concerns $\|L\|_{32}^{-}$, we observe that

$$\|L\|_{32}^{-}\leq\frac{\|\eta-u\|M}{m_4} \tag{B.34}$$

if and only if

$$\frac{m_4\|\eta-u\|M-\sqrt{-\left(m_2^2\frac{\mu_{34}}{\mu_{12}}-m_4^2\right)\frac{2Q_Rm_2^2}{\mu_{12}}+m_2^2\frac{\mu_{34}}{\mu_{12}}\|\eta-u\|^2M^2}}{m_2^2\frac{\mu_{34}}{\mu_{12}}-m_4^2}\leq\frac{\|\eta-u\|M}{m_4},$$

that is,

$$-\sqrt{-\left(m_2^2\frac{\mu_{34}}{\mu_{12}}-m_4^2\right)\frac{2Q_Rm_2^2}{\mu_{12}}+m_2^2\frac{\mu_{34}}{\mu_{12}}\|\eta-u\|^2M^2}\leq\frac{\|\eta-u\|M}{m_4}\left(m_2^2\frac{\mu_{34}}{\mu_{12}}-2m_4^2\right),$$

where the term on the right hand side is non-positive. In fact, thanks to condition (B.33), we have

$$m_2^2\frac{\mu_{34}}{\mu_{12}}-2m_4^2\leq 0. \tag{B.35}$$

Consequently, condition (B.34) holds if and only if

$$-\left(m_2^2\frac{\mu_{34}}{\mu_{12}}-m_4^2\right)\frac{2Q_Rm_2^2}{\mu_{12}}+m_2^2\frac{\mu_{34}}{\mu_{12}}\|\eta-u\|^2M^2\geq\frac{\|\eta-u\|^2M^2}{m_4^2}\left(m_2^2\frac{\mu_{34}}{\mu_{12}}-2m_4^2\right)^2,$$

that is,

$$-\left(m_2^2\frac{\mu_{34}}{\mu_{12}}-m_4^2\right)\frac{2Q_Rm_2^2}{\mu_{12}} \geq \frac{\|\eta-u\|^2M^2}{m_4^2}\left[\left(m_2^2\frac{\mu_{34}}{\mu_{12}}-2m_4^2\right)^2-m_4^2m_2^2\frac{\mu_{34}}{\mu_{12}}\right]. \tag{B.36}$$

Here, the term on the right hand side is negative, since

$$\begin{aligned}
&\left(m_2^2\frac{\mu_{34}}{\mu_{12}}-2m_4^2\right)^2-m_4^2m_2^2\frac{\mu_{34}}{\mu_{12}} \\
&= m_2^4\frac{\mu_{34}^2}{\mu_{12}^2}+4m_4^4-5m_4^2m_2^2\frac{\mu_{34}}{\mu_{12}} \\
&= \frac{m_2^4m_3^2m_4^2}{m_1^2m_2^2}+4m_4^4-5m_2^2m_4^2\frac{m_3m_4}{m_1m_2} \\
&= \frac{m_4^2}{m_1^2}\left(m_2^2m_3^2+4m_1^2m_4^2-5m_1m_2m_3m_4\right) \\
&= \frac{m_4^2}{m_1^2}\left[(m_2m_3-2m_1m_4)^2-m_1m_2m_3m_4\right] \\
&< 0
\end{aligned} \tag{B.37}$$

thanks to the second hypothesis within this first situation. Thus, from condition (B.36), we obtain

$$\frac{-\left(m_2^2\frac{\mu_{34}}{\mu_{12}}-m_4^2\right)\frac{2Q_Rm_2^2m_4^2}{\mu_{12}M^2}}{\left(m_2^2\frac{\mu_{34}}{\mu_{12}}-2m_4^2\right)^2-m_4^2m_2^2\frac{\mu_{34}}{\mu_{12}}} \leq \|\eta-u\|^2$$

and finally

$$\|\eta-u\| \geq \sqrt{\frac{-\left(m_2^2\frac{\mu_{34}}{\mu_{12}}-m_4^2\right)\frac{2Q_Rm_2^2m_4^2}{\mu_{12}M^2}}{\left(m_2^2\frac{\mu_{34}}{\mu_{12}}-2m_4^2\right)^2-m_4^2m_2^2\frac{\mu_{34}}{\mu_{12}}}}. \tag{B.38}$$

Then we conclude that condition (B.34) holds if and only if condition (B.38) holds.

Finally, we have to compare the quantities $\sqrt{\frac{-\left(m_2^2\frac{\mu_{34}}{\mu_{12}}-m_4^2\right)\frac{2Q_R m_2^2 m_4^2}{\mu_{12}M^2}}{\left(m_2^2\frac{\mu_{34}}{\mu_{12}}-2m_4^2\right)^2-m_4^2m_2^2\frac{\mu_{34}}{\mu_{12}}}}$ and $\sqrt{\left(m_2^2\frac{\mu_{34}}{\mu_{12}}-m_4^2\right)\frac{2Q_R}{\mu_{34}M^2}}$. We have

$$\sqrt{\left(m_2^2\frac{\mu_{34}}{\mu_{12}}-m_4^2\right)\frac{2Q_R}{\mu_{34}M^2}} \le \sqrt{\frac{-\left(m_2^2\frac{\mu_{34}}{\mu_{12}}-m_4^2\right)\frac{2Q_R m_2^2 m_4^2}{\mu_{12}M^2}}{\left(m_2^2\frac{\mu_{34}}{\mu_{12}}-2m_4^2\right)^2-m_4^2m_2^2\frac{\mu_{34}}{\mu_{12}}}}, \qquad \text{(B.39)}$$

since it is equivalent to

$$\left(m_2^2\frac{\mu_{34}}{\mu_{12}}-m_4^2\right)\frac{2Q_R}{\mu_{34}M^2} \le \frac{-\frac{2Q_R}{M}\left(m_2^2\frac{\mu_{34}}{\mu_{12}}-m_4^2\right)}{\frac{m_2m_3^2}{m_1}+\frac{4m_4^2m_1}{m_2}-5m_3m_4},$$

or to

$$(m_2m_3-2m_1m_4)^2 \ge 0,$$

which is trivially verified. In this first situation, if

$$\sqrt{\left(m_2^2\frac{\mu_{34}}{\mu_{12}}-m_4^2\right)\frac{2Q_R}{\mu_{34}M^2}} < \|\eta-u\| < \sqrt{\frac{-\left(m_2^2\frac{\mu_{34}}{\mu_{12}}-m_4^2\right)\frac{2Q_R m_2^2 m_4^2}{\mu_{12}M^2}}{\left(m_2^2\frac{\mu_{34}}{\mu_{12}}-2m_4^2\right)^2-m_4^2m_2^2\frac{\mu_{34}}{\mu_{12}}}},$$

then

$$\frac{\|\eta-u\|M}{m_4} < \|L\|_{32}^- < \|L\|_{32}^+$$

which contradicts the fact that conditions (B.26) and (B.31) must be verified.

On the other hand, if

$$\|\eta - u\| > \sqrt{\frac{-\left(m_2^2\frac{\mu_{34}}{\mu_{12}} - m_4^2\right)\frac{2Q_R m_2^2 m_4^2}{\mu_{12}M^2}}{\left(m_2^2\frac{\mu_{34}}{\mu_{12}} - 2m_4^2\right)^2 - m_4^2 m_2^2\frac{\mu_{34}}{\mu_{12}}}}$$

then

$$\|L\|_{32}^{-} < \frac{\|\eta - u\|M}{m_4} < \|L\|_{32}^{+},$$

and from conditions (B.26) and (B.31) we get $\|L\|_{32}^{-} \leq \|L\| \leq \frac{\|\eta - u\|M}{m_4}$.

Second. $m_2m_3 \leq 2m_1m_4$ and $(m_2m_3 - 2m_1m_4)^2 \geq m_1m_2m_3m_4$

In this situation, conditions (B.33) and (B.35) still hold true. Moreover, we now have (see condition (B.37))

$$\left(m_2^2\frac{\mu_{34}}{\mu_{12}} - 2m_4^2\right)^2 - m_4^2 m_2^2\frac{\mu_{34}}{\mu_{12}} \geq 0. \tag{B.40}$$

Consequently, we get

$$\|L\|_{32}^{-} > \frac{\|\eta - u\|M}{m_4}.$$

In fact

$$
\begin{aligned}
&\|L\|_{32}^{-} > \frac{\|\eta - u\|M}{m_4} \\
\Leftrightarrow &\frac{m_4\|\eta-u\|M-\sqrt{-\left(m_2^2\frac{\mu_{34}}{\mu_{12}}-m_4^2\right)\frac{2Q_Rm_2^2}{\mu_{12}}+m_2^2\frac{\mu_{34}}{\mu_{12}}\|\eta-u\|^2M^2}}{m_2^2\frac{\mu_{34}}{\mu_{12}}-m_4^2} > \frac{\|\eta-u\|M}{m_4} \\
\Leftrightarrow &-\sqrt{-\left(m_2^2\frac{\mu_{34}}{\mu_{12}}-m_4^2\right)\frac{2Q_Rm_2^2}{\mu_{12}}+m_2^2\frac{\mu_{34}}{\mu_{12}}\|\eta-u\|^2M^2} \\
&\qquad > \frac{\|\eta-u\|M}{m_4}\left(m_2^2\frac{\mu_{34}}{\mu_{12}}-2m_4^2\right) \\
\Leftrightarrow &-\left(m_2^2\frac{\mu_{34}}{\mu_{12}}-m_4^2\right)\frac{2Q_Rm_2^2}{\mu_{12}}+m_2^2\frac{\mu_{34}}{\mu_{12}}\|\eta-u\|^2M^2 \\
&\qquad < \frac{\|\eta-u\|^2M^2}{m_4^2}\left(m_2^2\frac{\mu_{34}}{\mu_{12}}-2m_4^2\right)^2 \\
\Leftrightarrow &-\left(m_2^2\frac{\mu_{34}}{\mu_{12}}-m_4^2\right)\frac{2Q_Rm_2^2}{\mu_{12}} < \frac{\|\eta-u\|^2M^2}{m_4^2}\left[\left(m_2^2\frac{\mu_{34}}{\mu_{12}}-2m_4^2\right)^2-m_4^2m_2^2\frac{\mu_{34}}{\mu_{12}}\right],
\end{aligned}
$$

which is trivially verified, since the left hand side is negative and the right hand side is non-negative. However, condition $\|L\|_{32}^{-} > \frac{\|\eta-u\|M}{m_4}$ contradicts the fact that conditions (B.26) and (B.31) must be verified.

Third. $m_2m_3 > 2m_1m_4$ and $(m_2m_3 - 2m_1m_4)^2 < m_1m_2m_3m_4$

In this situation, we have

$$m_2^2\frac{\mu_{34}}{\mu_{12}} - 2m_4^2 > 0 \tag{B.41}$$

and

$$\left(m_2^2\frac{\mu_{34}}{\mu_{12}} - 2m_4^2\right)^2 - m_4^2 m_2^2\frac{\mu_{34}}{\mu_{12}} < 0. \tag{B.42}$$

Consequently, we have

$$\|L\|_{32}^{+} \geq \frac{\|\eta - u\|M}{m_4} \quad \text{if and only if} \quad \|\eta{-}u\|{\geq}\sqrt{\frac{-\left(m_2^2\frac{\mu_{34}}{\mu_{12}} - m_4^2\right)\frac{2Q_R m_2^2 m_4^2}{\mu_{12}M^2}}{\left(m_2^2\frac{\mu_{34}}{\mu_{12}} - 2m_4^2\right)^2 - m_4^2 m_2^2\frac{\mu_{34}}{\mu_{12}}}}.$$

In fact,

$$\begin{aligned}
&\|L\|_{32}^{+} \geq \frac{\|\eta - u\|M}{m_4} \\
&\Leftrightarrow \frac{m_4\|\eta{-}u\|M{+}\sqrt{-\left(m_2^2\frac{\mu_{34}}{\mu_{12}}{-}m_4^2\right)\frac{2Q_R m_2^2}{\mu_{12}}{+}m_2^2\frac{\mu_{34}}{\mu_{12}}\|\eta{-}u\|^2 M^2}}{m_2^2\frac{\mu_{34}}{\mu_{12}}{-}m_4^2} \geq \frac{\|\eta{-}u\|M}{m_4} \\
&\Leftrightarrow -\left(m_2^2\frac{\mu_{34}}{\mu_{12}} - m_4^2\right)\frac{2Q_R m_2^2}{\mu_{12}} + m_2^2\frac{\mu_{34}}{\mu_{12}}\|\eta - u\|^2 M^2 \\
&\qquad\qquad \geq \frac{\|\eta - u\|^2 M^2}{m_4^2}\left(m_2^2\frac{\mu_{34}}{\mu_{12}} - 2m_4^2\right)^2 \\
&\Leftrightarrow -\left(m_2^2\frac{\mu_{34}}{\mu_{12}}{-}m_4^2\right)\frac{2Q_R m_2^2}{\mu_{12}} \geq \frac{\|\eta{-}u\|^2 M^2}{m_4^2}\left[\left(m_2^2\frac{\mu_{34}}{\mu_{12}}{-}2m_4^2\right)^2{-}m_4^2 m_2^2\frac{\mu_{34}}{\mu_{12}}\right] \\
&\Leftrightarrow \frac{-\left(m_2^2\frac{\mu_{34}}{\mu_{12}} - m_4^2\right)\frac{2Q_R m_2^2 m_4^2}{\mu_{12}M^2}}{\left(m_2^2\frac{\mu_{34}}{\mu_{12}} - 2m_4^2\right)^2 - m_4^2 m_2^2\frac{\mu_{34}}{\mu_{12}}} \leq \|\eta - u\|^2 \\
&\Leftrightarrow \|\eta - u\| \geq \sqrt{\frac{-\left(m_2^2\frac{\mu_{34}}{\mu_{12}} - m_4^2\right)\frac{2Q_R m_2^2 m_4^2}{\mu_{12}M^2}}{\left(m_2^2\frac{\mu_{34}}{\mu_{12}} - 2m_4^2\right)^2 - m_4^2 m_2^2\frac{\mu_{34}}{\mu_{12}}}}.
\end{aligned} \tag{B.43}$$

Moreover, the term on the right hand side verifies condition (B.39), as before.

For what concerns $\|L\|_{32}^{-}$, we have

$$\|L\|_{32}^{-} \leq \frac{\|\eta - u\|M}{m_4}, \tag{B.44}$$

since

$$\begin{aligned}
&\|L\|_{32}^{-} \leq \frac{\|\eta - u\|M}{m_4} \\
&\Leftrightarrow \frac{m_4\|\eta-u\|M-\sqrt{-\left(m_2^2\frac{\mu_{34}}{\mu_{12}}-m_4^2\right)\frac{2Q_R m_2^2}{\mu_{12}}+m_2^2\frac{\mu_{34}}{\mu_{12}}\|\eta-u\|^2M^2}}{m_2^2\frac{\mu_{34}}{\mu_{12}}-m_4^2} \leq \frac{\|\eta-u\|M}{m_4} \\
&\Leftrightarrow -\sqrt{-\left(m_2^2\frac{\mu_{34}}{\mu_{12}} - m_4^2\right)\frac{2Q_R m_2^2}{\mu_{12}} + m_2^2\frac{\mu_{34}}{\mu_{12}}\|\eta - u\|^2M^2} \\
&\qquad\qquad \leq \frac{\|\eta - u\|M}{m_4}\left(m_2^2\frac{\mu_{34}}{\mu_{12}} - 2m_4^2\right),
\end{aligned}$$

where the left hand side is negative and the right hand side is positive.

In this third situation, the conclusion is the following.

If

$$\sqrt{\left(m_2^2\frac{\mu_{34}}{\mu_{12}} - m_4^2\right)\frac{2Q_R}{\mu_{34}M^2}} < \|\eta - u\| < \sqrt{\frac{-\left(m_2^2\frac{\mu_{34}}{\mu_{12}} - m_4^2\right)\frac{2Q_R m_2^2 m_4^2}{\mu_{12}M^2}}{\left(m_2^2\frac{\mu_{34}}{\mu_{12}} - 2m_4^2\right)^2 - m_4^2 m_2^2\frac{\mu_{34}}{\mu_{12}}}}$$

then we have, see conditions (B.43) and (B.44),

$$\|L\|_{32}^{-} < \|L\|_{32}^{+} < \frac{\|\eta - u\|M}{m_4},$$

and from conditions (B.26) and (B.31) we get $\|L\|_{32}^{-} \leq \|L\| \leq \|L\|_{32}^{+}$.

On the other hand, if

$$\|\eta - u\| > \sqrt{\frac{-\left(m_2^2\frac{\mu_{34}}{\mu_{12}} - m_4^2\right)\frac{2Q_R m_2^2 m_4^2}{\mu_{12}M^2}}{\left(m_2^2\frac{\mu_{34}}{\mu_{12}} - 2m_4^2\right)^2 - m_4^2 m_2^2\frac{\mu_{34}}{\mu_{12}}}}$$

then

$$\|L\|_{32}^{-} < \frac{\|\eta - u\|M}{m_4} < \|L\|_{32}^{+},$$

and from conditions (B.26) and (B.31) we get $\|L\|_{32}^{-} \leq \|L\| \leq \frac{\|\eta-u\|M}{m_4}$.

Fourth. $m_2m_3 > 2m_1m_4$ and $(m_2m_3 - 2m_1m_4)^2 \geq m_1m_2m_3m_4$

In this situation, we have

$$m_2^2\frac{\mu_{34}}{\mu_{12}} - 2m_4^2 > 0 \tag{B.45}$$

and

$$\left(m_2^2\frac{\mu_{34}}{\mu_{12}} - 2m_4^2\right)^2 - m_4^2 m_2^2\frac{\mu_{34}}{\mu_{12}} \geq 0. \tag{B.46}$$

Consequently,

$$\|L\|_{32}^{+} \leq \frac{\|\eta - u\|M}{m_4}, \tag{B.47}$$

since

$$
\begin{aligned}
&\|L\|_{32}^{+} \leq \frac{\|\eta-u\|M}{m_4} \\
&\Leftrightarrow \frac{m_4\|\eta-u\|M+\sqrt{-\left(m_2^2\frac{\mu_{34}}{\mu_{12}}-m_4^2\right)\frac{2Q_R m_2^2}{\mu_{12}}+m_2^2\frac{\mu_{34}}{\mu_{12}}\|\eta-u\|^2M^2}}{m_2^2\frac{\mu_{34}}{\mu_{12}}-m_4^2} \leq \frac{\|\eta-u\|M}{m_4} \\
&\Leftrightarrow \sqrt{-\left(m_2^2\frac{\mu_{34}}{\mu_{12}}-m_4^2\right)\frac{2Q_R m_2^2}{\mu_{12}}+m_2^2\frac{\mu_{34}}{\mu_{12}}\|\eta-u\|^2M^2} \\
&\qquad\qquad\qquad \leq \frac{\|\eta-u\|M}{m_4}\left(m_2^2\frac{\mu_{34}}{\mu_{12}}-2m_4^2\right) \\
&\Leftrightarrow -\left(m_2^2\frac{\mu_{34}}{\mu_{12}}-m_4^2\right)\frac{2Q_R m_2^2}{\mu_{12}}+m_2^2\frac{\mu_{34}}{\mu_{12}}\|\eta-u\|^2M^2 \\
&\qquad\qquad\qquad \leq \frac{\|\eta-u\|^2M^2}{m_4^2}\left(m_2^2\frac{\mu_{34}}{\mu_{12}}-2m_4^2\right)^2 \\
&\Leftrightarrow -\left(m_2^2\frac{\mu_{34}}{\mu_{12}}-m_4^2\right)\frac{2Q_R m_2^2}{\mu_{12}} \leq \frac{\|\eta-u\|^2M^2}{m_4^2}\left[\left(m_2^2\frac{\mu_{34}}{\mu_{12}}-2m_4^2\right)^2-m_4^2m_2^2\frac{\mu_{34}}{\mu_{12}}\right],
\end{aligned}
$$

which is trivially verified, since the left hand side is negative and the right hand side is non-negative. Thus, we conclude that

$$\|L\|_{32}^{-} < \|L\|_{32}^{+} \leq \frac{\|\eta-u\|M}{m_2},$$

and from conditions (B.26) and (B.31), we get

$$\|L\|_{32}^{-} \leq \|L\| \leq \|L\|_{32}^{+}.$$

<u>*Case B*</u> - If the term on the right-hand-side of condition (B.29) is positive,

that is

$$m_4 - \frac{\|\eta - u\| M}{\|L\|} > 0, \tag{B.48}$$

or equivalently

$$\|L\| > \frac{\|\eta - u\| M}{m_4}, \tag{B.49}$$

then, from condition (B.29), we may write

$$m_2^2 \left(\frac{\mu_{34}}{\mu_{12}} + \frac{2Q_R}{\mu_{12}\|L\|^2} \right) \geq m_4^2 + \frac{\|\eta - u\|^2 M^2}{\|L\|^2} - 2m_4 \frac{\|\eta - u\| M}{\|L\|}, \tag{B.50}$$

or

$$\left(m_2^2 \frac{\mu_{34}}{\mu_{12}} - m_4^2 \right) \|L\|^2 + 2m_4 \|\eta - u\| M \|L\| + \frac{2Q_R m_2^2}{\mu_{12}} - \|\eta - u\|^2 M^2 \geq 0, \tag{B.51}$$

where the coefficient of $\|L\|^2$ is positive, see Eq. (B.20). Thus, if the discriminant of the quadratic polynomial on the left hand side of Eq. (B.51) is non-positive, then condition (B.51) is verified for an arbitrary L. Conversely, if it is positive, then L must satisfy certain constraints in order to condition (B.51) be verified. Let us analyze this case. We have

$$4m_4^2 \|\eta - u\|^2 M^2 + 4 \left(m_2^2 \frac{\mu_{34}}{\mu_{12}} - m_4^2 \right) \left(-\frac{2Q_R m_2^2}{\mu_{12}} + \|\eta - u\|^2 M^2 \right) > 0,$$

that is

$$m_2^2 \frac{\mu_{34}}{\mu_{12}} \|\eta - u\|^2 M^2 > \left(m_2^2 \frac{\mu_{34}}{\mu_{12}} - m_4^2 \right) \frac{2Q_R m_2^2}{\mu_{12}} \tag{B.52}$$

where the terms in both sides are positive, see again Eq. (B.20). Thus

$$\|\eta - u\| > \sqrt{\left(m_2^2 \frac{\mu_{34}}{\mu_{12}} - m_4^2 \right) \frac{2Q_R}{\mu_{34} M^2}}. \tag{B.53}$$

The two zeros of the quadratic polynomial on the left-hand side of Eq. (B.51) are given by

$$\|L\|_{32B}^{+} = \frac{-m_4\|\eta - u\|M + \sqrt{-\left(m_2^2\frac{\mu_{34}}{\mu_{12}} - m_4^2\right)\frac{2Q_R m_2^2}{\mu_{12}} + m_2^2\frac{\mu_{34}}{\mu_{12}}\|\eta - u\|^2 M^2}}{m_2^2\frac{\mu_{34}}{\mu_{12}} - m_4^2} \tag{B.54}$$

and

$$\|L\|_{32B}^{-} = \frac{-m_4\|\eta - u\|M - \sqrt{-\left(m_2^2\frac{\mu_{34}}{\mu_{12}} - m_4^2\right)\frac{2Q_R m_2^2}{\mu_{12}} + m_2^2\frac{\mu_{34}}{\mu_{12}}\|\eta - u\|^2 M^2}}{m_2^2\frac{\mu_{34}}{\mu_{12}} - m_4^2}. \tag{B.55}$$

It is immediate that $\|L\|_{32B}^{-} < 0$. Let us study the sign of $\|L\|_{32B}^{+}$. We have

$$\|L\|_{32B}^{+} > 0 \qquad \text{if and only if} \qquad \|\eta - u\| > \sqrt{\frac{2Q_R m_2^2}{\mu_{12} M^2}}. \tag{B.56}$$

In fact,

$$\begin{aligned}
&\|L\|_{32B}^{+} > 0 \\
\Leftrightarrow\ & \frac{-m_4\|\eta - u\|M + \sqrt{-\left(m_2^2\frac{\mu_{34}}{\mu_{12}} - m_4^2\right)\frac{2Q_R m_2^2}{\mu_{12}} + m_2^2\frac{\mu_{34}}{\mu_{12}}\|\eta - u\|^2 M^2}}{m_2^2\frac{\mu_{34}}{\mu_{12}} - m_4^2} > 0 \\
\Leftrightarrow\ & m_4\|\eta - u\|M < \sqrt{-\left(m_2^2\frac{\mu_{34}}{\mu_{12}} - m_4^2\right)\frac{2Q_R m_2^2}{\mu_{12}} + m_2^2\frac{\mu_{34}}{\mu_{12}}\|\eta - u\|^2 M^2} \\
\Leftrightarrow\ & \left(m_2^2\frac{\mu_{34}}{\mu_{12}} - m_4^2\right)\|\eta - u\|^2 M^2 > \left(m_2^2\frac{\mu_{34}}{\mu_{12}} - m_4^2\right)\frac{2Q_R m_2^2}{\mu_{12}} \\
\Leftrightarrow\ & \|\eta - u\|^2 M^2 > \frac{2Q_R m_2^2}{\mu_{12}} \\
\Leftrightarrow\ & \|\eta - u\| > \sqrt{\frac{2Q_R m_2^2}{\mu_{12} M^2}}.
\end{aligned}$$

Having in mind condition (B.22), remember that the term $\sqrt{\frac{2Q_R m_2^2}{\mu_{12}M^2}}$ of Eq. (B.22) and the term $\sqrt{\left(m_2^2\frac{\mu_{34}}{\mu_{12}} - m_4^2\right)\frac{2Q_R}{\mu_{34}M^2}}$, above, are such that

$$\sqrt{\frac{2Q_R m_2^2}{\mu_{12}M^2}} > \sqrt{\left(m_2^2\frac{\mu_{34}}{\mu_{12}} - m_4^2\right)\frac{2Q_R}{\mu_{34}M^2}}.$$

Since this <u>*Case B*</u> is characterized by condition (B.49), it is also convenient to compare $\|L\|_{32B}^{+}$ with the term $\frac{\|\eta-u\|M}{m_4}$ that figures in Eq. (B.49). We have

$$\|L\|_{32B}^{+} < \frac{\|\eta - u\|M}{m_4}, \tag{B.57}$$

since

$$\|L\|_{32B}^{+} < \frac{\|\eta - u\|M}{m_4}$$

$$\Leftrightarrow \frac{-m_4\|\eta-u\|M + \sqrt{-\left(m_2^2\frac{\mu_{34}}{\mu_{12}} - m_4^2\right)\frac{2Q_R m_2^2}{\mu_{12}} + m_2^2\frac{\mu_{34}}{\mu_{12}}\|\eta-u\|^2M^2}}{m_2^2\frac{\mu_{34}}{\mu_{12}} - m_4^2} < \frac{\|\eta-u\|M}{m_4}$$

$$\Leftrightarrow \sqrt{-\left(m_2^2\frac{\mu_{34}}{\mu_{12}} - m_4^2\right)\frac{2Q_R m_2^2}{\mu_{12}} + m_2^2\frac{\mu_{34}}{\mu_{12}}\|\eta-u\|^2M^2} < \frac{\|\eta-u\|M}{m_4}\,\frac{m_2^2\mu_{34}}{\mu_{12}}$$

$$\Leftrightarrow -\left(m_2^2\frac{\mu_{34}}{\mu_{12}} - m_4^2\right)\frac{2Q_R m_2^2}{\mu_{12}} + m_2^2\frac{\mu_{34}}{\mu_{12}}\|\eta-u\|^2M^2 < \frac{\|\eta-u\|^2M^2m_2^4\mu_{34}^2}{\mu_{12}^2m_4^2}$$

$$\Leftrightarrow -\left(m_2^2\frac{\mu_{34}}{\mu_{12}} - m_4^2\right)\frac{2Q_R m_2^2}{\mu_{12}} < \|\eta-u\|^2M^2m_2^2\frac{\mu_{34}}{\mu_{12}}\left(\frac{m_2^2\mu_{34}}{m_4^2\mu_{12}} - 1\right)$$

$$\Leftrightarrow -\left(m_2^2\frac{\mu_{34}}{\mu_{12}} - m_4^2\right)\frac{2Q_R m_2^2}{\mu_{12}} < \|\eta-u\|^2M^2m_2^2\frac{\mu_{34}}{\mu_{12}}\left(\frac{m_2m_3 - m_1m_4}{m_1m_4}\right),$$

where the left hand side is negative and the right hand side is positive.

Consequently, as we explain in the following, in this <u>*Case B*</u> we conclude that condition (B.28) is verified only if $\|L\|$ is such that

$$\frac{\|\eta - u\|M}{m_4} < \|L\| < +\infty. \qquad \text{(B.58)}$$

In fact, if

$$\|\eta - u\| < \sqrt{\left(m_2^2\frac{\mu_{34}}{\mu_{12}} - m_4^2\right)\frac{2Q_R}{\mu_{34}M^2}}$$

then the discriminant of the quadratic polynomial on the left hand side of Eq. (B.51) is negative and the solution of condition (B.51), together with condition (B.49), lead to $\frac{\|\eta-u\|M}{m_4} < \|L\| < +\infty$. On the other hand, if

$$\sqrt{\left(m_2^2\frac{\mu_{34}}{\mu_{12}} - m_4^2\right)\frac{2Q_R}{\mu_{34}M^2}} < \|\eta - u\| < \sqrt{\frac{2Q_R m_2^2}{\mu_{12}M^2}}$$

then the discriminant of the quadratic polynomial on the left hand side of Eq. (B.51) is positive, and the two zeros of such polynomial, $\|L\|_{32B}^-$ and $\|L\|_{32B}^+$, are such that $\|L\|_{32B}^- < \|L\|_{32B}^+ < 0$. Thus, the solution of condition (B.51), together with condition (B.49), lead to $\frac{\|\eta-u\|M}{m_4} < \|L\| < +\infty$.
Finally, if

$$\|\eta - u\| > \sqrt{\frac{2Q_R m_2^2}{\mu_{12}M^2}}$$

then the discriminant of the quadratic polynomial on the left hand side of Eq. (B.51) is positive, and the two zeros of the polynomial are such that $\|L\|_{32B}^- < 0 < \ |L\|_{32B}^+ < \frac{\|\eta-u\|M}{m_4}$. Thus, the solution of condition (B.51), together with condition (B.49), lead to $\frac{\|\eta-u\|M}{m_4} < \|L\| < +\infty$.

Now we have to combine condition (B.58) of this *Case B* with the one obtained in Eq. (B.26) for the specification of the domain D_L. To this end, we first compare the quantities $\|L\|_{32}^-$ and $\|L\|_{32}^+$ with $\frac{\|\eta-u\|M}{m_4}$, in the four different situations considered before in *Case A*.

Moreover we underline that, see Eq. (B.22),

$$\|\eta - u\| > \sqrt{\left(m_2^2\frac{\mu_{34}}{\mu_{12}} - m_4^2\right)\frac{2Q_R}{\mu_{34}M^2}}$$

in the four considered situations.

First. $m_2m_3 \leq 2m_1m_4$ and $(m_2m_3 - 2m_1m_4)^2 < m_1m_2m_3m_4$
In this situation, if

$$\sqrt{\left(m_2^2\frac{\mu_{34}}{\mu_{12}} - m_4^2\right)\frac{2Q_R}{\mu_{34}M^2}} < \|\eta - u\| < \sqrt{\frac{-\left(m_2^2\frac{\mu_{34}}{\mu_{12}} - m_4^2\right)\frac{2Q_Rm_2^2m_4^2}{\mu_{12}M^2}}{\left(m_2^2\frac{\mu_{34}}{\mu_{12}} - 2m_4^2\right)^2 - m_4^2m_2^2\frac{\mu_{34}}{\mu_{12}}}}$$

then conditions (B.32) and (B.38) give

$$\frac{\|\eta - u\|M}{m_4} < \|L\|_{32}^- < \|L\|_{32}^+,$$

and from conditions (B.26) and (B.58) we get the following condition for the domain D_L

$$\|L\|_{32}^- \leq \|L\| \leq \|L\|_{32}^+$$

On the other hand, if

$$\|\eta - u\| > \sqrt{\frac{-\left(m_2^2\frac{\mu_{34}}{\mu_{12}} - m_4^2\right)\frac{2Q_Rm_2^2m_4^2}{\mu_{12}M^2}}{\left(m_2^2\frac{\mu_{34}}{\mu_{12}} - 2m_4^2\right)^2 - m_4^2m_2^2\frac{\mu_{34}}{\mu_{12}}}}$$

then

$$\|L\|_{32}^- < \frac{\|\eta - u\|M}{m_4} < \|L\|_{32}^+,$$

and from conditions (B.26) and (B.58) we get

$$\frac{\|\eta - u\|M}{m_4} \leq \|L\| \leq \|L\|_{32}^{+}$$

Second. $m_2m_3 \leq 2m_1m_4$ and $(m_2m_3 - 2m_1m_4)^2 \geq m_1m_2m_3m_4$
In this situation we have $\|L\|_{32}^{-} > \frac{\|\eta-u\|M}{m_4}$ and from conditions (B.26) and (B.58) we get

$$\|L\|_{32}^{-} \leq \|L\| \leq \|L\|_{32}^{+}$$

Third. $m_2m_3 > 2m_1m_4$ and $(m_2m_3 - 2m_1m_4)^2 < m_1m_2m_3m_4$
In this situation, if

$$\sqrt{\left(m_2^2\frac{\mu_{34}}{\mu_{12}} - m_4^2\right)\frac{2Q_R}{\mu_{34}M^2}} < \|\eta - u\| < \sqrt{\frac{-\left(m_2^2\frac{\mu_{34}}{\mu_{12}} - m_4^2\right)\frac{2Q_R m_2^2 m_4^2}{\mu_{12}M^2}}{\left(m_2^2\frac{\mu_{34}}{\mu_{12}} - 2m_4^2\right)^2 - m_4^2m_2^2\frac{\mu_{34}}{\mu_{12}}}}$$

then conditions (B.43) and (B.44) give

$$\|L\|_{32}^{-} < \|L\|_{32}^{+} < \frac{\|\eta - u\|M}{m_4},$$

and this contradicts conditions (B.26) and (B.58).

On the other hand, if

$$\|\eta - u\| > \sqrt{\frac{-\left(m_2^2\frac{\mu_{34}}{\mu_{12}} - m_4^2\right)\frac{2Q_R m_2^2 m_4^2}{\mu_{12}M^2}}{\left(m_2^2\frac{\mu_{34}}{\mu_{12}} - 2m_4^2\right)^2 - m_4^2m_2^2\frac{\mu_{34}}{\mu_{12}}}}$$

then

$$\|L\|_{32}^{-} < \frac{\|\eta - u\|M}{m_4} < \|L\|_{32}^{+},$$

and from conditions (B.26) and (B.58) we get

$$\frac{\|\eta - u\|M}{m_4} \leq \|L\| \leq \|L\|_{32}^{+}.$$

Fourth. $m_2m_3 > 2m_1m_4$ and $(m_2m_3 - 2m_1m_4)^2 \geq m_1m_2m_3m_4$
In this situation we have $\|L\|_{32}^{-} < \|L\|_{32}^{+} < \frac{\|\eta-u\|M}{m_4}$, which contradicts conditions (B.26) and (B.58). For the situations already described, the results obtained in both cases lead to the following conclusions.

The analysis of <u>*Case B*</u> is complete. The next step consists in combining the results obtained in <u>*Case B*</u> with those previously obtained in <u>*Case A*</u>. For the sub-cases described in the four situations, the results can be summarized as follows.

First. $m_2m_3 \leq 2m_1m_4$ and $(m_2m_3 - 2m_1m_4)^2 < m_1m_2m_3m_4$

(i) If $\|\eta - u\| < \sqrt{\left(m_2^2\frac{\mu_{34}}{\mu_{12}} - m_4^2\right)\frac{2Q_R}{\mu_{34}M^2}}$
then $D_L = \emptyset$;

(ii) If $\sqrt{\left(m_2^2\frac{\mu_{34}}{\mu_{12}} - m_4^2\right)\frac{2Q_R}{\mu_{34}M^2}} < \|\eta - u\| < \sqrt{\frac{-\left(m_2^2\frac{\mu_{34}}{\mu_{12}}-m_4^2\right)\frac{2Q_Rm_2^2m_4^2}{\mu_{12}M^2}}{\left(m_2^2\frac{\mu_{34}}{\mu_{12}}-2m_4^2\right)^2-m_4^2m_2^2\frac{\mu_{34}}{\mu_{12}}}}$
then $\|L\|_{32}^{-} \leq \|L\| \leq \|L\|_{32}^{+}$;

(iii) If $\|\eta - u\| > \sqrt{\frac{-\left(m_2^2\frac{\mu_{34}}{\mu_{12}}-m_4^2\right)\frac{2Q_Rm_2^2m_4^2}{\mu_{12}M^2}}{\left(m_2^2\frac{\mu_{34}}{\mu_{12}}-2m_4^2\right)^2-m_4^2m_2^2\frac{\mu_{34}}{\mu_{12}}}}$
then $\|L\|_{32}^{-} \leq \|L\| \leq \frac{\|\eta-u\|M}{m_4} \quad \vee \quad \frac{\|\eta-u\|M}{m_4} \leq \|L\| \leq \|L\|_{32}^{+}$,
or, equivalently, $\|L\|_{32}^{-} \leq \|L\| \leq \|L\|_{32}^{+}$.

Second. $m_2m_3 \leq 2m_1m_4$ and $(m_2m_3 - 2m_1m_4)^2 \geq m_1m_2m_3m_4$

(i) If $\|\eta - u\| < \sqrt{\left(m_2^2 \frac{\mu_{34}}{\mu_{12}} - m_4^2\right) \frac{2Q_R}{\mu_{34} M^2}}$
then $D_L = \emptyset$;

(ii) If $\|\eta - u\| > \sqrt{\left(m_2^2 \frac{\mu_{34}}{\mu_{12}} - m_4^2\right) \frac{2Q_R}{\mu_{34} M^2}}$
then $\|L\|_{32}^{-} \leq \|L\| \leq \|L\|_{32}^{+}$.

Third. $m_2 m_3 > 2m_1 m_4$ and $(m_2 m_3 - 2m_1 m_4)^2 < m_1 m_2 m_3 m_4$

(i) If $\|\eta - u\| < \sqrt{\left(m_2^2 \frac{\mu_{34}}{\mu_{12}} - m_4^2\right) \frac{2Q_R}{\mu_{34} M^2}}$
then $D_L = \emptyset$;

(ii) If $\sqrt{\left(m_2^2 \frac{\mu_{34}}{\mu_{12}} - m_4^2\right) \frac{2Q_R}{\mu_{34} M^2}} < \|\eta - u\| < \sqrt{\frac{-\left(m_2^2 \frac{\mu_{34}}{\mu_{12}} - m_4^2\right) \frac{2Q_R m_2^2 m_4^2}{\mu_{12} M^2}}{\left(m_2^2 \frac{\mu_{34}}{\mu_{12}} - 2m_4^2\right)^2 - m_4^2 m_2^2 \frac{\mu_{34}}{\mu_{12}}}}$
then $\|L\|_{32}^{-} \leq \|L\| \leq \|L\|_{32}^{+}$;

(iii) If $\|\eta - u\| > \sqrt{\frac{-\left(m_2^2 \frac{\mu_{34}}{\mu_{12}} - m_4^2\right) \frac{2Q_R m_2^2 m_4^2}{\mu_{12} M^2}}{\left(m_2^2 \frac{\mu_{34}}{\mu_{12}} - 2m_4^2\right)^2 - m_4^2 m_2^2 \frac{\mu_{34}}{\mu_{12}}}}$
then $\|L\|_{32}^{-} \leq \|L\| \leq \frac{\|\eta - u\| M}{m_4} \quad \vee \quad \frac{\|\eta - u\| M}{m_4} \leq \|L\| \leq \|L\|_{32}^{+}$,
or, equivalently, $\|L\|_{32}^{-} \leq \|L\| \leq \|L\|_{32}^{+}$.

Fourth. $m_2 m_3 > 2m_1 m_4$ and $(m_2 m_3 - 2m_1 m_4)^2 \geq m_1 m_2 m_3 m_4$

(i) If $\|\eta - u\| < \sqrt{\left(m_2^2 \frac{\mu_{34}}{\mu_{12}} - m_4^2\right) \frac{2Q_R}{\mu_{34} M^2}}$
then $D_L = \emptyset$;

(i) If $\|\eta - u\| > \sqrt{\left(m_2^2 \frac{\mu_{34}}{\mu_{12}} - m_4^2\right) \frac{2Q_R}{\mu_{34} M^2}}$

then $\|L\|_{32}^{-} \leq \|L\| \leq \|L\|_{32}^{+}$.

The results summarized above show that the condition obtained for the specification of the domain D_L is the same for the considered situations.

Finally, we consider the more restrictive condition (B.26) in order to completely specify the domain D_L. Since the results of the combination of <u>*Case A*</u> and <u>*Case B*</u> lead to the unique condition $\|L\|_{32}^{-} \leq \|L\| \leq \|L\|_{32}^{+}$, the conclusion for D_L is the following:

(a) If $\sqrt{\left(m_2^2 \frac{\mu_{34}}{\mu_{12}} - m_4^2\right) \frac{2Q_R}{\mu_{34} M^2}} < \|\eta - u\| < \sqrt{\frac{2Q_R m_2^2}{M^2 \mu_{12}}}$

then D_L is specified by

$$\|L\|_{32}^{-} \leq \|L\| \leq \|L\|_{32}^{+}; \tag{B.59}$$

(b) If $\|\eta - u\| > \sqrt{\frac{2Q_R m_2^2}{M^2 \mu_{12}}}$

then D_L is specified by

$$0 \leq \|L\| \leq \|L\|_{32}^{+}. \tag{B.60}$$

Conditions (B.59) and (B.60) define the lower and upper bounds for the internal integral defining the operator $R_3^{(2)}$, whereas conditions (a) and (b) on $\|\eta - u\|$ are traduced in terms of suitable Heaviside step functions.
Now we come back to the expression (B.12) of the operator $R_3^{(2)}$. As previously anticipated, our idea is to express L in spherical coordinates, with θ being the angle between L and $\eta - u$, and use the appropriate conditions to specify the domain D_L in the new coordinate system. Before writing the

detailed expression of the operator $R_3^{(2)}$, we introduce the following notation, for sake of simplicity.

$$\Delta_3^{(2)} = \beta_{34}\sigma_{34}^2(n_2n_4)^{1/2}\left(\frac{m_2m_4}{(2\pi kT)^2}\right)^{3/4}\frac{\mu_{34}}{\mu_{12}}$$
$$\times\exp\left[-\frac{m_4}{2kT}\left(u-\frac{w-u-\frac{1}{M}\left(m_2\sqrt{\frac{\mu_{34}}{\mu_{12}}+\frac{2Q_R}{\mu_{12}\|L\|^2}}-m_4\right)L}{\frac{1}{M}\left(m_2\sqrt{\frac{\mu_{34}}{\mu_{12}}}-m_4\right)}-L\right)^2\right.$$
$$-\frac{m_2}{2kT}\left(u+\frac{1}{M}\left(-m_1\sqrt{\frac{\mu_{34}}{\mu_{12}}+\frac{2Q_R}{\mu_{12}\|L\|^2}}-m_4\right)L\right.$$
$$\left.\left.+\frac{1}{M}\left(-m_1\sqrt{\frac{\mu_{34}}{\mu_{12}}}-m_4\right)\frac{w-u-\frac{1}{M}\left(m_2\sqrt{\frac{\mu_{34}}{\mu_{12}}+\frac{2Q_R}{\mu_{12}\|L\|^2}}-m_4\right)L}{\frac{1}{M}\left(m_2\sqrt{\frac{\mu_{34}}{\mu_{12}}}-m_4\right)}\right)^2\right]$$
$$\times\Theta(\|L\|-\Gamma_{34})\left\|\frac{\frac{1}{M}\left(m_2\sqrt{\frac{\mu_{34}}{\mu_{12}}}-m_4\right)}{w-u-\frac{1}{M}\left(m_2\sqrt{\frac{\mu_{34}}{\mu_{12}}+\frac{2Q_R}{\mu_{12}\|L\|^2}}-m_4\right)L}\right\|\|L\|^2\sin\theta,$$

with

$$L = (\|L\|\cos\theta, \|L\|\sin\theta\cos\varphi, \|L\|\sin\theta\sin\varphi),$$

$$\cos\theta = \frac{1}{M}\left(m_2\sqrt{\frac{\mu_{34}}{\mu_{12}}-\frac{2Q_R}{\mu_{12}\|L\|^2}}-m_4\right)\frac{\|L\|}{\|w-u\|},$$

and since $\theta\in[0,\pi]$, we have $\sin\theta\geq 0$, so that

$$\sin\theta = \sqrt{1-\cos^2\theta}. \tag{B.61}$$

Finally, we are able to re-write the operator $R_3^{(2)}$ of expression (B.12) with

D_L explicitly defined. We get

$$R_3^{(2)}(\underline{\hat{h}}) = \int_{\mathbb{R}^3}\int_0^{2\pi}\left[\int_{\|L\|_{32}^-}^{\|L\|_{32}^+}\Delta_3^{(2)}\,d\|L\|\hat{h_1}(\eta)\right.$$
$$\times\Theta\left(\|\eta-u\|-\sqrt{\left(m_2^2\frac{\mu_{34}}{\mu_{12}}-m_4^2\right)\frac{2Q_R}{\mu_{34}M^2}}\right)\Theta\left(\sqrt{\frac{2Q_Rm_2^2}{\mu_{12}M^2}}-\|\eta-u\|\right)$$
$$\left.+\int_0^{\|L\|_{32}^+}\Delta_3^{(2)}\,d\|L\|\Theta\left(\|\eta-u\|-\sqrt{\frac{2Q_Rm_2^2}{\mu_{12}M^2}}\right)\right]\left(\frac{M}{m_2\sqrt{\frac{\mu_{34}}{\mu_{12}}}-m_4}\right)^3 d\varphi d\eta.$$

Thus, the kernel of $R_3^{(2)}$ can be extracted in the form

$$N(R_3^{(2)})(u,w) = \int_0^{2\pi}\left[\int_{\|L\|_{32}^-}^{\|L\|_{32}^+}\Delta_3^{(2)}\,d\|L\|\right.$$
$$\times\Theta\left(\|w-u\|-\sqrt{\left(m_2^2\frac{\mu_{34}}{\mu_{12}}-m_4^2\right)\frac{2Q_R}{\mu_{34}M^2}}\right)\Theta\left(\sqrt{\frac{2Q_Rm_2^2}{\mu_{12}M^2}}-\|w-u\|\right)$$
$$\left.+\int_0^{\|L\|_{32}^+}\Delta_3^{(2)}\,d\|L\|\Theta\left(\|w-u\|-\sqrt{\frac{2Q_Rm_2^2}{\mu_{12}M^2}}\right)\right]\left(\frac{M}{m_2\sqrt{\frac{\mu_{34}}{\mu_{12}}}-m_4}\right)^3 d\varphi,$$

and this leads to the expression of Eq. (4.120) of Subsection 4.6.2.

Bibliography

[1] Abouseif, G. E. and Toong, T. Y., Theory of unstable one-dimensional detonations. *Combustion & Flame* **45** (1982) 67-94.

[2] Abouseif, G. E. and Toong, T. Y., Theory of unstable two-dimensional detonations: Genesis of the transverse waves. *Combustion & Flame* **63** (1986) 191-207.

[3] Austina, J. M., Pintgenb, F. and Shepherd, J. E., Reaction zones in highly unstable detonations. *Proc. Comb. Inst.* **30** (2005) 1849-1857.

[4] Bdzil, J. B. and Stewart, D. S., Modeling two-dimensional detonation with detonation shock dynamics. *Phys. Fluids* **1** (1989) 1261-1267.

[5] Bianchi, M. P. and Soares, A. J., A kinetic model for a reacting gas mixture: steady detonation and speeds of sound. *Phys. Fluids* **8** (1996) 3423-3432.

[6] Bianchi, M. P. and Soares, A. J., Modelling and solutions to the linear stability of detonation wave in the kinetic frame. *Journal of Difference Equations and Applications* **17** (2011) 1169-1184.

[7] Bisi, M., Groppi, M. and Spiga, G., Flame structure from a kinetic model for chemical reactions. *KRM* **3** (2010) 17-34.

[8] Bourlioux, A., Majda, A. and Roytburd, V., Theoretical and numerical structure for unstable one-dimensional detonations. *SIAM J. Appl. Math* **51** (1991) 303-343.

[9] Bourlioux, A. and Majda, A. J., Theoretical and numerical structure for unstable two-dimensional detonations. *Combustion & Flame* **90** (1992) 211-229.

[10] Buckmaster, J. D. and Ludford, G. S. S., The effect of structure on the stability of detonations I. role of the induction zone. *Proc. XX Simp. Comb.* (1986) 1669-1676.

[11] Buckmaster, J. D. and Neves, J., One-dimensional detonation stability: The spectrum for infinite activation energy. *Phys. Fluids* **31** (1988) 3571-3576.

[12] Carleman, T. S., *Problème Mathématique dans la Théorie Cinétique des Gases.* Almqvist and Wiksel, Uppsala, 1957.

[13] Carvalho, F. and Soares, A. J., Steady detonation wave solutions under the reaction heat effect. *In Waves and Stability in Continuous Media*, (Palermo, Italy, 2009) edited by Greco, A. M. Rionero, M. Ruggeri, T. World Scientific Proceedings, Singapore, 87-92.

[14] Carvalho, F. and Soares, A. J., Influence of the reaction heat on the linear stability spectra of steady detonation in the kinetic frame. *In 27th Int. Symp. on Rarefied Gas Dynamics* (California, USA, 2010) American Institute of Physics, 6974.

[15] Carvalho, F. and Soares, A. J., On the dynamics and linear stability of one-dimensional steady detonation waves. *J. Phys. A: Math. Theor.* **45** (2012) 255501 (23pp).

[16] Carvalho, F., Polewczak, J. and Soares, A. J., work in preparation about the Kernels of the simple reacting spheres linearized theory.

[17] Cercignani, C., *Theory and Application of the Boltzmann Equation*. Scottish Academic Press, Edinburgh, 1975.

[18] Cercignani, C., Illner, R. and Pulvirenti, M., *The Mathematical Theory of Dilute Gases*. Springer, 1994.

[19] Cercignani, C., *Rarefied Gas Dynamics: From Basic Concepts to Actual Calculations*. Cambridge University press, 2000.

[20] Chapman, S. and Cowling, T. G., *The Mathematical Theory of Non-uniform Gases*. Cambridge University Press, Cambridge, 1970.

[21] Chevalier, J. M., Carion, N., Protat, J. C. and Redasse, J. C., Propagation phenomena on the detonation wave front. *Phys. Rev. Lett.* **71** (1993) 712-715.

[22] Conforto, F., Monaco, R., Schürrer, F. and Ziegler, I., Steady detonation waves via the Boltzmann equation for a reacting mixture. *J. Phys. A: Math. Gen.* **36** (2003) 5381-5398.

[23] Conforto, F., Groppi, M., Monaco, R. and Spiga, G., Steady detonation waves for gases undergoing dissociation/recombination and bimolecular reactions. *Continuum Mech. Thermodyn.* **16** (2004) 149-161.

[24] Conforto, F., Groppi, M., Monaco, R. and Spiga, G., Steady detonation problem for slow and fast chemical reaction. *in Modelling and Numerics of Kinetics Dissipative Sistems* (New York, 2006) edited by Pareschi, L. Russo, G. and Toscani, G. Nova Science, 105-117.

[25] Conforto, F., Groppi, M., Monaco, R. and Spiga, G., Kinetic Approach to deflagration processes in a recombination reaction. *Kinetic and Related Models* **4** (2011) 259-276.

[26] Cooper, M., Jacksony, S., Austin, J., Wintenberger, E. and Shepherdz, J. E., Direct experimental impulse measurements for detonations and deflagrations. *J. Propulsion and Power* **18** (2002) 1033-1041.

[27] Desvillettes, L. and Villani, C., On the trend to global equilibrium for spatially inhomogeneous systems: the Boltzmann equation. *Invent. Math.* **159** (2005) 245-316.

[28] Erpenbeck, J. J., Stability of steady-state equilibrium detonations. *Phys. Fluids* **5** (1962) 604-614.

[29] Erpenbeck, J. J., Structure and stability of the square wave detonation. *In Ninth Symposium on Combustion* (New York, 1963) New York: Academic Press 442-453.

[30] Erpenbeck, J. J., Stability of idealized one-reaction detonations. *Phys. Fluids* **7** (1964) 684-696.

[31] Ferziger J. H. and Kaper, H. G., *Mathematical Theory of Trasport Processes in Gase.* North-Holland Publishing Company, 1972.

[32] Fickett, W. and Wood, W. W., Calculation for pulsating one-dimensional detonations. *Phys. Fluids* **9** (1966) 903-916.

[33] Fickett, W. and Davis, W. C., *Detonation, Theory and Experiment.* University of California, Berkeley, 1979.

[34] Fickett, W., *Introduction to Detonation Theory.* University of California, Berkeley, 1986.

[35] Giovangigli, V. and Massot, M., Asymptotic stability of equilibrium states for multicomponent reactive flows. *Mathematical Models Methods in Applied Science* **8** (1998) 251-297.

[36] Giovangigli, V., *Multicomponent Flow Modeling.* Birkhäuser, Boston, 1999.

[37] Gorchkov, V., Kiyanda, C. B., Short, M. and Quirk, J. J., A detonation stability formulation for arbitrary equations of state and multi-step reaction mechanisms. *Proc. Combust. Instit* **31** (2007) 2397-2405.

[38] Grad, H., On the kinetic theory of rarefied gases. *Communications on Pure and Applied Mathematics* **2** (1949) 331-407.

[39] Grad, H., Theory of rarefied gases. *Rarefied Gas Dynamics* (1960) 100-138.

[40] Grad, H., Asymptotic Theory of the Boltzmann Equation II. *In Rarefied Gas Dynamics* **1** (Paris, 1962) Edited by J.A. Laurmann. New York: Academic Press, 26-59.

[41] Grad, H., Asymptotic Theory of the Boltzmann Equation. *The Physics of Fluids* **6** (1963) 147-181.

[42] Groppi, M. and Spiga, G., Kinetic approach to chemical reactions and inelastic transitions in a rarefied gas. *J. Math. Chem.* **26** (2000) 197-219.

[43] Groppi, M. and Polewczak, J., On Two Kinetic Models for Chemical Reactions: Comparisons and Existence Results. *Journal of Statistical Physics* **117** (2004) 211-241.

[44] He, L. and Lee, J. H. S., The dynamical limit of one-dimensional detonations. *Phys. Fluids* **7** (1995) 1151-1158.

[45] Kasimov, A. and Stewart, D. S., Spinning instability of gaseous detonations. *J. Fluid Mech.* **466** (2002) 179-203.

[46] Kasimov, A. and Stewart, D. S., On the dynamics of self-sustained one-dimensional detonations: a numerical study in the shock-attached frame. *Phys. Fluids* **16** (2004) 3566-3578.

[47] Kasimov, A. and Stewart, D. S., Theory of detonation with an embedded sonic locus. *SIAM J. Appl. Math.* **66** (2005) 384-407.

[48] Kato, T., *Perturbation Theory of Linear Operators.* Springer, New York, 1966.

[49] Kremer, G. and Soares, A. J., Effect of reaction heat on Maxwellian distribution functions and rate of reactions. *J. Stat. Mech* **P12003** (2007) 1-16.

[50] Kremer, G., Oliveira, F. and Soares, A. J., H-Theorem and Trend to Equilibrium of Chemically Reacting Mixtures of Gases *Kinetic and Related Models* **2** (2009) 333-343.

[51] Kremer, G., *Introduction to the Boltzmann Equation and Transport Processes in Gases*. Springer, Berlin, 2010.

[52] Kuo, K. K., *Principles of Combustion*. New York, Wiley, 2005.

[53] Lee, H. I. and Stewart, D. S., Calculation of linear detonation stability: one dimensional instability of plane detonation. *J. Fluid Mech.* **216** (1990) 103-132.

[54] Lee, J. H. S., *The Detonation Phenomenon*. Cambridge University Press, Cambridge, 2008.

[55] Liang, Z., Khastoo, B. and Bauwens, L., Effect of reaction order on stability of planar detonation. *Int. J. Comput. Fluid Dyn.* **19** (2004) 131-142.

[56] Majda, A. J. and Rosales, R., A Theory for Spontaneous Mach Stem Formation in Reacting Shock Fronts, I. The Basic Perturbation Analysis. *SIAM J. Appl. Math.* **43** (1983) 1310-1334.

[57] Marron, M. T., Simple Collision Theory of Reactive Hard Spheres. *Journal of Chemical Physics* **52** (1970) 4060-4061.

[58] Mazaheri, K., Hashemi, S. S. and Lee, J. H., Numerical study of detonation instability for a two-step kinetics model. *Scientia Iranica* **11** (2004) 292-301.

[59] Moreau, M., Formal study of a chemical reaction by Grad expansion of the Boltzmann equation. *Physica A* **79** (1975) 18-51.

[60] Müller, I., Flame Structure in ordinary and extended thermodynamics. *Proc. Asymptotic Methods in Nonlinear Wave Phenomena, Singapore, World Scientific* (2007) 144-153.

[61] Papalexandris, M. V., Numerical simulation of detonations in mixtures of gases and solid particles. *J. Fluid Mech.* **507** (2004) 95-142.

[62] Pintgena, F., Ecketta, C. A., Austin, J. M. and Shepher, J. E., Direct observations of reaction zone structure in propagating detonations. *Combustion & Flame* **133** (2003) 211-229.

[63] Polak, L. S. and Khachoyan, A.V., Generalization of Boltzmann's H-theorem for a reacting gas mixture. *Soviet J. Chem. Phys.* **2** (1985) 1474-1485.

[64] Polewczak, J., The Kinetic Theory of Simple Reacting Spheres: I. Global Existence Result in a Dilute-Gas Case. *Journal of Statistical Physics* **100** (2000) 327-362.

[65] Polewczak, J., Soares, A. J. and Carvalho F., Work in preparation about the linearized systems of simple reacting spheres.

[66] Present, R. D., On the velocity distribution in a chemically reacting gas. *J. chem. Phys.* **31** (1959) 747-797.

[67] Present, R. D., Chapman-Enskog Method in Chemical Kinetics. *The Journal of Chemical Physics* **48** (1968) 4875-4877.

[68] Prigogine, I. and Xhrouet, E., On the perturbation of Maxwell distribution function by chemical reaction in gases. *Physica* **XV** (1949) 913-932.

[69] Resibois, P. and Leener, M., *Classical Kinetic Theory of Fluids*. Wiley-Interscirnce Puplications, 1977.

[70] Ross, J. and Mazur, P., Some deductions from a formal statistical mechanical theory of chemical kinetics. *J. Chem. Phys.* **35** (1961) 19-28.

[71] Rossani, A. and Spiga, G., A note on the kinetic theory of chemically reacting gases. *Physica A* **272** (1999) 563-573.

[72] Sharpe, G. J., Linear stability of idealized detonations. *R. Soc. Lond. A* (1997) 2623-2605.

[73] Sharpe, G. J., Linear stability of pathological detonations. *J. Fluid Mech.* **401** (1999) 311-338.

[74] Sharpe, G. J. and Falle, S. A. E. G., One-dimensional numerical simulations of idealized detonations. *Proc. R. Soc. Lond. A* **455** (1999) 1203-1214.

[75] Sharpe, G. J. and Falle, S. A. E. G., One-dimensional nonlinear stability of pathological detonations. *J. Fluid Mech.* **414** (2000) 339-366.

[76] Sharpe, G. J. and Falle, S. A. E. G., Numerical simulations of pulsating detonations: I. Nonlinear stability os steady detonations. *Combust. Theory Modelling* **4** (2000) 557-574.

[77] Shizgal, B. and Karplus, M., Nonequilibrium contributions to the Rate of Reaction. I. Perturbation of the Velocity Distribution Function. *The Journal of Chemical Physics* **52** (1970) 4262-4278.

[78] Short, M. and Stewart, D. S., Cellular detonation stability. Part 1. A normal-mode linear analysis. *J. Fluid Mech.* **368** (1998) 229-262.

[79] Short, M., Theory and modeling of detonation wave stability: a brief look at the past and toward the future. *20th Int. Colloq. Dyn. Expl. React. Syst.* (2005) 1-19.

[80] Sone, Y., *Molecular Gas Dynamics, Theory, Techniques and Applications.* Birkhäuser, 2007.

[81] Stewart, D. S. and Kasimov, A., On the dynamics of self-sustained one-dimensional detonations: A numerical study in the shock-attached frame. *Physics of fluids* **16** (2004) 3566-3578.

[82] Stewart, D. S. and Kasimov, A., State of Detonation Stability Theory and Its Application to Propulsion. *J. Propulsion and Power* **22** (2006) 1230-1244.

[83] Stewart, I. and Tall, D., *Complex Analysis.* Cambridge University Press, 1985.

[84] Strehlow, R. A., Multi-dimensional detonation wave structure. *Astro. Acta* **15** (1970) 345-357.

[85] Villani, C., A Review of Mathematical Topics in Collisional Kinetic Theory. *Handbook of Mathematical Fluid Dynamics* **1** 2002.

[86] Xystris, N. and Dahler, J. S., Mass and momentum transport in dilute reacting gases. *J. Chem. Phys.* **68** (1978) 354-373.

[87] Xystris, N. and Dahler, J. S., Kinetic Theory of Simple Reactive Spheres. *J. Chem. Phys.* **68** (1978) 387-401.

[88] Yoshida, K., *Functional Analysis and Its Applications.* New York: Springer-Verlag, 1971.

[89] Yungster, S. and Radhakrishnam, K., Structure and stability of one-dimensional detonations in ethylene-air mixtures. *Shock Waves* **14** (2005) 61-72.

[90] Zhang, F., *Shock Wave Science and Technology Reference Library: Heterogeneous Detonation.* **4** Springer-Verlag, Berlin Heidelberg, 2009.

Index